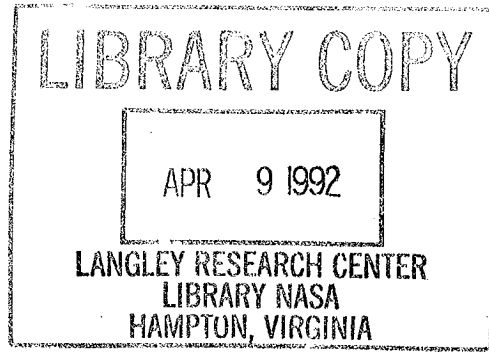NASA—CR— /0 7, UU/

NASA Contractor Report 189051

NASA-CR-189051
19920011168

Analysis of Shell-Type Structures Subjected to Time-Dependent Mechanical and Thermal Loading

G.J. Simitses
Georgia Institute of Technology
Atlanta, Georgia

November 1991

NASA
National Aeronautics and
Space Administration

ANALYSIS OF SHELL-TYPE STRUCTURES SUBJECTED TO TIME-DEPENDENT MECHANICAL AND THERMAL LOADING

By

G. J. Simitses
School of Aerospace Engineering
Georgia Institute of Technology
Atlanta, Georgia

ABSTRACT

This report deals with the development of a general mathematical model and solution methodologies for analyzing structural response of thin, metallic shell-like structures under dynamic and/or static thermomechanical loads. In the mathematical model, geometric as well as material-type of nonlinearities are considered. Traditional as well as novel approaches are reported and detailed applications are presented in the appendices. The emphasis for the mathematical model, the related solution schemes, and the applications, is on thermal viscoelastic and viscoplastic phenomena, which can predict creep and ratchetting.

1. INTRODUCTION

The prediction of inelastic behavior of metallic materials at elevated temperatures has increased in importance in recent years. The operating conditions within the hot section of a rocket motor or a modern gas turbine engine present an extremely harsh thermo-mechanical environment. Large thermal transients are induced each time the engine is started or shut down. Additional thermal transients from an elevated ambient occur, whenever the engine power level is adjusted to

meet flight requirements. The structural elements employed to construct such hot sections, as well as any engine component located therein, must be capable of withstanding such extreme conditions. Failure of a component would, due to the critical nature of the hot section, lead to an immediate and catastrophic loss in power and thus cannot be tolerated. Consequently, assuring satisfactory long term performance for such components is a major concern for the designer.

Traditionally, this requirement for long term durability has been a more significant concern for gas turbine engines rather than rocket motors. However, with the advent of reusable space vehicles, such as the Space Shuttle, the requirement to accurately predict future performance following repeated elevated temperature operations must now be extended to include the more extreme rocket motor application. These blades operate in severe thermal transients that result in large inelastic strains, and several types of behavior must be considered. The elevated temperatures can lead to thermal buckling and, in addition, creep can be expected to occur. Thus, a combination of thermal-creep buckling behavior leading to large deflections can be anticipated. Because of the cyclic character of the mechanical and thermal loads, progressive growth or ratchetting effects must also be considered. Thus, geometric and material nonlinearities (of high orders) can be anticipated and must be considered in the mathematical model.

Consequently, the industry is concerned with the behavior of thin shell-like structural elements subjected to severe time-dependent thermomechanical loading. Such thin elements, including beams, rings, arches, plates and shells, are presenting generic types of components, which might be located within or adjacent to the hot section of a rocket or a gas turbine engine.

The experience in the gas turbine engine industry indicates, however, that existing analytic tools are not sufficiently reliable to accomplish this task. State of the art methods for predicting hot section component behavior are generally not sufficiently accurate to perform extended use evaluations.

Under this kind of severe loading conditions, the structural behavior is highly nonlinear due to the combined action of geometrical and physical nonlinearities. On one side, finite

2

deformation in a stressed structure introduces nonlinear geometric effects. On the other side, physical nonlinearities arise even in small strain regimes, whereby inelastic phenomena play a particularly important role. From a theoretical standpoint, nonlinear constitutive equations should be applied only in connection with nonlinear transformation measures (implying both deformation and rotations). However, in almost all of the works in this area, the two identified sources of nonlinearities are always separated. This separation yields, at one end of the spectrum, problems of large kinematics, while at the other end, problems of viscous and/or non-isothermal behavior in the presence of small strain.

Because of the nature of the causes, special care is needed in the selection or development of a constitutive law that includes time and temperature effects. Although there exists a sizeable body of literature on phenomenological constitutive equations for the rate- and temperature-dependent plastic deformation of metallic materials, to date rational and thermodynamically consistent elastic-thermoviscoplastic constitutive relations capable of incorporating the effects of large strains and rotations have not been demonstrated.

Constitutive models for small strain in engineering literature may generally be grouped into three categories: classical plasticity, nonlinear visoelasticity, and theories based on microstructural phenomena. Each group can be further separated into "unified" and "uncoupled" theories, where the two differ in their approach to the treatment of rate-independent and rate-dependent inelastic deformation. The uncoupled theories decompose the inelastic strain rate into a time-independent plastic strain rate and a time-dependent creep rate with independent constitutive relations describing plastic and creep behavior. Such uncoupling of the strain components provides for simpler theories to be developed but precludes any creep-plasticity interaction. Recognizing that cyclic plasticity, creep and recovery are not independent phenomena but rather are very interdependent, a number of "unified" models for inherently time-dependent nonelastic deformation have been developed recently.

Classical incremental plasticity theories are macrophenomenological because they base the derivation of state variables purely on experimental results without direct reference to the microstructure of the material. Most incremental plasticity theories have four major components: (1) stress-elastic strain relations, (2) a yield function describing the onset of plastic deformation, (3) a hardening rule which prescribes the strain-hardening of the material and the modification of the yield surface during plastic flow, and (4) a flow rule which defines the components of strain that are plastic or nonrecoverable.

Research in this area is voluminous. For example, Zienkiewicz and Cormeau [1] developed a rate-dependent unified theory which allows for nonassociative plasticity and strain softening, but does not model the Bauschinger effect or temperature dependence. Extensions of classical plasticity to model both rate and temperature effects were presented recently by Allen and Haisler [2], Haisler and Cronenworth [3], and Yamada and Sakurai [4].

In the nonlinear viscoelastic approach, the constitutive relation is expressed as a single integral or convoluted form. This type of constitutive model employs the thermodynamic laws along with physical constraints to complete the formulation. A detailed review of several existing theories is presented by Walker [5]. Walker's [5] theory is based on a unified viscoplastic integral developed by modifying the constitutive relations for a linear three parameter viscoelastic solid. The theory contains clearly defined material parameters, a rate-dependent equilibrium stress, and a proposed multiaxial model. An important shortcoming of Walker's theory is its failure to model transient temperature conditions. Many other nonlinear viscoelastic theories have been proposed including those by Cernocky and Krempl [6], Valanis [7], and Chabache[8].

The microphenomenological theories attempt to represent the response of polycrystalline materials in terms of various micromechanisms of deformation and failure. Various dislocation theories have been developed to predict plastic deformation in terms of dislocation interaction, slip, glide, density, etc. Most of the material models developed, to date, depend primarily on the number of state variables used and their growth or evolutionary laws. Many of the recent 'unified'

microphenomenological theories have been discussed and evaluated by Walker [9] and Chan et al. [10].

One example of a microphysically based constitutive law is an elastic-viscoplastic theory based on two internal state variables as proposed by Bodner, et al. [11]. These authors, demonstrate the ability of the constitutive equations to represent the principal features of cyclic loading behavior including softening upon stress reversal, cyclic hardening or softening, cyclic saturation, cyclic relaxation, and cyclic creep. One limitation of the formulation though is that the computed stress-strain curves are independent of the strain amplitude and therefore too "flat" or "square".

Miller [12] has reported research on the modeling of cyclic plasticity with "unified" constitutive equations. He also recognizes the shortcomings of many theories in predicting hysteresis loops, which are oversquare in comparison to observed experimental behavior. Improvement is accomplished by making the kinematic work-hardening coefficient depend on the back stress and the sign of the nonelastic strain term. Theories that are similar in format to Miller's have been proposed by Krieg, Swearengen and Rhode [13] and by Hart [14]. The models use two internal state variables to reflect current microstructure state and are based upon models for dislocation processes in pure metals. All these constitutive theories were formulated without the use of a yield criterion. Since these models do not contain a completely elastic regime, the function that describes the inelastic strain rate should be such that the inelastic strain rate is very small for low stress levels. Theories with a yield function and a full elastic regime have been developed for the case of isotropic and directional hardening by Lee and Zavrel [15].

As previously noted, the quantities utilized in the small strain theory of viscoplasticity (stress, strain, stress rate, and strain rate) are defined only within the assumption of "small strain", but this is always left unstated. Whether or not the strains for a given case are "small" cannot be determined a priori by geometric considerations. In general, one cannot know in advance whether for a given loading of a material the "small strain" assumption (always left undefined) will hold or

not. The question of whether the small-strain approximations are valid is always avoided in the "small strain" literature. Furthermore, as Hill [16] points out, the really typical plastic problems involve changes in geometry that cannot be disregarded. In many cases, for example, it is sufficient to take into account finite plastic strains and small elastic strains or vice versa. From the theoretical viewpoint it is desirable in all cases to have a theory which intrinsically allows for both the elastic and plastic strains to be large. Such a theory of course, must reduce to the earlier mentioned special cases, as limiting cases. Furthermore, such theories provide a check for those which are obtained by generalizing small strain theories.

The mathematical theories of deformation and flow of matter deal essentially with the gross properties of a medium. Heat and mechanical work are considered as additional causes for a change of the state of the medium. The resulting phenomena in any particular material are not unrelated. Therefore, a thermodynamical treatment of the foundation of the theory of flow and deformation is appropriate, and indeed the obvious approach. Two very different main approaches to a thermodynamic theory of a continuum can be identified. These differ from each other in the fundamental postulates upon which the theories are based. An essential controversy can be traced through the whole discussion of the thermodynamic aspects of continuum mechanics. None of these approaches is concerned with the atomic structure of the material. They, therefore, represent purely phenomenological approximations. Both theories are characterized by the same fundamental requirement that the results should be obtained without having recourse to statical or kinetic methods.

Within each of these approaches there are two distinct methods of describing history and dissipative effects: the functional theory [18], in which all dependent variables are assumed to depend on the entire history of the independent variables, and the internal variable approach [19], wherein history dependence is postulated to appear implicitly in a set of internal variables. For experimental as well as analytical reasons[20, 21] the use of internal variables in modeling inelastic

solids is gaining widespread usage, in current research. The main differences among the various modern theories lie in the choice of these internal variables.

The predictive value of an elastic- viscoplastic material model for non-isothermal, large deformation analyses depends therefore on three basic elements:

a) the nonlinear kinematic description of the elastic-plastic deformation.

b) termodynamic considerations, and

c) the choice of external and internal thermodynamic variables as well as on their interactions.

The problem of viscoplastic deformations in shells has been treated at several levels of approximation and generality.

The simplest approaches (see [22]) are based on the assumption of infinitesimal displacement gradients (which implies infinitesmal strains) and a material model of stationary creep, sometimes with an approximate inclusion of primary creep.

A more general analysis utilizes shell kinematics for moderately large displacement gradients (at least some of them), infinitesimal strains, and material models of stationary or simple non-stationary creep (see [22]). This type of assumption is capable of solving problems of creep buckling [23], and it does reproduce the sometimes stiffening effect of the interaction between the normal forces and the normal deflection. Extension of this kind of formulation with a viscoplastic material model is presented in [24-26]. The use of numerical methods [27] makes possible the solution for many non-trivial types of structures.

The problems of large strains, which arise in the analysis of large creep or thermal deformation of shells, have not been treated at all in a general manner. Recognizing that finite strain effects are present in these problems, reliable prediction demands that such effects be included rationally and properly in the analysis. In addition to the necessary basic kinematical and dynamical equations of the shell theory, such an analysis must incorporate a correctly invariant formulation of the material equations and requires an evaluation of the strain-rate tensors through

the thickness of the shell. Such an analysis cannot be found in explicit form, at least in the readily accessible engineering literature.

Several authors have developed mathematical description of the kinematics of the three dimensional deformation of elastic or viscoelastoplastic materials [28, 29]. However, it is not clear how to best select the reference space and configuration for the stress tensor, bearing in mind the rheologies of realistic materials. Although an intrinsic relation, which satisfies material objectivity can be used [30, 31], the choice is not unique (see for example [29], [32], [33]).

For shell-like structures, failure may be caused by buckling. Thus, stability can be a primary consideration in the structure design. In a high temperature environment, there will be much more concern on this issue, because the inelastic deformation may lead to a geometrical imperfection which, in turn, may further decrease the load carrying capability. Therefore, stability of shell-like structures can become the main concern for designers, and buckling and postbuckling behavior of shell-like structures (see [34]) must be studied.

In the analysis of shell-like structures, it is worthwhile to note that Donnell [35] and Sanders [36] made great contributions in the formulation of nonlinear shell theories. Many applications are based on their formulation and simplifications.

For a long time, the research efforts have been put into the subject on how to improve the discrepancy between the theoretical and experimental results. The present trend in buckling and postbuckling analyses is to relax several of the assumptions in classical theories and employ nonlinear kinematic and constitutive relations.

As the complexity of shell-like structures increases and as the computational capability improves, numerical methods play a major role in predicting buckling and in enhancing our understanding of postbuckling response.

The finite element analysis for shell structures has been the subject of interest for many years. There have been many published works in this field. Most of them deal with elastic-plastic material behavior. Some of them also deal with geometric nonlinearity and postbuckling behavior.

8

Ahmad, Irons and Zienkiewicz [37] first proposed the 'degenerated' three dimensional isotropic element which can be used in the linear analysis of thin shells. The basic assumption used in [37] is that the normal will remain normal to the deflected midsurface, straight and inextensional after deformation. With this assumption, the displacement field in the shell can be expressed in terms of five degrees of freedom (three translations and two rotations) of the nodes which are located in the middle surface.

The 'degenerated' 3-D element was extended to the geometrically nonlinear analysis of shells by Ramm [38]. He used both quadratic and cubic interpolation functions in his work. The development is based on total Lagrangian formulation.

Bolouchi [39] developed various shell elements with 8-16 nodes. His work is based on both total Lagrangian and updated Lagrangian formulations.

At the same time, finite element analysis has been adopted to the area of nonlinear continuum mechanics. It made it possible to obtain solutions to a large class of nonlinear problems with acceptable accuracy.

J.T. Oden [40, 41] extended the elastic theory of finite elements to the hyper-elastic and visco-elastic field.

In 1968, H.D. Hibbitt, D.V. Marcal and J.R. Rice [42] first introduced hypo-elastic formulation into the finite element analysis. They adopted the incremental theory based on a Lagrangian reference frame and their formulation is suitable for large strain and large displacement response. In their work, they used a linear relation between the Jaumann stress increments and increments of the deformation tensor which are invariant with respect to rigid body rotation. The formulation for small strain and large rotation approximation is also proposed in their work.

Needleman [43] derived similar finite element equations from variational principles given by Hill [44]. The work is also based on the Lagrangian formulation.

The Eulerian formulation which is based on the current configuration has been used by Yaghmai and Popov [45]. They derived the equations by means of variational principles and

solved some elastic and elastic-plastic problems. Similar work was done by Gunasekera and Alexander [46]. They gave their equations for Prandtl-Reuss plastic materials and derived the equations from the principle of virtual work.

In 1974, R.M. McMeeking and J.R. Rice [47] introduced Eulerian finite element formulation for large elastic-plastic flow, which is parallel to the treatment of [42]. The method is based on Hill's variational principle for incremental deformations. It is ideally suited for isotropically hardening Prandtl-Reuss materials.

T.Y. Chang and K. Sawamiphakdi [38] adopted the hypoelastic theory to the degenerated 3-D isoparametric element for laminated anisotropic shells. The nonlinear geometric stiffness matrix which is based on Lagrangian description was developed and some example problems were presented.

Generally, the Newton-Raphson integration method is used to achieve the correct equilibrium positions in the nonlinear finite element computations. However, it is no longer appropriate to use it in establishing post buckling response. The reason is that the stiffness matrix tends to be singular resulting in an increasing number of iterations. Finally, the result will diverge at the critical point. In order to overcome these problems and to trace the response beyond the critical point, several efficient methods have been developed [48, 49].

Bergan [50] introduced the 'current' stiffness parameter' to guide the equilibrium iterations. When the parameter reaches the prescribed value, the execution of iterations stops. At that time, the displacement continues to increase until a new parameter value is reached. This means that the iterations are suppressed near the critical point. The algorithm of this method is simple and the program is easy to develop from the Newton-Raphson method. The drawback is that the load step in the neighborhood of the critical point need still be small.

Argyris [52] and several other researchers introduced the displacement control method. In this scheme, a single displacement component is selected as a control parameter and the corresponding load level is considered to be unknown. In the initial paper, the symmetry of the

stiffness matrix is damaged. The method, then, was improved as a two step method [52, 53], in order to preserve the symmetry of the stiffness matrix. The displacement control method is relatively widely used since it is both efficient and easy to control. The limitation of this method is that it will fail whenever the structure snaps back from one load level to a lower one.

Riks [54, 55], and Wempner [56] independently introduced the constant-arc-length method. The load increment in this method is confined by the equation of arc length. The increments of load and displacement vector are mixed. The final equilibrium position is located by continuing drawing a normal plane to the new tangent of the load-displacement curve. Generally speaking, this method is efficient in the entire load range and can be applied to all possible nonlinear structural responses.

Crisfield [57, 58] further modified Riks' method. He introduced line searches into the constant-arc-length algorithm. In addition, he developed a scheme in which a single parameter is employed to accelerate the speed of convergence using the line search concept. His work makes Riks' method more efficient and also much easier for programming.

2. SUMMARY OF WORK

The progress made and the work performed have been elaborated upon in an interim scientific report submitted to the sponsor in late 1986, and in a series of semiannual progress reports. The most recent of these is dated October 1989.

2.1 Traditional Approach

Following a traditional approach, a method was developed for bounding the response of problems of viscoelastic material behavior, based on nonlinear kinematic behavior. Upper and lower bounds are established through bounding of the convolution integral of the governing nonlinear Volterra-type integral equation. Details of the method can be found in the first paper of Appendix A.

11

Next, a differential (as opposed to integral) methodology for solution of one-dimensional, kinematically nonlinear, visoelastic problems was developed. Using the example of an eccentrically loaded cantilever beam-column, the results from the differential formulation were compared to the results obtained from the integral solution technique. The details of this are found in the second paper of Appendix A. This paper also includes a discussion of the various factors affecting the numerical accuracy and rate of convergence of the two procedures. Moreover, the influences of some "higher order" effects, such as straining along the centroidal axis, are also discussed.

Finally, an analytic study of beams and arches subjected to significant thermal cycling from ambient temperatures up to 800°C is presented. In this study, Walker's [9] unified nonlinear hereditary type of viscoelastoplastic constitutive law is employed to characterize the time-and temperature-dependent properties of a typical aerospace alloy, Hastelloy X.

The details are given in the third paper of Appendix A. A shorter version of this paper was published in the ASME Journal of Engineering Materials and Technology (January 1990 issue). The PVP-Vol. 153 version is made part of this report, because it contains more detail.

2.2 Novel Approach

A complete true ab-initio rate theory of kinematics and kinetics for continuum and curved thin structures, without any restriction on the magnitude of the strains or the deformation, was formulated. The time dependence and large strain behavior are incorporated through the introduction of the time rate of the metric and curvature in two coordinate system; a fixed (spatial) one and a convected (material) coordinate system. The relations between the time derivative and the covariant derivatives (gradients) have been developed for curved space and motion, so that the velocity components supply the connection between the equations of motion and the time rate of change of the metric and curvature tensors.

The metric tensor (time rate of change) in the convected material coordinate system is linearly decomposed into elastic and plastic parts. In this formulation, a yield function is assumed,

12

which is dependent on the rate of change of stress, metric, temperature, and a set of internal variables. Moreover, a hypoelastic law was chosen to describe the thermoelastic part of the deformation.

A time and temperature dependent viscoplastic model was formulated in this convected material system to account for finite strains and rotations. The history and temperature dependence were incorporated through the introduction of internal variables. The choice of these variables, as well as their evolution, was motivated by phenomenological thermodynamic considerations.

The nonisothermal elastic-viscoplastic deformation process was described completely by "thermodynamic state" equations. Most investigators (in the area of viscoplasticity) employ plastic strains as state variables. Our study shows that, in general, use of plastic strains as state variables may lead to inconsistencies with regard to thermodynamic considerations. Furthermore, the approach and formulation employed by all previous investigators lead to the condition that all plastic work is completely dissipated. This, however, is in contradiction with experimental evidence, from which it emerges that part of the plastic work is used for producing residual stresses in the lattice, which, when phenomenologically considered, causes hardening. Both limitations are not present in our deformation, because of the inclusion of the "thermodynamic state" equations.

The obtained complete rate field equations consist of the principles of the rate of the virtual power and the rate of conservation of energy, of the constitutive relations, and of boundary and initial conditions. These formulations provide a sound basis for the formulation of the adopted finite element solution procedures.

The derived shell theory, in the least restricted form, before any simplifying assumptions are imposed, has the following desirable features:

(a)   The two-dimensional, impulse-integral form of the equations of motion and the Second Law of Thermodynamics (Clausius-Duhem inequality) for a shell follow naturally and exactly from their three-dimensional counterparts.

13

(b)   Unique and concrete definitions of shell variables such as stress resultants and couples, rate of deformation, spin and entropy resultants can be obtained in terms of weighted integrals of the three-dimensional quantities through the thickness.

(c)   There are no series expansions in the thickness direction.

(d)   There is no need for making use of the Kirchhoff Hypotheses in the kinematics.

(e)   All approximations can be postponed until the descretization process of the integral forms of the First Law of Thermodynamics.

(f)   A by-product of the descent from three-dimensional theory is that the two-dimensional temperature field (that emerges) is not a through-the-thickness average, but a true point by point distribution. This is contrary to what one finds in the literature concerning thermal stresses in the shell.

To develop geometrically nonlinear, doubly curved finite shell elements the basic equations of nonlinear shell theories have to be transferred into the finite element model. As these equations in general are written in tensor notation, their implementation into the finite element matrix formulation requires considerable effort.

The nonlinear element matrices are directly derived from the incrementally formulated nonlinear shell equations, by using a tensor-oriented procedure. The classical thin shell theory based on the Kirchoff-Love hypotheses (Formulation D) was employed for this purpose. For this formulation, we are using the "natural" degrees of freedom per midsurface shell node: three incremental velocities and the rates of rotation about the material coordinates in a mixed form.

The quasi-linear nature of the principle of the rate of virtual power suggests the adoption of an incremental approach to numerical integration with respect to time. The availability of the field formulation provides assurance of the completeness of the incremental equations and allows the use of any convenient procedure for spatial integration over the domain V. In the present instance, the choice has been made in favor of a simple first order expansion in time for the construction of

14

incremental solutions from the results of finite element spatial integration of the governing equations.

The procedure employed permits the rates of the field formulation to be interpreted as increments in the numerical solution. This is particularly convenient for the construction of incremental boundary condition histories.

Even under the condition of static external loads and slowly growing creep effects, the presence of snap-through buckling makes the inertia effects significant. In dynamic analyses, the applied body forces include inertia forces. Assuming that the mass of the body considered is preserved, the mass matrix can be evaluated prior to the time integration using the initial configuration.

Finite element solution of any boundary-value problem involves the solution of the equilibrium equations (global) together with the constitutive equations (local). Both sets of equations are solved simultaneously in a step by step manner. The incremental form of the global and local equations can be achieved by taking the integration over the incremental time step $t=t_{j+1}-t_j$. The rectangular rule has been applied to execute the resulting time integration.

Clearly, the numerical solution involves iteration. A simplified version of the Riks-Wempner constant-arch-length method has been utilized. This iteration procedure which is a generalization of the displacement control method also allows to trace the nonlinear response beyond bifurcation points. In contrast to the conventional Newton-Raphson techniques, the iteration of the method takes place in the velocity and load rate space. The load step of the first solution in each increment is limited by controlling the length ds of the tangent. Either the length is kept constant in each step or it is adapted to the characteristics of the solution. In each step the triangular-size stiffness matrix has to be checked for negative diagonal terms, indicating that a critical point is reached.

The study is limited only to the simplest of the developed shell theory formulations (Formulation D).

15

The various shell theory approximations (formulations) are based on the use of certain simplifying assumptions regarding the geometry and kinematics of the shell configuration. These are:

Assumption I: The material points which are on the normal to the reference surface before deformation will be on the same normal after deformation.

Assumption II: The shell is sufficiently thin so that we can assume linear dependence of the position of any material point (in the deformed state) to the normal (to the reference surface) coordinate (in the deformed state). The linear dependence can easily be changed to parabolic, cubic, or any desired degree of approximation.

Assumption III: The rate of change of the velocity gradients with respect to in-plan coordinates on the two bounding shell surfaces is negligibly small.

Assumption IV; The rate of change of the distance of a material from the reference surface is negligibly small.

On the basis of the above four simplifying assumptions, several formulations result, for the analysis of thin shells. These formulations are denoted below by capital letters.

Formulation A: This formulation makes use of Assumption I, only.

Formulation B: This formulation employs Assumptions I and II.

Formulation C: This formulation employs Assumption I, II and III.

Formulation D: This is the classical thin shell theory based on the Kirchoff-Love hypotheses of Assumptions I, II, III, IV, as applied to large deformation theory.

These formulations are arranged in such a manner that we move from the least restrictive (A) to the most restrictive (D).

In addition to this, a fifth formulation (E) can easily be devised and this formulation in terms of order of restriction is similar to Formulation A. Formulation E makes use of Assumption II only.

Three papers are included as Appendix B. These papers reflect the work associated with the novel approach and provide detail in formulation as well as in application.

3. <u>PUBLICATIONS AND PRESENTATIONS</u>

Several presentations and publications resulted from this project. Moreover, two Ph.D. students were supported (one has already received the degree, the second is expected to complete the requirements by the end of 1990), as well as one postdoctoral fellow and three faculty members (Drs. R.L. Carlson, R. Riff and G.J. Simitses) of the Georgia Institute of Technology.

A list of the presentations and publications is given below:

3.1 Presentations

1. "Thermodynamically Consistent Constitutive Equations for Nonisothermal, Large Strain, Elasto-Plastic Creep Behavior," 26th AIAA/ASME/ASCE/AHS Structures Structural Dynamics and Materials Conference, Orlando, FL., April 14-17, 1985.

2. "Dynamic Creep Buckling: Analysis of Shell Structures Subjected to Time-Dependent Mechanical and Thermal Loading," NASA Conference on Structural Integrity and Durability of Reusable Space Propulsion Systems, Cleveland, OH., June 4-5, 1985.

3. "Bounding Solutions of Geometrically Nonlinear Viscoelastic Problems," 27th Structures, Structural Dynamics and Materials Conference, San Antonio, TX, May 4-6, 1986.

4. "Dynamic Analysis of Shell Structures Subjected to Mechanical and Thermal Loading," AFOSR/ARO Conference on Non-Linear Vibrations, Stability, and Dynamics of Structures and Mechanisms, Blacksburg, VA, March 23-25, 1987.

5. "Solution Methods for One-Dimensional Nonlinear Viscoelastic Problems," 28th AIAA/ASME/ASCE/AHS Structures, Structural Dynamics and Materials Conference, Monterey, CA, April 6-8, 1987.

6. "Non-Isothermal Elastoviscoplastic Snap-Through and Creep Buckling of Shallow Arches," 28th AIAA/ASME/ASCB/AHS Structures, Structural Dynamics and Materials Conference, Monterey, CA, April 6-8, 1987.

7. "Creep Analysis of Beams and Arches Based on a Hereditary Visco-Elastic-Plastic Law," ASME Winter Annual Meeting, Chicago, IL., Nov. 28-Dec. 2, 1988.

8. "Non-Isothermal Buckling Behavior of Viscoplastic Shell Structures," 30th AIAA/ASME/ASCE/AHS/AS C Structures, Structural Dynamics and Materials Conference, Mobile, AL, April 3-5, 1989.

3.2 Publications

1. "Bounding Solutions of Geometrically Nonlinear Viscoelastic Problems," AIAA J., Vol. 11, 1986, pp 1843-1850; also in Proceedings of AIAA/..../AHS 27th S.D.M. Conference, Part 1, 1986, pp 343-352 (J. Stubstad and G.J. Simitses).

2. "Thermodynamically Consistent Constitutive Equations for Non-Isothermal Large Strain, Elasto-Plastic, Creep Behavior," AIAA J., Vol. 25, No. 1, 1987, pp. 114-122 (R. Riff, R.L. Carlson and G.J. Simitses).

3. "Solution Methods for One-Dimensional Viscoelastic Problems," AIAA J., Vol. 26, No. 9, 1988, pp 1127-1134 (J. Stubstad and G.J. Simitses)

4. "Non-Isothermal Elastoviscoplastic Snap-Through and Creep Buckling of Shallow Arches," AIAA J., Vol. 27, No. 8, 1990, pp. 1110-1115 (R. Riff).

5. "Creep Analysis of Beams and Arches Based on a Hereditary Visco-Elastic-Plastic Law," J. Engng. Mat'ls and Technology, To be Published. (J. Stubstad and G.J. Simitses).

6. "Non-Isothermal Buckling Behavior of Viscoplastic Shell Structures," AIAA Paper, AIAA-89-1315 (R. Riff).

7. "Dynamic Creep Buckling: Analysis of Shell Structures Subjected to Time-Dependent Mechanical and Thermal Loading," NASA Conference Publication No. 2381, 1985, pp. 117-120.

4. REFERENCES

1. Zienkiewicz, O.C. and Cormeau, I.C., "Visco-Plasticity-- Plasticity and Creep in Elastic Solids-- A Unified Numerical Approach", International Journal for Numerical Methods in Engineering, Vol. 8, 1974, pp. 821-845.

2. Allen, D. H. and Haisler, W.E., "A Theory for Analysis for Thermoplastic Materials," Computers and Structures. Vol. 13, 1981, pp. 129-135.

3. Haisler, W.E. and Cronenworth, J., "An Uncoupled Viscoplastic Constitutive Model for Metals at Elevated Temperature," AIAA/ASME/ASCE/AHS 24th Structure, Structural Dynamics and Materials Conference, Collection of Technical Papers, Part 1, 1983, pp. 664-673.

4. Yamada, Y. and Sakurai, T., "Basic Formulation and a Computer Program for Large Deformation Analysis," Pressure Vessel Technology, Part I, ASME, 1977, pp. 342-352.

5. Walker, K.P., "Representation of Hastelloy-X Behavior at Elevated Temperature with a Functional Theory of Viscoplasticity," Proceedings of ASME Pressure Vessels Conference, San Francisco, August 12, 1980.

6. Cernocky, E.P. and Krempl, E., "A Nonlinear Uniaxial Integral Constitutive Equation Incorporating Rate Effects, Creep and Relaxation", International Journal of Nonlinear Mechanics, Vol. 14, 1979, pp. 183-203.

7. Valanis, K.D., "Some Recent Developments in the Endochronic Theory of Plasticity--The Concept of Internal Barriers," in Constitutive Equations in Viscoplasticity: Phenomenological and Physical Aspects, AMD Vol. 21, 1976, pp. 15-32.

8. Chaboche, J.L., "Thermodynamic and Phenomenological Description of Cyclic Viscoplasticity with Damage," European Space Agency Technical Translation Service, Publication No. ESA-TT-548, May 1979.

9. Walker, K.P., "Research and Development Program for Nonlinear Structural Modding with Advanced Time-Temperature Dependent Constitutive Relationships," NASA Contract Report, NASA CR 165533, 1981.

10. Chan, K.S., Bodner, S.R., Walker, K.P., and Lindholm, U.S., "A Survey of Unified Constitutive Theories," NASA Contract Report, NASA CR 23925, 1984.

11. Bodner, S.R., Partom, I., and Partom, Y., "Uniaxial Cyclic Loading of Elastic-Viscoplastic Materials," Journal of Applied Mechanics, Vol. 46, 1979, pp. 805-810.

12. Miller, A.K., "Modelling Cyclic Plasticity with Unified Constitutive Equations: Improvements in Simulating Normal and Anomalous Bauschinger Effects," Journal of Engineering Materials and Technology, Vol. 102, 1980, pp. 215-222.

13. Krieg, R.D., Swearengen, J.C., and Rodhe, R.W., "A Physically-Based Internal Variable Model for Rate-Dependent Plasticity," Proceedings ASME/CSME PVP Conference, 1978, pp. 15-27.

14. Hart, E.W., "Constitutive Relations for the Nonelastic Deformation of Metals," ASME Journal Engineering Material and Technology, Vol. 98, 1976, pp. 193-202.

15. Lee, D., and Zavrel, F., Jr., "A Generalized Strain Rate Constitutive Equation for Anisotropic Metals," Acta Metallurgica, Vol. 26, 1978, pp. 1771-1780.

16. Hill, R., "A General Theory of Uniqueness and Stability in Elastic-Plastic Solids," J. Mechanics and Physics of Solids, Vol. 6, 1978, pp. 236-249.

17. Coleman, B.D., and Gurtin, M.E., "Thermodynamics of Material with Memory, Archives for Rational Mechanics and Analysis, Vol. 17, 1966, pp. 1-46.

18. Coleman, B.D., and Gurtin, M.E., "Thermodynamics with Internal State Variables," Journal of Chemical Physics, Vol. 47, 1967, pp. 597-613.

19. Lubliner, J., "On the Thermodynamic Foundation of Non-Linear Solid Mechanics," International Journal of Non-Linear Mechanics, Vol. 7, 1972, pp. 237-254.

20. Perzyna, P., "Internal Variable Description of Plasticity," in Problems of Plasticity, Ed. A. Sawczuk, 1974, pp. 145-176.

21. Botros, F.R., and Bieniek, M.P., "Creep Buckling of Structures," 24th AIAA/ASME/ASCE/AHS Structures, Structural Dynamics and Materials Conference, May 1983, Paper No. 33-0864.

22. Hoff, N.J., "Creep Buckling of Plates and Shells," Proceedings, 13th Int. Congr. of Theor. and Appl. Mech., Springer Verlag, 1973.

23. Wojewodzki, W., and Bukowski, R., "Influence of the Yield Function Nonlinearity and Temperature in Dynamic Buckling of Viscoplastic Cylindrical Shells," J. of Applied Mechanics, Vol. 51, March 1984, pp. 114-120.

24. Bukowski, R., and Wojewodzki, W., "Dynamic Buckling of Viscoplastic Spherical Shells," Int. J. Solids Structures, Vol. 20, No. 8, pp. 761-776.

25. Atkatsh, R.S., Bienek, M.P., and Sandler, I.S., "Theory of Viscoplastic Shells for Dynamic Response," J. of Applied Mechanics, Vol. 50, March 1983, pp. 131-136.

26. Saigal, S., and Yang, T.Y., "Elastic-Viscoplastic, Large Deformation Formulation of a Curved Quadrilateral Thin Shell Element," Int. J. for Numerical Methods in Engng., Vol. 21, 1985, pp. 1987-1909.

27. Lee, E.H., "Elastic-Plastic Deformation at Finite Strains," J. Appl. Mech., Vol. 36, 1969.

28. Mandel, J., "Plasticite Classique et Viscoplasticite",. Cours au C.I.S.M., Udine, 1972.

29. Germain, P., "Cours de Mecanique des Milieux Continus," Masson, Paris, 1973.

30. Truesdell, C.A., The Elements of Continuum Mechanics, Springer-Verlag, New York, 1966.

31. Sidoroff, F., "Incremental Constitutive Equations for Large Strain Elasto-Plasticity," Int. J. Eng. Sci. Vol. 20, No. 1, 1982, pp. 19-24.

32. Stoltz, C., "Contribution a L'Etude des Grandes Transformations en Elastoplasticite," These de Docteur-Ingenieur, Paris, 1982.

33. Simitses. G.J., "Buckling and Postbuckling of Imperfect Cylindrical Shells: A Review," Appl. Mech. Rev. Vol. 39, 1986, pp. 1517-1524.

34. Donnell, L.H., "A New Theory for the Buckling of Thin Cylinders under Axial Compression," Trans. ASME, Vol. 56, pp 795-800.

35. Sanders, J.L., "Nonlinear Theories for Thin Shells," Quart. Appl. Math., Vol. 21, 1963, pp. 21-36.

36. Ahmad, S., Irons B.M. and Zienkiewicz, O.C., "Analysis of Thick and Thin Shell Structures by Curved Finite Element," Int'l J. Num. Meth. Engng., Vol. 2, 1970, pp. 419-451.

37. Ramm, E., "A Plate/Shell Element for Large Deflections and Rotations," in Formulations and Computational Algorithms in Finite Element Analysis, Edited by K.J. Bathe, J.T. Oden and W. Wunderlick, M.I.T. Press, Cambridge, Mass. (1977), pp. 264-293.

38. Chang, T.Y. and Sawamiphakdi, K., "Large Deformation Analysis of Laminated Shells by Finite Element Method," Computers and Structures, Vol. 13, 1981, pp. 331-340.

39. Oden, J.T., "On a Generalization of the Finite Element Concept and Its Applications to a Class of Problems in Nonlinear Viscoelasticity," Developments in Theoretical and Applied Mechanics, Vol. IV. Pergamon Press, 1968 (Proc. Fourth South Eastern Conf. on Theoretical and Applied Mechanics, March 1968).

40. Oden, J.T. and Key, J.E., "Numerical Analysis of Finite Axisymmetric Deformations of Incompressible Elastic Solids of Revolution," Int. J. Solids Struct., Vol. 5, 1970, pp. 497-518.

41. Hibbitt, H.D., Marcal, P.V. and Rice, J.R., "A Finite Element Formulation For Problems of Large Strain and Large Displacement," Int. J. Solids Struct., Vol. 6, 1970, pp. 1069-1086.

42. Needleman, A., "A Numerical Study of Necking in Circular Cylindrical Bars," J. Mech. Phys. Solids Vol. 20, 1972, pp. 111-117.

43. Hill, R., "Some Basic Principles in the Mechanics of Solids Without Natural Time," J. Mech. Phys Solids Vol. 7, 1959, pp. 209-214.

44. Yaghmai, S. and Popov, E.P., "Incremental Analysis of Large Deflections of Shells of Revolution," Int. J. Solids Struct., Vol. 7, 1971, pp. 1375-1379.

45. Gunasekera, J.S. and Alexander, J.M., "Matrix Analysis of the Large Deformation of an Elastic-plastic Axially Symmetrical Continuum," Proceedings of Symposium on Foundations of Plasticity, Noordhoff, Leyden, 1973.

46. McMeeking, R.M. and Rice, J.R., "Finite-Element Formulations for Problems of Large Elastic-Plastic Deformation," Int. J. Solids Struc., Vol. 11, 1975, pp. 601-616.

47. Bathe, K.J. and Cimento, A.P., "Some Practical Procedures for the Solution of Nonlinear Finite Element Equations," Computer Methods in Applied Mechanics and Engineering. Vol. 22, 1980, pp. 59-85.

48. Ramm, E., "Stratages for Tracing Non-linear Responses Near Limit Points," in Non-linear Finite Element Analysis in Structural Mechanics. (Eds. W. Wunderlich, E. Stein and K.J. Bathe), Springer-Verlag, New York, 1981, pp. 63-89.

49. Bergan, P.G., "Solution Algorithms for Nonlinear Structural Problems," Int. Conf. on Engng. Appl. of the F.E. Method, Norway, 1979.

50. Argyris, J.H., "Continua and Discontinua," Matrix Mech. and Struct. Mech., Wright-Patterson, Ohio, 1965, pp. 11-189.

51. Pian, T.H. and Tong, P., "Variational Formulation of Finite Displacement Analysis," High Speed Computing for Elastic Structures, Liege, 1970, pp. 43-63.

52. Zinkiewicz, O.V., "Incremental Displacement in Non-Linear Analysis," Int. J. Num. Meth. Eng., Vol. 3, 1971, pp. 587-588.

53. Riks, E., "The Application of Newton's Method to the Problem of Elastic Stability," J. Appl. Mech., Vol. 39, 1972, 1060-1066.

54. Riks, E., "Some Computational Aspects of the Stability Analysis of Nonlinear Structures, " Computer Methods in Appl. Mech. Eng., Vol. 47, 1984, pp. 219-259.

55. Wempner, G.A., "Discrete Approximation Related to Nonlinear Theories of Solids," Int. J. Solids Struct., Vol. 7, 1971, pp. 1581-1599.

56. Crisfield, M.A., "An Arc-Length Method Including Line Search and Accelerations," Int. J. Num. Meth. Eng., Vol. 19, 1983, pp. 1269-1289.

57. Crishfield, M.A., "A Fast Incremental/Iterative Solution Procedure That Handles 'Snap-Through'," Computers and Structures, Vol. 13, 1981, pp. 55-62.

APPENDIX A

Traditional Approach Papers

Bounding Solutions of Geometrically Nonlinear Viscoelastic Problems

John M. Stubstad* and George J. Simitses†
Georgia Institute of Technology, Atlanta, Georgia

A method is presented for bounding solutions to problems of linear viscoelastic material behavior formulated using nonlinear kinematic measures of deformation. Upper and lower bounds are established through bounding of the convolution integral of the governing nonlinear Volterra-type integral equation. A significant feature of the manner in which these bounding solutions are generated is that time may be treated as a parameter, thereby casting the bounding solutions into a quasielastic context. Consequently, numerical evaluation is simplified since the necessity of continually approximating convolution integrals of the deformation history, required for exact solution, is eliminated. This, in turn, results in a substantial reduction in the computational effort required for numerical evaluation. In one of the example problems considered, this reduction translates into more than a thirtyfold difference in computer time needed for determination of the exact and bounding solutions. Application of the bounding technique is demonstrated through two examples and includes a limited comparison with some recently published experimental data.

Nomenclature

a	= load eccentricity
E_1, E_2	= elastic constants of ideal viscoelastic material
$g(s,u)$	= Green's function for the spatial integrals
I	= moment of inertia
$J(t)$	= creep compliance
$\mathcal{J}(p)$	= Laplace transform of creep compliance
$k(t-\tau)$	= generic kernel of convolution integral
$K(t)$	= integrated form of $k(t-\tau)$
L	= length of beam
$\mathcal{L}_p$	= Laplace transform operator
$M(s',\tau)$	= bending moment at position s' and time τ
p	= Laplace transform variable
P	= time-independent load
P_E	= Euler load
$R(t)$	= time-dependent load
s',s	= dimensional and nondimensional distance along the beam, respectively
t,τ	= time
x,y	= spatial coordinates
$\alpha(\tau)$	= angle of rotation of the end of the cantilever column
$\Delta(\tau), \delta(\tau)$	= lateral and transverse deflection of the end of the beam, respectively
η_1	= viscous coefficient of ideal viscoelastic material
$\theta(s,t)$	= generic representation of a spatial integral
$\kappa(s',t)$	= curvature at position s' and time t
λ	= scalar parameter
μ	= relaxation constant of ideal viscoelastic material
$\varphi(s',\tau)$	= angle of rotation of the cantilever at position s' and time τ
$\Phi(s',p)$	= Laplace transform of angle of rotation

Subscripts

qe	= quasielastic solution
ub, lb	= upper and lower bounds, respectively

Introduction

INTEGRAL transform techniques, such as the Laplace transform, provide simple and direct methods for solving viscoelastic problems formulated within a context of linear material response and using linear measures for deformation. Application of the transform operator reduces the governing linear integrodifferential equations to a set of algebraic relations between the transforms of the unknown functions, the viscoelastic operators, and the initial and boundary conditions. Inversion, either directly or through the use of the appropriate convolution theorem, provides the time domain response, once the unknown functions have been expressed in terms of sums, products, or ratios of known transforms. When exact inversion is not possible, approximate techniques, such as suggested by Schapery,[1] may provide accurate results.

The overall problem becomes substantially more complex when nonlinear effects must be included. We consider here situations where a linear material constitutive law can still be productively employed, but where the magnitude of the resulting time-dependent deformations warrants the use of a nonlinear kinematic analysis. The governing equations will be nonlinear integrodifferential equations for this class of problems. Thus, traditional as well as approximate techniques, such as cited above, cannot be employed since the transform of a nonlinear function is not explicitly expressible.

Rogers and Lee[2] considered such a problem in an investigation of the finite deflection of a viscoelastic cantilever beam. Employing an analogy of an associated elastic problem, they derived a solution to the viscoelastic problem in a form involving a time convolution of a nonlinear space and time-dependent integral function. Numerical evaluation was accomplished using Picard's method of successive substitutions. Newton-Coates quadratures were employed to approximate the spatially dependent integral relationship; a mean-value-based finite-difference formula was used for the time convolution.

Solution procedures of this type are generally well suited for computer implementation. However, they can become

computationally inefficient when the response must be determined over an extended time period. Each increment in time requires a reevaluation of the convolution integrals. Thus, the entire deformation history must be retained in memory during the calculations. Since each completed set of computations adds another set of results to this history, this generates an ever-increasing memory requirment. In addition, the total number of computations performed during each succeeding iteration also increases.

In this regard, an approximation technique proposed by Schapery[3] can provide an attractive alternative. Commonly referred to as the *quasielastic* approximation, it has most recently been employed by Vinogradov[4] and Vinogradov and Wijeweera[5] in studies of the behavior of eccentrically loaded viscoelastic cantilever columns.

The method is based on the observation that the solution procedure developed by Rogers and Lee[2] may be interpreted as a sequence of short-time interval quasielastic solutions. This suggests that approximate solutions may be generated by replacing the original viscoelastic problem by an "equivalent" time-dependent elastic one. In this replacement problem, the elastic properties are equated to the instantaneous values of the relaxation moduli or creep compliances of the viscoelastic material.

The inherent numerical advantage provided by this technique is that it eliminates the potentially inefficient calculation of convolution integrals. Thus, the speed and efficiency at which the time-dependent response is calculated is independent of elapsed time. The obvious potential disadvantage is that, since it is an approximation, significant differences may exist between the actual response of the viscoelastic body and those predicted quasielastically. In addition, the quasielastic method does not provide a direct method for assessing whether any errors incurred are conservative.

In this paper, we present an approximation technique that provides both upper- and lower-bound predictions for the class of viscoelastic problems under consideration. From these bounds, one may readily deduce when the approximation provides sufficiently accurate results or when more involved techniques must be used. Finally, we demonstrate that solutions for this class of viscoelastic problems can be accomplished within a Laplace transform context, even though the transformed functions cannot be expresssed as explicit functions of the transform variable.

Preliminaries

As a motivation for the development, consider an integral equation of the form

$$\varphi(x,t) = \lambda \int_0^t k(t-\tau)\theta(x,\tau)d\tau \qquad (1)$$

where $\varphi(x,\tau)$ and $\theta(x,\tau)$ may be scalar, vector, or tensor functions of position vector x and time τ. We shall assume that the kernel $k(\tau)$ is positive semidefinite over the range of integration and λ is some scalar parameter. In addition, we assume that $k(\tau)$, $\varphi(x,\tau)$, $\theta(x,\tau)$, and their first partial derivatives with respect to τ are continuous over the interval $0^+ \leq \tau \leq t$. Finally, we assume that $\varphi(x,\tau)$ and $\theta(x,\tau)$ are continuous with respect to x over some closed domain D and possess continuous first and second partial derivatives with respect to x over at least the interior of the domain.

For the class of problems under consideration, the function $\theta(x,\tau)$ represents a spatial integral in which $\varphi(x,\tau)$ appears in the integrand in a nonlinear manner. Depending upon the boundary conditions, $\theta(x,\tau)$ may also include additive nonlinear forms of $\varphi(x,\tau)$. Thus, Eq. (1) may be viewed as a Volterra-type integral equation of the second kind.

Let us assume that, even before specific solutions have been generated, we are able to infer some information about the general manner in which $\theta(x,\tau)$ behaves. Suppose, for

example, that $\theta(x,\tau)$ represents some measure of deflection which (we deduce) must be a nondecreasing function with respect to time. Thus, over the interval $0^+ \leq \tau \leq t$, this would imply

$$\theta(x,0^+) \leq \theta(x,\tau) \leq \theta(x,t) \qquad (2)$$

This suggests that if we establish the approximate solutions

$$\varphi_{lb} = \lambda \int_0^t k(t-\tau)\theta(x,0^+)d\tau \qquad (3a)$$

$$\varphi_{ub} = \lambda \int_0^t k(t-\tau)\theta(x,t)d\tau \qquad (3b)$$

where subscripts ub and lb denote upper and lower bounds, respectively, we can then define difference functions $\Delta\varphi_{lb}$ and $\Delta\varphi_{ub}$ by

$$\Delta\varphi_{lb} = \varphi(x,t) - \varphi_{lb} \qquad (4a)$$

$$\Delta\varphi_{ub} = \varphi_{ub} - \varphi(x,t) \qquad (4b)$$

Then substitution of Eqs. (1) and (3) into Eq. (4) yields

$$\Delta\varphi_{lb} = \lambda \int_0^t k(t-\tau)[\theta(x,\tau) - \theta(x,0^+)]d\tau \qquad (5a)$$

$$\Delta\varphi_{ub} = \lambda \int_0^t k(t-\tau)[\theta(x,t) - \theta(x,\tau)]d\tau \qquad (5b)$$

As a direct consequence of Eq. (2), the quantities enclosed by square brackets in Eqs. (5) must be positive semidefinite for all values of time τ. Because both $\theta(x,0^+)$ and $\theta(x,t)$ are constant with respect to τ, the square bracket terms must be continuous in τ since, by prior assumption, $\theta(x,\tau)$ is continuous in τ. Thus, for a continuous and positive semdefinite kernel, the integrand is continuous and positive semidefinite over the entire range of integration. Consequently, for positive λ, the differences $\Delta\varphi_{lb}$ and $\Delta\varphi_{ub}$ must be positive for all time. Therefore, the approximate solution φ_{ub} must represent an upper bound for the exact solution. Similarly, φ_{lb} must inherently bound the exact solution from below.

The numerical advantages provided by working with the bounding functions are easily demonstrated. Letting

$$K(t) = \lambda \int_0^t k(t-\tau)d\tau \qquad (6)$$

and noting that $\theta(x,0^+)$ and $\theta(x,t)$ are independent of τ imply that Eqs. (3) have the form

$$\varphi_{lb} = K(t)\theta(x,0^+) \qquad (7a)$$

and

$$\varphi_{ub} = K(t)\theta(x,t) \qquad (7b)$$

Thus, the time convolution of the exact solution [Eq. (1)] has, in the bounding formulation, been replaced by a format in which time appears only as a parameter. Consequently, numerical solution of Eqs. (7) requires integration only over the spatial coordinates, whereas the exact solution requires both spatial and temporal integrations.

The preceding development was based upon the assumption that $\theta(x,\tau)$ was a nondecreasing function with respect to time. The technique is easily adapted to cases where $\theta(x,\tau)$ is a nonincreasing function. Thus, if

$$\theta(x,0^+) \geq \theta(x,\tau) \geq \theta(x,t) \qquad (8)$$

we can replace Eqs. (3) with

$$\varphi_{lb} = \lambda \int_0^t k(t-\tau)\theta(x,t)d\tau \qquad (9a)$$

and

$$\varphi_{ub} = \lambda \int_0^t k(t-\tau)\theta(x,0^+)d\tau \qquad (9b)$$

Thereafter, proceeding as before generates the desired bounding behavior. In a similar manner, a simple series of modifications to the definitions of the bounding functions are needed when λ is a negative rather than positive scalar.

Applications of the bounding technique, including comparisons with exact solutions, are provided in the following sections.

Applications

End-Loaded Cantilever Beam

As noted earlier, Rogers and Lee[2] developed the first, and a numerically exact, solution for the problem of an end-loaded linearly viscoelastic cantilever beam. The solution, in the general form of Eq. (1), was evaluated by employing Newton-Coates quadratures for the spatially dependent integral function $\theta(x,\tau)$ and a mean value based finite-difference formula for the convolution with $k(t-\tau)$. Several years later, Schapery,[3] in a paper describing the quasielastic method, presented an approximate solution for this problem. Since this approximate solution was in the form of Eqs. (7), Schapery was able to generate numerical results directly from the elastic analysis presented in Ref. 2. Thus, his solution required only numerical evaluation of a spatially dependent integral equation with time treated as a parameter.

Here, we analyze the same problem using the bounding procedure. It is demonstrated that Schapery's approximate solution is, in fact, a lower-bound solution for a suitably restricted range of deformation. In addition, it is shown that a reasonably close upper-bound solution may be readily obtained.

Derivation of the governing integrodifferential equation is documented in Ref. 2 and thus only summarized here. The beam is assumed to be thin and composed of a linearly viscoelastic material. Its geometry in the deformed configuration is illustrated in Fig. 1. The loading is assumed to be applied quasistatically and thus inertia terms are neglected.

Reference line extensional strains are assumed to be negligibly small. Thus, a coordinate s' is employed to specify position in both the initial and the deformed states. A non-dimensional coordinate s is defined by dividing s' by the beam length L. Assuming a linear distribution of strains through the depth, bending thus occuring within a Bernoulli-Euler context, results in the moment-curvature relationship given by

$$\kappa(s',t) = \left(\frac{1}{I}\right)\int_{-\infty}^t J(t-\tau)\left[\frac{\partial M(s',\tau)}{\partial \tau}\right]d\tau \qquad (10)$$

where $\kappa(s',t)$ denotes the curvature and $M(s',\tau)$ the bending moment at location s'. I is the moment of inertia of the beam and $J(t)$ the creep compliance of the material. The moment at position s' is given by

$$M(s',\tau) = R(\tau)[L-x(s',\tau)-\Delta(\tau)] \qquad (11)$$

where $R(\tau)$ is the end load (see Fig. 1).

From kinematic considerations, we note that

$$\kappa(s',t) = \frac{\partial\varphi(s',t)}{\partial s'} \qquad (12a)$$

$$\frac{\partial x(s',t)}{\partial s'} = \cos\varphi(s',t) \qquad (12b)$$

$$\frac{\partial y(s',t)}{\partial s'} = \sin\varphi(s',t) \qquad (12c)$$

Substitution of Eqs. (11) and (12a) into Eq. (10), differentiation with respect to s' and use of Eq. (12b) yield, after nondimensionalization

$$\frac{\partial^2\varphi(s,t)}{\partial s^2} = -\left(\frac{L^2}{I}\right)\int_{-\infty}^t J(t-\tau)\left\{\frac{\partial[R(\tau)\cos\varphi(s,\tau)]}{\partial\tau}\right\}d\tau \qquad (13)$$

The associated boundary conditions are

$$\varphi(0,t) = 0 \qquad (14a)$$

$$\frac{\partial\varphi(1,t)}{\partial s} = 0 \qquad (14b)$$

It is assumed the beam is undeformed for $\tau < 0$. Then, by taking the Laplace transform of Eqs. (13) and (14), we obtain

$$\frac{\partial^2\Phi(s,p)}{\partial s^2} = -\left(\frac{L^2}{I}\right)p\mathcal{J}(p)\mathcal{L}_p[R(\tau)\cos\varphi(s,\tau)] \qquad (15a)$$

$$\Phi(0,p) = 0 \qquad (15b)$$

$$\frac{\partial\Phi(1,p)}{\partial s} = 0 \qquad (15c)$$

where $\mathcal{L}_p[\ ]$ is the Laplace transform operator, p the transform variable, and $\mathcal{J}(p)$ and $\Phi(s,p)$ the transforms of $J(t)$ and $\varphi(s,t)$, respectively. Here, we have tacitly assumed that the Laplace transform of the expression within the brackets exists, in the usual sense, even though a formal expression for it is not available.

Assuming that the transform variable appears only as a parameter, Eq. (15a) can be viewed as a type of *ordinary* differential equation. Integration thus yields

$$\frac{\partial\Phi(s,p)}{\partial s} - \frac{\partial\Phi(0,p)}{\partial s}$$

$$= -\left(\frac{L^2}{I}\right)p\mathcal{J}(p)\int_0^s\left[\int_0^\infty e^{-p\tau}R(\tau)\cos\varphi(u,\tau)d\tau\right]du \qquad (16)$$

where the Laplace transform has been expressed in the explicit manner. Application of the boundary condition, as
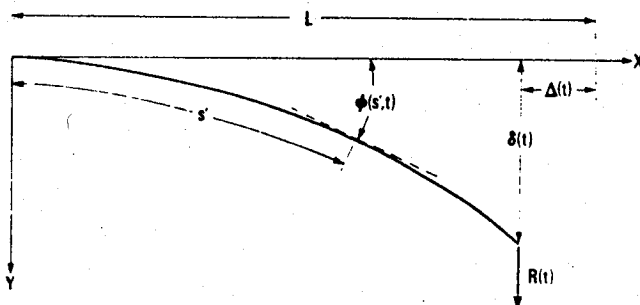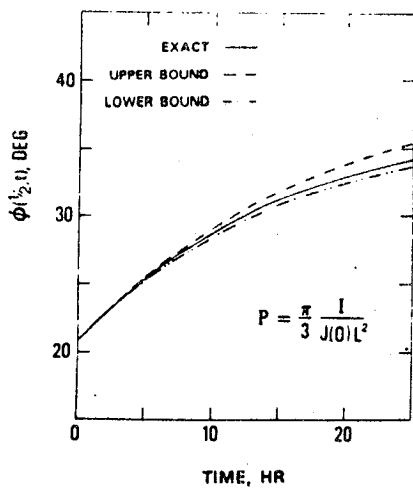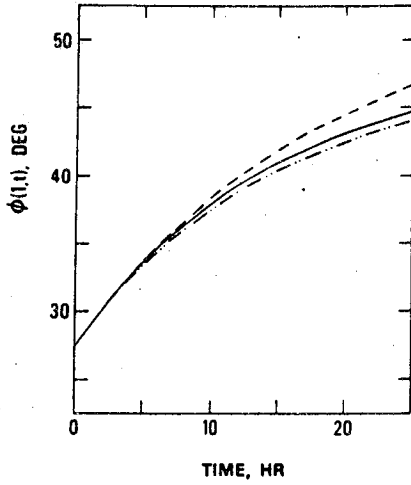

Fig. 1 Geometry of the end-loaded cantilever beam.

28

a) At midspan.

b) At loaded end.

Fig. 2 Angle of deflection of the end-loaded cantilever beam.

given by Eq. (15c), yields

$$\frac{\partial \Phi(0,p)}{\partial s} = \left(\frac{L^2}{I}\right) p \mathcal{J}(p) \int_0^\infty e^{-p\tau} R(\tau) \left[\int_0^1 \cos\varphi(u,\tau)du\right] d\tau \tag{17}$$

Note that we have interchanged the order of integration of Eq. (16). This follows directly from the assumption of inextensionality; therefore, s and τ represent independent variables. Substitution of Eq. (17) into Eq. (16) yields

$$\frac{\partial \Phi(s,p)}{\partial s} = -\left(\frac{L^2}{I}\right) p \mathcal{J}(p) \int_0^\infty e^{-p\tau} R(\tau)$$
$$\times \left[\int_1^s \cos\varphi(u,\tau)du\right] d\tau \tag{18}$$

Integration of Eq. (18) with respect to s, use of the boundary condition [Eq. (15b)], and manipulation as before yield

$$\Phi(s,p) = -\left(\frac{L^2}{I}\right) p \mathcal{J}(p) \int_0^\infty e^{-p\tau} R(\tau)$$
$$\times \left[\int_0^s \int_1^r \cos\varphi(u,\tau)du\,dr\right] d\tau$$

The term in the brackets may be simplified through integration by parts and by employing

$$g(s,u) = u, \quad 0 \le u \le s$$
$$= s, \quad s \le u \le 1 \tag{20}$$

to yield

$$\Phi(s,p) = \left(\frac{L^2}{I}\right) p \mathcal{J}(p) \mathcal{L}_p \left[R(\tau)\int_0^1 g(s,u)\cos\varphi(u,\tau)du\right] \tag{21}$$

Thus defining $\theta(s,\tau)$ by

$$\theta(s,\tau) = \int_0^1 g(s,u)\cos\varphi(u,\tau)du \tag{22}$$

results in

$$\Phi(s,p) = (L^2/I)p\mathcal{J}(p)\mathcal{L}_p[R(\tau)\theta(s,\tau)] \tag{23}$$

Next, the Laplace convolution theorem is employed to invert Eq. (23) to yield

$$\varphi(s,t) = \left(\frac{L^2}{I}\right) \int_0^t J(t-\tau) \frac{\partial[R(\tau)\theta(s,\tau)]}{\partial\tau} d\tau \tag{24}$$

Upon a final integration by parts we have

$$\varphi(s,t) = \left(\frac{L^2}{I}\right)\left[J(0)R(t)\theta(s,t) + \int_0^t J'(t-\tau)R(\tau)\theta(s,\tau)d\tau\right] \tag{25}$$

where $(\;)'$ denotes differentiation with respect to the argument of the function. Note that Eq. (25) is the viscoelastic solution reported in Ref. 2.

Bounding solutions are developed in the following manner. Provided, after quasistatic application, the load $R(\tau)$ is held constant at some value P, it is reasonable to presume that the angle of deflection $\varphi(s,\tau)$ will be a nondecreasing function in time. Thus, for the interval $0^+ \le \tau \le t$,

$$\varphi(s,0^+) \le \varphi(s,\tau) \le \varphi(s,t) \tag{26}$$

Consequently, restricting our attention to a range of deflection such that $0 \le \varphi \le \pi/2$ we may conclude that

$$\cos\varphi(s,0^+) \ge \cos\varphi(s,\tau) \ge \cos\varphi(s,t) \tag{27}$$

Thus, from Eqs. (22) and (27) we have

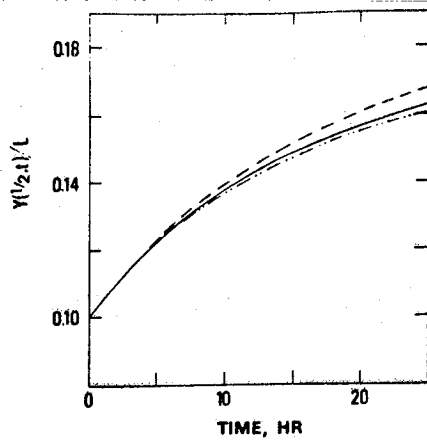$$\theta(s,0^+) \ge \theta(s,\tau) \ge \theta(s,t) \tag{28}$$

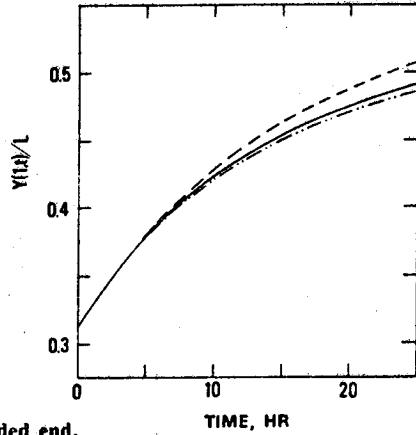Through the use of Eq. (28), we can bound the convolution integral of Eq. (25) as follows:

$$P\theta(s,0^+)\int_0^t J'(t-\tau)d\tau \ge \int_0^t J'(t-\tau)R(\tau)\theta(s,\tau)d\tau$$
$$\ge P\theta(s,t)\int_0^t J'(t-\tau)d\tau \tag{29}$$

Integration of the first and third integrals in Eq. (29) and substitution of these results into Eq. (25) yield, after rearrangement,

$$\varphi_{lb}(s,t) = J(t)\left(\frac{PL^2}{I}\right)\theta(s,t) \tag{30a}$$

29

a) At midspan.

b) At loaded end.

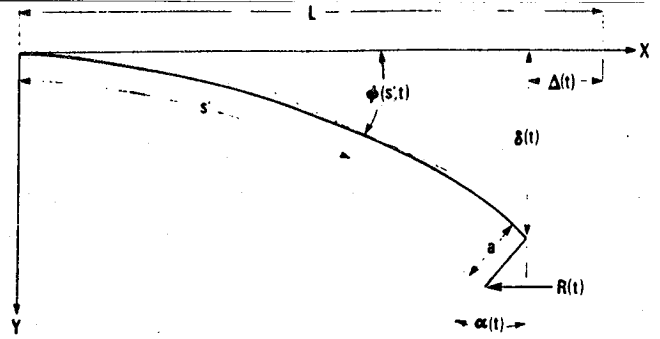Fig. 3 Vertical deflection of the end-loaded cantilever beam.

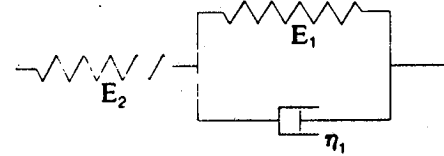Fig. 4 Geometry of the eccentrically loaded cantilever column.

Fig. 5 Ideal three-element "limited" creep model.

approximated by using Newton-Coates formulas; a fixed-step trapezoidal rule is used for the time convolution. All computations are performed on a CDC Cyber 180/855 located at the Georgia Institute of Technology.

Figures 2 and 3 compare the results obtained with the bounding formulation to the exact solution for the loading case reported in Refs. 2 and 3. The form of the creep compliance for this example is

$$J(t)/J(0) = 1 + 7.6 \times 10^{-4} t + 1.12(1 - e^{-0.055t}) \tag{34}$$

Figure 2 demonstrates that the bounding solutions provide a reasonably narrow band at both the midspan and the loaded end locations. For this particular case, the lower bound tends to more closely approximate the actual solution. For both the upper and lower bounds, the discrepancy between the approximate result and the exact solution tends to increase with elapsed time and distance from the clamped end.

Figure 3 compares the calculated vertical deflections at midspan and at the loaded end. It can be noted that the descrepancies between the bounding and exact solutions behave in the same manner as described above. In terms of absolute accuracy, after 24 h, the upper-bound end deflection exceeds the exact result by approximately 3.3%. The lower bound, at the same point and time, is only 1.2% less than the exact deflection. Using a 0.1 h fixed-length time step, the exact solution required 15.6s of CPU time to compute. Calculated for the same number of time intervals, each of the bounding solutions required only 4.1 CPU s. Note, however, that the accuracy of the bounding solutions is independent of the length of the time step. Thus, identical bounding solution results can be obtained with, for example, a 1.0 h time step. Using this larger time step, the computation time for each of the bounding solutions was reduced to only 0.5 CPU s. Accurate results could not be obtained from the exact solution using a time step this large due to errors in approximating the convolution integrals.

$$\varphi_{ub}(s,t) = J(0) \left(\frac{PL^2}{I} \right) \left\{ \theta(s,t) + \left[\frac{J(t)}{J(0)} - 1 \right] \theta(s,0^+) \right\}$$

(30b)

Note that Eq. (30a) is the quasielastic solution proposed by Schapery.

Bounding of the deflection of the beam can be readily accomplished by using Eqs (30). Nondimensionalization and then integration of Eq. (12c) yield

$$\frac{y(s,t)}{L} = \int_0^s \sin\varphi(u,t)du \tag{31}$$

Thus, since $\varphi_{lb}(s,t) \leq \varphi(s,t) \leq \varphi_{ub}(s,t)$, we note that, for $0 \leq \varphi \leq \pi/2$

$$\sin\varphi_{lb}(s,t) \leq \sin\varphi(s,t) \leq \sin\varphi_{ub}(s,t) \tag{32}$$

which yield, upon substitution into Eq. (31)

$$\frac{y_{lb}(s,t)}{L} = \int_0^s \sin\varphi_{lb}(u,t)du \tag{33a}$$

$$\frac{y_{ub}(s,t)}{L} = \int_0^s \sin\varphi_{ub}(u,t)du \tag{33b}$$

Numerical solutions of Eqs. (25), (30), and (33) are generated in a manner similar to Ref. 2. Picard's method of successive substitutions is employed to numerically solve the integral equations, Eqs. (25) and (30). Spatial integrals are

Eccentrically Loaded Cantilever Column

Although formally similar to the prior example, this problem is of interest because the eccentric loading generates additive nonlinear boundary terms in the general solution. The presence of these terms substantially influences the accuracy of the predictions of the system response.
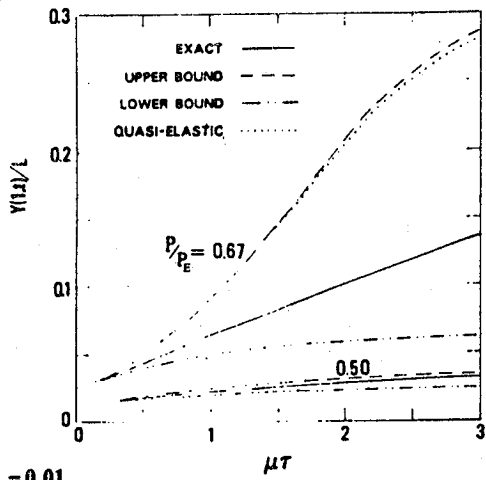
a) $a/L = 0.01$.
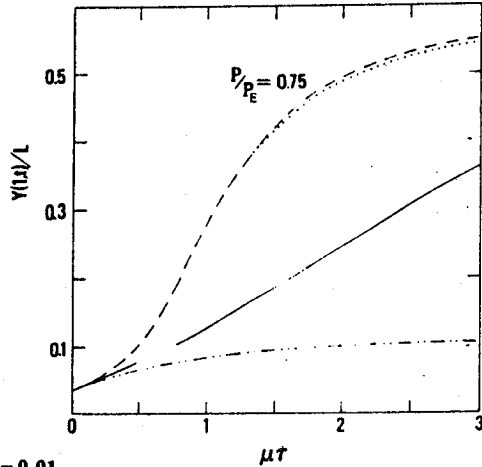
b) $a/L = 0.01$.

Fig. 6 End deflection of the eccentrically loaded cantilever column for the three-element model.

A quasielastic solution of this problem was recently presented by Vinogradov.[4] Included with the analysis were numerical results for two ideal constitutive models, using two eccentricity ratios and a wide range of applied loads. Subsequently, Vinogradov and Wijeweera[5] and Wijeweera[6] published comparisons of results obtained using the quasielastic approximation of Ref. 4 to experimental data from tests conducted on PTFE G-700 columns. The loading and eccentricity ratios employed in those tests were, however, restricted to relatively narrow ranges in value.

Bounding solutions for the problem are developed in a similar manner to the prior example. The column is assumed to be inextensional, linearly viscoelastic, and loaded quasi-statically. Its geometry in the deformed configuration is illustrated in Fig. 4. Note that the applied load remains parallel to the x axis.

For this geometry, the moment at any position s' is given by

$$M(s',\tau) = R(\tau)[\delta(\tau) + a\cos\alpha(\tau) - y(s',\tau)] \qquad (35)$$

Substitution of Eq. (35) into Eq. (10), differentiation with respect to s', use of Eqs. (12a) and (12c) followed by non-dimensionalization yield

$$\frac{\partial^2 \varphi(s,t)}{\partial s^2} = -\left(\frac{L^2}{I}\right)\int_{-\infty}^{t} J(t-\tau)\left\{\frac{\partial[R(\tau)\sin\varphi(s,\tau)]}{\partial\tau}\right\}d\tau$$

We note that the boundary conditions for this problem are

$$\varphi(0,t) = 0 \qquad (37a)$$

$$M(1,t) = aR(t)\cos\varphi(1,t) \qquad (37b)$$

where, for a rigid "extension,"

$$\alpha(t) = \varphi(1,t) \qquad (37c)$$

Through the use of Eqs. (10) and (12a), the second boundary condition [Eq. (37b)] can, after nondimensionalization, be expressed entirely in terms of φ by

$$\frac{\partial\varphi(1,t)}{\partial s} = \left(\frac{L}{I}\right)\int_{-\infty}^{t} J(t-\tau)\left\{\frac{\partial[aR(\tau)\cos\varphi(1,\tau)]}{\partial\tau}\right\}d\tau \quad (37d)$$

Assuming that the column is undeformed for $\tau < 0$ and that following the procedure detailed in Eqs. (15-25) again yield a solution of the form of Eq. (25) except that, in this case,

$$\theta(s,t) = \left(\frac{sa}{L}\right)\cos\varphi(1,t) + \int_0^1 g(s,u)\sin\varphi(u,t)du \qquad (38)$$

Note that the nonlinear boundary term $\cos\varphi(1,t)$ appears inside the convolution integral as well as in the integrated term of Eq. (25).

Under a constant load P it is again plausible to assume that $\varphi(s,\tau)$ will be a nondecreasing function with respect to τ. Thus, in addition to Eqs. (26) and (27), we note

$$\sin\varphi(s,0^+) \le \sin\varphi(s,\tau) \le \sin\varphi(s,t) \qquad (39)$$

Because of the differences in bounding behavior in Eqs. (27) and (39), the convolution integral of the general solution [Eq. (25)] is split into two separate integrals that are bounded individually.

Substitution of the appropriate bounding functions from Eqs. (27) and (39) into Eq. (38) and substitution of these results into Eq. (25) yield, after integration and rearrangement of terms

$$\varphi_{lb}(s,t) = J(0)\left(\frac{PL^2}{I}\right)\left\{\int_0^1 g(s,u)\sin\varphi(u,t)du \right.$$

$$+ \left[\frac{J(t)}{J(0)}\right]\left(\frac{sa}{L}\right)\cos\varphi(1,t)$$

$$\left. + \left[\frac{J(t)}{J(0)} - 1\right]\int_0^1 g(s,u)\sin\varphi(u,0^+)du\right\} \qquad (40a)$$

$$\varphi_{ub}(s,t) = J(0)\left(\frac{PL^2}{I}\right)\left\{\left(\frac{sa}{L}\right)\cos\varphi(1,t)\right.$$

$$+ \left[\frac{J(t)}{J(0)} - 1\right]\left(\frac{sa}{L}\right)\cos\varphi(1,0^+)$$

$$\left. + \left[\frac{J(t)}{J(0)}\right]\int_0^1 g(s,u)\sin\varphi(u,t)du\right\} \qquad (40b)$$

Numerical evaluation of Eqs. (40), as well as the exact solution given by Eqs. (25) and (38), is accomplished in the same manner as the prior example. Figures 6 and 7 present the results of these computations for the ideal "limited creep" model used in Refs. 5 and 6 and illustrated on Fig. 5. For this particular constitutive model, the creep compliance $J(t)$ has the form

$$\frac{J(t)}{J(0)} = 1 + \left(\frac{E_2}{E_1}\right)e^{-\mu t} \qquad (41a)$$

31
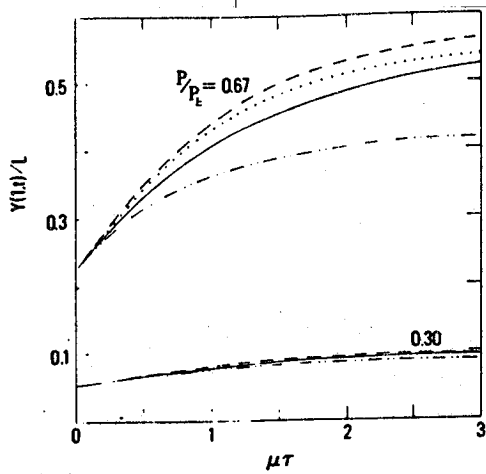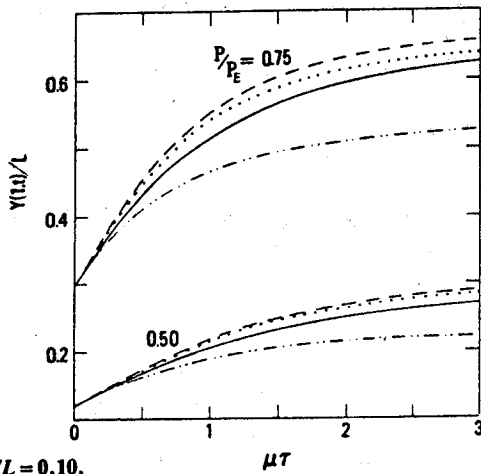
a) $a/L = 0.10$.

b) $a/L = 0.10$.

Fig. 7 End deflection of the eccentrically loaded cantilever column for the three-element model.

a) $P/P_E = 0.40$ and $a/L = 0.07$.

b) $P/P_E = 0.125$ and $a/L = 0.03$.

Fig. 8 Reported and normalized experimental data for the six-element model.

where we have employed

$$J(0) = 1/E_2 \qquad (41b)$$

$$\mu = E_1/\eta_1 \qquad (41c)$$

Figure 6 presents results for $E_2/E_1 = 0.5$ and $a/L = 0.01$ for a range of load ratios. In this figure, and all succeeding ones, we employ a viscoelastic "Euler" load P_E to non-dimensionalize the loading, where
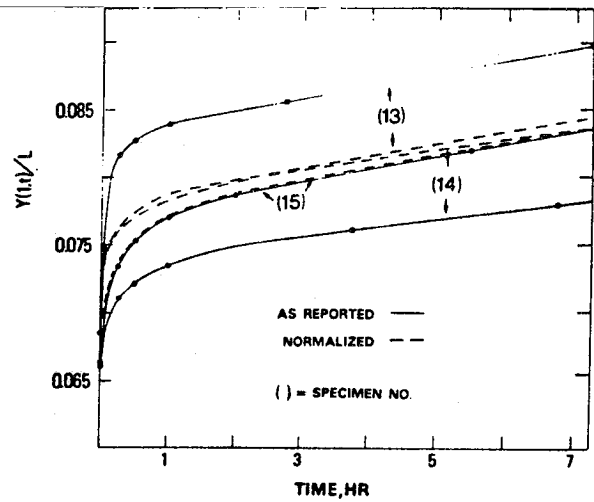
$$P_E = \frac{\pi^2 I}{4J(0)L^2} \qquad (42)$$

For comparison, this figure also includes results from a "standard" quasielastic solution φ_{qe} of the general form

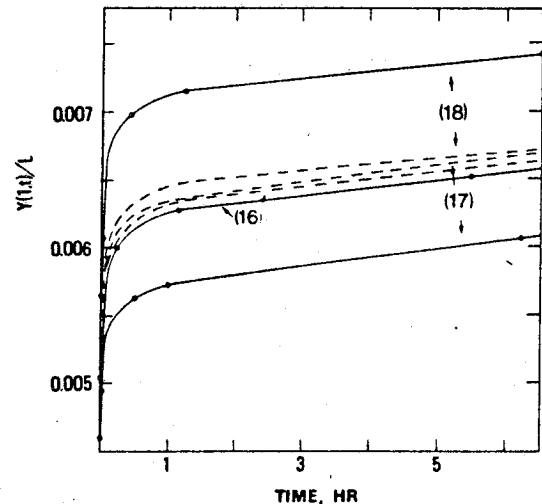$$\varphi_{qe}(s,t) = \left(\frac{PL^2}{I}\right) J(t)\theta(s,t) \qquad (43)$$

where the various functions on the right-hand side are as previously defined.

It can be observed that the quasielastic solution is almost identical to the upper-bound result for the load ratios of 0.67 and 0.75. At the load ratio of 0.50, the upper-bound and quasielastic results differ only in the fourth decimal place. Thus, only the upper-bound result has been indicated in the figure for this load case.

Although the upper-bound and quasielastic results compare favorably with each other, neither of them nor the

lower-bound solution provides a good approximation to the exact result except at the lowest load ratio, 0.50. Thus, reliance on only a quasielastic type of solution, especially for the higher loading instances, could lead to erroneous results.
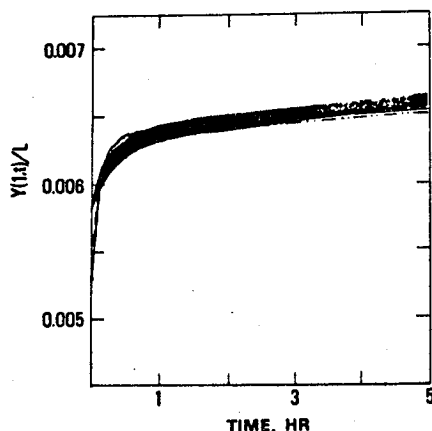
With only a quasielastic solution, it is impossible to determine its accuracy without calculating the exact solution. Thus, it is not possible to assess the magnitude or character (i.e., conservative or nonconservative) of the potential errors. In contrast, the amount of separation between the bounding solutions provides such a capability. The narrow separation evident at a load ratio of 0.50 might well provide sufficiently accurate results without resorting to the more involved analysis. The significant differences between the bounds at the higher loads, instead, indicate that exact solutions must be determined for accurate results.

Figure 7 provides results for the same ratio of modulii, but for a load eccentricity of 0.10. Again, at the lowest load ratio (0.30), the quasielastic and upper-bound solutions are virtually indistinguishable and only the upper bound is indicated.

Comparison of Figs. 6 and 7 illustrates that the increase in load eccentricity generates several pronounced effects. The quasielastic solution, in general, tends to provide a more accurate prediction of behavior at all load levels for the higher load eccentricity. Additionally, the larger eccentricity tends to decrease the spread between the upper- and lower-bound approximations. This is not, however, a completely general

32

a) $P/P_E = 0.40$ and $a/L = 0.07$.

b) $P/P_E = 0.125$ and $a/L = 0.03$.

Fig. 9 End deflection of the eccentrically loaded cantilever column for the six-element model.

value was only 0.0580. If the various results were to be normalized to eliminate this difference, the test data band would completely overlap the calculated results. However, using such a procedure for the lower-load case would decrease the correlation indicated on Fig. 8. Since the observed "instantaneous" deflection was only 0.00504, normalizing the data to the calculated deflection of 0.00530 would move the band of test data so that it would be somewhat above the calculated results. The main conclusion to be drawn is that, qualitatively, the calculated results agree with the observed data. Exact comparability is, however, hindered by the large differences in initial displacement evident in the test data.

Conclusions

A methodology is presented wherein problems of isothermal linear viscoelastic behavior, formulated using nonlinear kinematic measures of deformation, may be analyzed through the use of a bounding procedure. The bounding solutions developed by this technique are similar in form to that of a time-dependent elasticity problem. As such, numerical solutions may be generated without requiring the computation of convolution integrals of the entire history of deformation. In one of the examples considered, it is shown that this results in an increase in computational efficiency more than 30 times greater by comparison to the more traditional approach.

It is also demonstrated that the bounding procedure provides reasonably accurate results for a variety of loading conditions. In those cases where narrow bounds cannot be established, it is shown that a standard type quasielastic approach is not necessarily more reliable. The clear implication of the wide bounds is that the more involved traditional approach must be employed if highly accurate results are required.

As presented, the bounding technique can be directly employed for problems where the governing functions may be characterized as either nonincreasing or nondecreasing functions with respect to time. However, the range of applicability potentially can be expanded to include some forms of multimodal functions. In general, this would require that these functions be capable of being characterized, at least in a piecewise manner, as a sequence of unimodal segments. Similar to the procedure that was employed in the second example, each of these segments would then be bounded individually. The degree of accuracy that might be obtained using such a procedure, however, requires further study.

Acknowledgments

References

[1]Schapery, R. A., "Approximate Methods of Transform Inversion for Viscoelastic Stress Analysis," *Proceedings of 4th U. S. Congress on Applied Mechanics*, Vol. 2, 1962, pp. 1075-1085.

[2]Rogers, T. G. and Lee, E. H., "On the Finite Deflection of a Viscoelastic Cantilever," *Proceedings of 4th U. S. Congress on Applied Mechanics*, Vol. 2, 1962, pp. 977-987.

[3]Schapery, R. A., "A Method of Viscoelastic Stress Analysis Using Elastic Solutions," *Journal of the Franklin Institute*, Vol. 279, No. 4, 1985, pp. 268-289.

[4]Vinogradov, A. M., "Nonlinear Effects in Creep Buckling Analysis of Columns," *Journal of Engineering Mechanics, ASCE*, Vol. 111, No. 6, 1985, pp. 757-767.

[5]Vinogradov, A. M. and Wijeweera, H., "Theoretical and Experimental Studies on Creep Buckling," *Proceedings of AIAA/ASME/ASCE/AHS 26th Structures, Structural Dynamics and Materials Conference*, Vol. 1, 1985, pp. 160-164.

[6]Wijeweera, H., "Creep Buckling of Initially Imperfect Linear Viscoelastic Columns," M.S. Thesis, Dept. of Civil Engineering, University of Calgary, Canada, 1984.

trend, since at the load ratio of 0.50 the bounding is much more narrow for the lower eccentricity case.

Since some experimental results also are available,[5,6] a comparison with these data is worthwhile. Figure 8 provides reported as well as "normalized" data for two load-eccentricity cases. The normalized curves are generated by adding the relative displacement of a specimen from its time $= 0^+$ (i.e., 10 or 20 s deflection) to the average 0^+ displacement of that test group. In this way, the significant differences between the observed results in a test group due solely to the differences in "instantaneous" deflection could be eliminated. As indicated in the figure, this virtually eliminates the substantial differences between observed results.

Based on data from four point bending tests the specimen material (PTFE G-700) was modeled[6] as a six-element "unlimited creep" type of material. The numerical form for the creep compliance is given by

$$J(t)/J(0) = 1 + 3.7 \times 10^{-4}t + 0.17(1 - e^{-9.02t})$$

$$+ 0.13(1 - e^{-0.04t}) \tag{44}$$

Figure 9 presents the comparison of the exact quasielastic, upper- and lower-bound results to the normalized test data of Fig. 8. Note that, while there is an apparent significant difference between observed and calculated results for the higher-load case, differences in the 0^+ deflection account for most of it. The average reported "instantaneous" nondimensional deflection was 0.0633, whereas the calculated

Solution Methods for One-Dimensional Viscoelastic Problems

John M. Stubstad* and George J. Simitses†
Georgia Institute of Technology, Atlanta, Georgia

A recently developed differential methodology for solution of one-dimensional nonlinear viscoelastic problems is presented. Using the example of an eccentrically loaded cantilever beam-column, the results from the differential formulation are compared to results obtained from a previously published integral solution technique. It is shown that the results from these distinct methodologies exhibit a high degree of correlation with one another. A discussion of the various factors affecting the numerical accuracy and rate of convergence of these two procedures is also included. Finally, the influences of some "higher-order" effects, such as straining along the centroidal axis, are discussed.

Nomenclature

a = load eccentricity
A = area of cross section
E = Young's modulus
$g(s,u)$ = Green's function for the spatial integrals
I = moment of inertia
$J(t)$ = creep compliance
l = length of cantilever
L_p = Laplace transform operator
M, N = moment and force resultant, respectively
P = applied load
P_e = Euler load
$\hat{s}, s$ = dimensional and nondimensional distance along the beam, respectively
t, τ = time
u, w = axial and transverse displacement, respectively
x, y = spatial coordinates
γ_q = Newton-Cotes quadrature weights
ϵ_0 = centroidal axis strain
κ = curvature
ϕ = angle of rotation

Introduction

A NUMBER of solution methods are available for viscoelastic problems in which the behavior of the material may be adequately characterized by a linear viscoelastic operator and where the deformation of the body is sufficiently small to allow the use of a linear kinematic formulation.[1,2] Commonly, integral transform methods, separation of variables, series expansions, and other techniques provide methodologies wherein exact closed-form solutions may be derived. When exact solutions cannot be obtained, approximate techniques, such as one proposed by Schapery,[3] provide an alternate approach.

The inclusion of nonlinear effects in the analysis significantly reduces the mathematical tractability of the problem. These nonlinear influences can be induced by geometric factors resulting from the magnitude of the deformation or from gross rotation of cross sections. Alternatively, nonlinearities in the material response may need to be included to provide an accurate model for material behavior.

Independent of whether the nonlinearities are produced by geometric or material effects, they invariably result in non-linear governing equations. Thus, the solution methods mentioned here, applicable to linear problems, generally cannot be employed. Approximation methods,[4] however, have been developed and can be employed to analyze such problems.

One of these methods is to idealize the problem in a manner that inherently simplifies the governing relations. An example of this technique was the utilization of an ideal "I" cross-sectional geometry in early column creep-buckling studies.[5] With this approximation, the equilibrium equations were reduced to simpler forms, involving the "average" stresses in the ideal flanges, where closed-form solution was possible.

Another approach used extensively was to restrict considerations to only certain types of time-dependent material behavior.[6] In some cases, this involved retaining only secondary creep behavior in the material model. Alternatively, and especially when "power-law" type constitutive laws were used, the constants or exponents of the law were restricted to special values for which closed-form solution was possible.[7] In a few cases, this approximation, as well as the aforementioned geometric simplification technique, were employed simultaneously to enable solution. A survey of many of these techniques has been provided by Hoff.[8]

A more general technique for the solution of geometrically nonlinear viscoelastic problems was first presented by Rogers and Lee.[9] In this method, the solution was formulated as an integral equation that was nonlinear in both time and space. From this, numerical results were obtained using computational techniques. A recent paper by the authors[10] provided a method for bounding the solution of problems formulated in this manner.

Generally, both the exact and bounding technique can be employed for problems wherein the response of the material may be adequately characterized using a linear viscoelastic model, but where the resulting time-dependent deformation of the body warrants the use of a nonlinear kinematic formulation. Problems involving nonlinear viscoelastic material behavior, however, currently cannot be addressed with this method. Unfortunately, many materials, and especially the elevated temperature behavior of most metals, require a nonlinear constitutive characterization. Consequently, an alternate solution procedure for one-dimensional problems involving nonlinear kinematic and nonlinear material effects has been developed. This method, hereinafter referred to as the differential formulation, is based on the direct solution of the nonlinear differential equations of equilibrium.

Similar to the integral method, the differential formulation is predicated on the assumption of a quasistatic response. This, effectively, "decouples" the temporal and spatial dependence of the problem in a manner that allows the general solution to be treated as the sequential combination of solutions to a nonlinear "boundary value" problem and a nonlinear "initial value" problem. The first of these, the equations characterizing the time-dependent states of quasistatic equilibrium, are solved

through the use of a Newton-type method.[11] The "initial value" problem, resulting from the nonlinear constitutive law, governs the manner by which the body progresses from one state of quasistatic equilibrium to the succeeding one. Numerical solutions for this part of the problem are generated using a fourth-order Runge-Kutta method. This general method has recently been employed to examine the nonlinear thermoviscoelastic behavior of thin structural members.[12]

In addition to presenting the differential formulation technique, a comparison of results obtained using the integral and differential formulations is provided. The problem of an eccentrically loaded viscoelastic cantilever beam-column is employed as the vehicle through which the comparison is performed. Because of the inherent limitation of the integral technique, this comparison is restricted to the consideration of a linear viscoelastic material. The specific case considered is that of the three-parameter viscoelastic solid, which has been examined in a number of studies.[10,13,14] The results obtained from these two distinct methods of solution exhibit a surprisingly high degree of correlation with one another, thereby establishing a high level of confidence in the validity of the methods. Finally, the differential formulation is employed to examine the influences of some "higher-order" effects in the class of problems under consideration.

Integral Formulation

The Rogers and Lee formulation method,[9] hereafter referred to as the integral solution technique, is focused toward formulating the solution to the nonlinear viscoelastic problem in terms of an integral equation. The general method was evolved through analogy to the associated geometrically nonlinear elastic problem. Only a synopsis of the method is presented here since complete developments for the technique are available in the literature.[9,10]

In the integral formulation, the time dependence of the material behavior is expressed in the form of a Volterra-type integral operator. This operator acts upon a second integral expression, which characterizes the quasistatic equilibrium of the body. For application to beam-column-type problems, it is assumed that the beam-column is thin and composed of a linearly viscoelastic material. In addition, referenced line extensional strains are assumed to be negligibly small. Thus, the coordinate $\hat{s}$, denoting distance along the undeformed length, can be employed to specify position in both the initial and deformed configurations. For convenience, a nondimensional coordinate s is defined by dividing $\hat{s}$ by the length of the beam l. Figure 1 illustrates a typical geometry used with this method. For the sample problem, the eccentric load is assumed to be applied quasistatically, and its direction does not vary with time.

Assuming a linear distribution of the strains through the depth, bending, thus occurring within an Euler-Bernoulli context, results in a moment-curvature relationship of the form

$$\kappa(\hat{s},t) = \left(\frac{1}{I}\right) \int_{-\infty}^{t} J(t-\tau) \left[\frac{\partial M(\hat{s},\tau)}{\partial \tau}\right] d\tau \qquad (1)$$

where $\kappa(\hat{s},t)$ denotes the curvature and $M(\hat{s},\tau)$ the bending moment at location $\hat{s}$. I denotes the moment of inertia of the beam and $J(t)$ the creep compliance of the material. For the sample problem, the moment at position $\hat{s}$ would be given by

$$M(\hat{s},\tau) = P(\tau)[\delta(\tau) + a\cos\alpha(\tau) - y(\hat{s},\tau)] \qquad (2)$$

where $P(\tau)$ denotes the load applied at eccentricity α. Since

$$\kappa(\hat{s},t) = \frac{\partial \phi(\hat{s},t)}{\partial \hat{s}} \qquad (3)$$

then, for quiescent initial condition, the Laplace transformation of Eq. (1) yields

$$\frac{\partial \Phi(s,p)}{\partial s} = \frac{l}{I} pJ(p)L_p[M(s,t)] \qquad (4)$$

where $J(p)$ and $\Phi(s,p)$ denote the transforms of $J(t)$ and $\phi(s,t)$, respectively, and where p represents the Laplace variable. Note that the nondimensional coordinate s has also been employed in the preceding expression.

Assuming that the Laplace variable apears only algebraically, Eq. (4) has the form of a type of "ordinary" differential equation. Consequently, integrating with respect to s yields

$$\Phi(s,p) - \Phi(0,p) = \frac{l}{I} pJ(p)L_p \left[\int_0^s M(r,t) \, dr\right] \qquad (5)$$

Note that the order of integration and Laplace transformation has been interchanged. This is a direct result of the assumption of inextensionality; consequently, s and t represent independent variables.

Equation (5) reveals a very interesting aspect of this formulation. Namely, the underlying structure of the equation is completely determined by the manner in which the moment depends on the deformation. For example, even if the moment depends upon the spatial coordinate s, provided it is independent of the deformation, then the basic equation is, in principle, integrable to a closed-form solution. This solution is, in fact, the usual result obtained from a linear analysis.

Illustrating how the equation structure changes when the moment is related to the deflection is best demonstrated through analogy with the associated elastic problem. Note that the governing relation for the associated elastic problem can be obtained by replacing the creep compliance by the elastic compliance and eliminating the Laplace operator. This yields

$$\phi_e(s) - \phi_e(0) = \frac{l}{EI} \int_0^s M(r)dr \qquad (6)$$

Note that the governing equation for the associated elastic problem takes on the form of a linear Fredholm equation when the moment depends linearly upon the deflection. In contrast, a nonlinear Fredholm format is obtained for cases where the moment is nonlinearly dependent upon deformation. In a similar manner, the viscoelastic problem takes on a linear "quasi-Fredholm" form when the moment is linearly dependent upon the deformation. A nonlinear "quasi-Fredholm" format occurs when, as in the sample problem, the relationship between moment and deflection is nonlinear.

To complete the formulation for the sample problem, Eqs. (2) and (3) are substituted into Eq. (1). Following differentiation with respect to s, the kinematic relations

$$\frac{\partial x(\hat{s},t)}{\partial \hat{s}} = \cos\phi(\hat{s},t)$$

$$\frac{\partial y(\hat{s},t)}{\partial \hat{s}} = \sin\phi(\hat{s},t) \qquad (7)$$
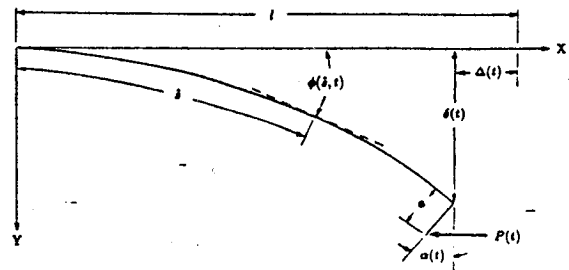

Fig. 1 Beam-column geometry for the integral method.

are employed to express all deformation-related quantities in terms of ϕ. For the sample problem, the boundary conditions are

$$\phi(0,t) = 0$$
$$M(l,t) = aP(t)\cos\phi(l,t) \qquad (8)$$

where $\alpha(t) = \phi(l,t)$ for a "rigid" extension. Thus, using the methodology detailed in Ref. 9 and assuming quiescent initial conditions yields the solution

$$\phi(s,t) = \left(\frac{l^2}{I}\right)\left[J(0)P(t)\Theta(s,t) + \int_0^t J'(t-\tau)P(\tau)\Theta(s,\tau)\,d\tau\right] \qquad (9)$$

where

$$\Theta(s,t) = \left(\frac{sa}{l}\right)\cos\phi(1,t) + \int_0^1 g(s,r)\sin\phi(r,t)\,dr \qquad (10)$$

and

$$g(s,r) = r, \qquad 0 \le r \le s$$
$$= s, \qquad s \le r \le 1 \qquad (11)$$

Note that the prime in Eq. (9) denotes differentiation with respect to the argument of the function.

Equation (9) represents a time convolution of a nonlinear spatial integral equation, Eq. (10). Numerical solutions are obtained using Picard's method of successive substitutions.[15] Newton-Coates formulas are used to approximate the spatial integral, and a fixed-step trapezoidal rule is employed for the time convolution. The general format of the algebraic expressions obtained in this manner is

$$\phi(s_i,t_n) = \frac{\pi^2}{4}\frac{P}{P_e}\Delta t\left[\left(1 + \frac{1}{2}J'(0)\right)\Theta(s_i,t_n)\right.$$
$$\left. + \sum_{j=2}^{n-1}J'(t_n - t_j)\Theta(s_i,t_j) + \frac{1}{2}J'(t_n)\Theta(s_i,0^+)\right] \qquad (12)$$

with

$$\Theta(s_i,t_j) = \frac{s_i a}{l}\cos\phi(1,t_j) + \Delta s\left[\sum_{k=1}^{i}\gamma_k r_k\sin\phi(r_k,t_j)\right.$$
$$\left. + \sum_{k=i}^{p}\gamma_k s_i\sin\phi(r_k,t_j)\right] \qquad (13)$$

Note that in Eq. (12), the number of terms in the summation increases linearly with each succeeding time step, whereas the number of terms in the summations represented by Eq. (13) is fixed. This increasing summation requirement in Eq. (12) has a significant impact on the relative speed of the integral formulation computations.

Differential Formulation

As previously noted, the differential formulation technique is based on the direct solution of the governing differential equations. Similar to the integral formulation, the differential formulation is also based on the assumption of quasistatic behavior. From this, the equations governing the successive states of quasistatic equilibrium may be expressed in terms of deformation functions and force and moment resultants. Consequently, these equations have the general format of a nonlinear boundary value problem. A Newton-type method, first suggested by Thurston,[11] is employed to derive solutions for this part of the problem.

On the other hand, the constitutive law, expressing the time dependence of the material response, governs the evolution of the force and moment resultants as the system progresses between successive states of quasistatic equilibrium. This repre-

sents a form of initial value problem with the values of the constitutive variables, such as accumulated viscoelastic strain, providing the initial conditions. For a nonlinear constitutive law, numerical procedures such as a Runge-Kutta or Euler method may be employed to predict the growth of these variables. Note that, for a "beam-theory" type formulation such as this, a spatial integration of the viscoelastic strain across the cross section is also required to enable evaluation of the force and moment resultants.

Similar to the integral formulation, the differential formulation for the sample problem is also based on the assumption that bending of the beam occurs in accordance with the Euler-Bernoulli hypotheses. Employing the functions $u(s,t)$ and $w(s,t)$ to denote, respectively, the axial and transverse deflection of the centroidal axis, then the extensional strain at the centroidal axis ϵ_0 is approximately given by

$$\epsilon_0 \approx \frac{\partial u}{\partial s} + \frac{1}{2}\left(\frac{\partial w}{\partial s}\right)^2 \qquad (14)$$

Note that the term $\frac{1}{2}(\partial u/\partial s)^2$ has been neglected as small in comparison to $\partial u/\partial s$. If, in addition, both the strain at the centroidal axis and $\partial u/\partial s$ are small in comparison to 1, then it is simple to show that

$$\frac{\partial\phi}{\partial s} \approx \frac{\partial w}{\partial s}\frac{\partial^2 u}{\partial s^2} - \frac{\partial^2 w}{\partial s^2} \qquad (15)$$

where ϕ denotes the angle of rotation of the cross section. Thus, the assumption of a linear variation of strain across the cross section yields

$$\epsilon_{11} = \epsilon_0 + \eta\frac{\partial\phi}{\partial s} \qquad (16)$$

Employing the principal of virtual work followed by integration by parts and subsequent algebraic manipulation yields the equilibrium equations

$$N = -F\left\{1 + \frac{\partial\phi}{\partial s}[a\cos\phi(l) + w(s) - w(l)]\right\} \qquad (17a)$$

$$M = F[a\cos\phi(l) + w(s) - w(l)] \qquad (17b)$$

where N and M, the force and moment resultants, respectively, are defined as

$$N = \int_A \sigma_{11}\,dA \qquad (18a)$$

$$M = \int_A \eta\sigma_{11}\,dA \qquad (18b)$$

Based on an additive decomposition for the total strain, $\epsilon_t = \epsilon_e + \epsilon_c$, where ϵ_e and ϵ_c represent the elastic and creep strain components, respectively, yields, after substitution into Eqs. (17) and (18),

$$EA\epsilon_0 = -F\left\{1 + \frac{\partial\phi}{\partial s}[a\cos\phi(l) + w(s) - w(l)]\right\} + N_c \qquad (19a)$$

$$EI\frac{\partial\phi}{\partial s} = F[a\cos\phi(l) + w(s) - w(l)] + M_c \qquad (19b)$$

where the "pseudoresultants" N_c and M_c are defined by

$$N_c = \int_A E\epsilon_c\,dA \qquad (20a)$$

$$M_c = \int_A \eta E\epsilon_c\,dA \qquad (20b)$$

Numerical solution for Eqs. (19) are computed using a modified Newton-type method suggested by Thurston.[11] To illustrate this method, consider a nonlinear differential term of the form $du'''dw''$ where du and dw are differentials of the functions u and w and m and n represent integer exponents. Assuming that close trial solutions $\tilde{w}$ and $\tilde{u}$ are available, which differ from the exact solution by the small quantities Δw and Δu so that $u = \tilde{u} + \Delta u$ and $w = \tilde{w} + \Delta w$, then

$$du'''dw'' = d\tilde{u}'''d\tilde{w}'' + m d\tilde{u}'''^{-1} d\tilde{w}''d(\Delta u)$$

$$+ n d\tilde{u}'''d\tilde{w}''^{-1}d(\Delta w) + f(\tilde{u},\tilde{w})O[\Delta u,\Delta w] \qquad (21)$$

where $f(\ )$ denotes a nonlinear function of $\tilde{u}$ and $\tilde{w}$ and $O[\ ]$ indicates terms of order $\Delta u \Delta w$ and higher. If the trial solution is indeed close to the true solution, then the corrections Δu and Δw will be small. Consequently, the quadratic and higher-order terms in the corrections will be negligible in comparison to the linear terms and therefore may be neglected. Thus, the left-hand side of Eq. (21) may be closely approximated by the linearized form consisting of just the first three terms on the right-hand side.

With this procedure, the original nonlinear differential equation is approximated by a linearized form. Employing standard finite-difference formulas, the linearized form is then converted into a system of algebraic equations where the unknowns are the corrections to the trial solution at the nodes of the finite-difference mesh. These relations are solved for these corrections, the trial solution is adjusted, and the process repeated until convergence is obtained.

Application of this procedure to the geometry of the sample problem, e.g., yields the finite-difference expressions

$$EI \frac{\partial \tilde{w}_i}{\partial s} \Delta u_{i-1} - 2EI \frac{\partial \tilde{w}_i}{\partial s} \Delta u_i + EI \frac{\partial \tilde{w}_i}{\partial s} \Delta u_{i+1}$$

$$- EI \left(1 + 2\Delta s \frac{\partial^2 \tilde{u}_i}{\partial s^2}\right) \Delta w_{i-1} + (2EI - \Delta s^2 P) \Delta w_i$$

$$- EI \left(1 - 2\Delta s \frac{\partial^2 \tilde{u}_i}{\partial s^2}\right) \Delta w_{i+1} + \Delta s^2 P \Delta w_n$$

$$+ 2\Delta s Pa \tan\tilde{\phi}(\Delta w_{n-1} - w_{n+1})$$

$$= \Delta s^2 \left[M_i^* + M_{c_i} - EI \frac{\partial \tilde{\phi}_i}{\partial s}\right] \qquad (22a)$$

and

$$M_i^* \left(\frac{\partial \tilde{w}_i}{\partial s} - 2\Delta s EA\right) \Delta u_{i-1} - 2M_i^* \frac{\partial \tilde{w}_i}{\partial s} \Delta u_i$$

$$- M_i^* \left(\frac{\partial \tilde{w}_i}{\partial s} + 2\Delta s EA\right) \Delta u_{i+1}$$

$$- \left[2\Delta s EA \frac{\partial \tilde{w}_i}{\partial s} + M_i^* \left(2\Delta s \frac{\partial^2 \tilde{u}_i}{\partial s^2} + 1\right)\right.$$

$$\left. + 2\Delta s P \tan\tilde{\phi}_i\right] \Delta w_{i-1} + \left(\frac{\partial \tilde{\phi}_i}{\partial s} \Delta s^2 P + 2M_i^*\right) \Delta w_i$$

$$+ \left[2\Delta s EA \frac{\partial \tilde{w}_i}{\partial s} + M_i^* \left(2\Delta s \frac{\partial^2 \tilde{u}_i}{\partial s^2} - 1\right)\right.$$

$$\left. + 2\Delta s P \tan\tilde{\phi}_i\right] \Delta w_{i+1} - \frac{\partial \tilde{\phi}_i}{\partial s} \Delta s^2 P \Delta w_n$$

$$- 2 \frac{\partial \tilde{\phi}_i}{\partial s} \Delta s Pa \tan\tilde{\phi}_n(\Delta w_{n-1} - \Delta w_{n+1})$$

$$= \Delta s^2 \left[-P \cos\tilde{\phi}_i + N_{c_i} - E\tilde{\epsilon}_0 - M_i^* \frac{\partial \tilde{\phi}_i}{\partial s}\right] \qquad (22b)$$

where

$$M_i^* = P(a \cos\tilde{\phi}_n + \tilde{w}_i - \tilde{w}_n) \qquad (23)$$

In these equations, the subscript i is used to represent interior nodes, and the subscript n is employed to indicate the node at the loaded end of the beam-column. Values obtained from the trial solution have been denoted by the placement of a tilde over the applicable term.

Numerical solution of Eqs. (22) requires evaluation of the "pseudoresultants" N_c and M_c at each interior point of the finite-difference mesh. This is accomplished by evaluating the accumulated creep strain at a select number of points across the cross section at each of the axial nodes. A three-point Newton-Cotes quadrature formula is then employed repetitively to approximate the area integrals. For the sample calculations reported herein, evaluation of the accumulated creep strain at each of these points is accomplished through the use of a fourth-order Runge-Kutta integration routine to integrate the constitutive law.

Example Problem

The specific example considered is that of a 30.5 cm (12 in.) long beam-column. For simplicity, a square cross section of dimension 12.7 mm (0.5 in.) has been assumed. It is also assumed that the beam-column is fabricated from a material that can be modeled as a three-parameter viscoelastic solid. The creep compliance for this model, illustrated in Fig. 2, is given by

$$J(t)/J(0) = 1 + [E_2/E_1]e^{-t/\tau_0} \qquad (24)$$

where $\tau_0 = v_1/E_1$. For the sample computations, the numerical values for the parameters have been selected so that $\tau_0 = 1$. Thus, integer values for time t are equal to multiples of the time constant of the material. The elastic modulus of the material, E_2, is assumed to be 196 GPa (28.5×10^6 psi), the room temperature modulus of Hastelloy X.

A five-point grid in the transverse direction is used in computing the "pseudoresultants" in the differential formulation. The points are equidistantly spaced, with the first and last located at the extreme fibers and the central point positioned on the centroidal axis.

Since the governing equations of both the differential and integral formulations are only satisfied at a discrete number of points over the length of the beam-column, the first question addressed is the sensitivity of the results to the number of points used in the approximation. Table 1, for example, compares initial elastic deflections determined using the differential formulation as the number of approximating points is doubled from 10 to 20 and then doubled again to 40. Table 2 provides a similar comparison for the integral formulation.

It can be seen that there is very little change in the computed transverse deflection as the number of approximating points is increased. In both cases, the initial elastic solution for the 10-element model is within 1.0% of the 40-element model results. Additionally, the relative magnitude of the errors between the 10- and 40- as well as the 20- and 40-element models of the differential formulation are very similar to those exhibited by the equivalent comparison of integral solution models. These specific results, of course, apply for an eccentricity ratio of 0.05 and an applied load of $P/P_e = 0.75$, where the Euler load P_e is based on a perfect geometry and use of the instantaneous compliance of the material $J(0)$. However, they, like other results reported herein, illustrate the general trends observed at other load levels and load eccentricities.

Thus, both formulations exhibit a similar low sensitivity to the number of elements used in the analysis. Concurrently, the results also indicate that a 10-element model can be used with either method without generating significant errors in the analysis. It should be noted that all of the differential formulation results presented in the first table are based on the use of an exact expression for evaluating the angle of rotation. The influence of employing an approximate formula for calculating the angle of rotation is discussed in a later section. Also note that

37

at this load and eccentricity, the initial end rotation of the beam-column exceeds 17 deg. Of course, smaller rotations are exhibited at the lower loads and lower eccentricities. Higher loads and larger eccentricities, conversely, produce greater rotations.

A direct comparison between the results generated by the two formulations is provided in Tables 3 and 4. Again, the comparison is based on the 0.05 eccentricity ratio, which produces reasonably large angles of rotation. Angles of rotation of the cross section, determined from the integral technique, are included in the tabulated data.

It should be noted that the differential solution results presented in Table 3 are based on the use of an exact expression for evaluation of $\sin\phi$. Differential solution results obtained using an approximate expression for $\sin\phi$ are provided in Table 4. The common approximation $\phi \approx \sin^{-1}(-\partial w/\partial s)$ is employed to calculate the angle of rotation for this second set of results. Except for this particular difference, these two differential formulations are otherwise completely identical.

These results indicate that little difference exists between the initial deformation predicted using the integral formulation and that predicted by either differential solution. The differences between the integral and differential methods are typically an order of magnitude lower than the differences observed for either technique when the number of elements was quadrupled. A potentially high-order effect may be indicated by the relative increase in differences at the highest loading examined. However, despite this increase, the magnitude of the differences is still so small as to be completely inconsequential with regard to engineering computations.

The data also indicate that no significant differences in the differential formulation (predicted transverse deflections) occur as a result of using an approximate formula for evaluation of $\sin\phi$. Even for an end rotation angle of 17 deg, the exact and approximate results differ only in the third or fourth decimal place. It should be noted that this high level of correlation continues to exist for even greater angles of rotation.

The probable reason for this high correlation is that, under compressive loading, the derivative of the axial displacement is negative. With reference to Eq. (14), this implies that the centroidal axis strain is numerically equal to the difference between the two components since the squared term (slope of the transverse deflection) is always positive. Thus, the magnitude of the centroidal axis strain must be less than the magnitude of either of its components. Because the difference between the exact and approximate expressions for $\sin\phi$ is related to the $\sqrt{1+2\epsilon_0}$ in the denominator of the exact expression, reducing the magnitude of the centroidal strain must inherently improve the accuracy of an approximation where this term is neglected.

This is best illustrated by the data of Table 5. Here, the integral solution is compared to an approximate differential solution in which the effect of the centroidal axis strain terms are suppressed. This suppression is accomplished by eliminating all the $(\partial w/\partial s)^2$ terms from the governing equations. In addition, the EA modulus-area product is artificially increased

through multiplication by a factor of 1000. This second change reduces the magnitude of the axial deflections u by approximately the same factor. The overall intent of this effort was to create a differential model that would simulate the axial "inex-

Table 1 Differential elastic solution vs number of nodes for $P/P_e = 0.75$ and $a/l = 0.05$

	Transverse deflection (cm) for various numbers of elements		
		Number of elements	
$s = \hat{s}/l$	40	20	% diff[a]
0.0	0.000000	0.000000	—
0.1	0.062669	0.062751	0.13
0.2	0.249400	0.249700	0.12
0.3	0.556448	0.557103	0.12
0.4	0.977725	0.978855	0.12
0.5	1.504980	1.506695	0.11
0.6	2.128050	2.130438	0.11
0.7	2.835125	2.838262	0.11
0.8	3.613038	3.616978	0.11
0.9	4.447532	4.452313	0.11
1.0	5.323528	5.329169	0.11
$s = \hat{s}/l$	40	10	% diff
0.0	0.000000	0.000000	—
0.1	0.062669	0.063015	0.55
0.2	0.249400	0.250858	0.59
0.3	0.556448	0.559534	0.56
0.4	0.977725	0.983259	0.57
0.5	1.504980	1.513218	0.55
0.6	2.128050	2.139785	0.55
0.7	2.835125	2.850330	0.54
0.8	3.613038	3.632429	0.54
0.9	4.447532	4.470819	0.52
1.0	5.323528	5.351315	0.52

[a]% differences are with respect to 40-element solution.

Table 2 Integral elastic solution vs number of nodes for $P/P_e = 0.75$ and $a/l = 0.05$

	Transverse deflection (cm) for various numbers of elements		
		Number of elements	
$s = \hat{s}/l$	40	20	% diff[a]
0.0	0.000000	0.000000	—
0.1	0.062525	0.062616	0.15
0.2	0.248836	0.249238	0.16
0.3	0.555208	0.555981	0.14
0.4	0.975561	0.977115	0.16
0.5	1.501648	1.503906	01.5
0.6	2.123316	2.126658	0.16
0.7	2.828762	2.833050	0.15
0.8	3.604837	3.610412	0.16
0.9	4.437309	4.443969	0.15
1.0	5.311148	5.319194	0.15
$s = \hat{s}/l$	40	10	% diff
0.0	0.000000	0.000000	—
0.1	0.062525	0.062944	0.67
0.2	0.248836	0.250833	0.80
0.3	0.555208	0.559112	0.70
0.4	0.975561	0.981829	0.64
0.5	1.501648	1.512425	0.72
0.6	2.123316	2.137987	0.69
0.7	2.828762	2.847177	0.65
0.8	3.604837	3.629746	0.69
0.9	4.437309	4.466392	0.66
1.0	5.311148	5.348440	0.70

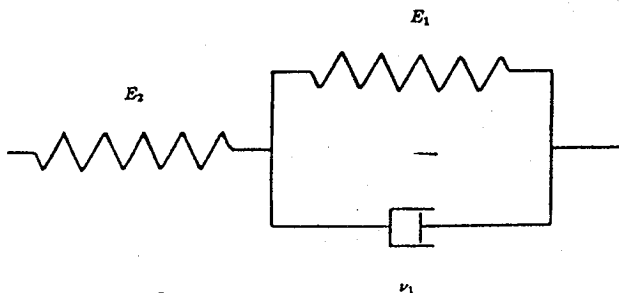[a]% differences are with respect to 40-element solution.

Fig. 2 Ideal three-element "limited" creep model.

Table 3 Comparison[a] of integral and differential[b] elastic solutions for various loads with $a/l = 0.05$

Transverse deflection (cm) from various solutions

$s = \bar{s}/l$	Integral	Differential	% diff[c]	Angle, deg
		$P/P_e = 0.25$		
0.0	0.000000	0.000000	—	0.00
0.1	0.006642	0.006645	0.04	0.25
0.2	0.026543	0.026538	−0.02	0.50
0.3	0.059548	0.059550	0.00	0.74
0.4	0.105461	0.105489	0.03	0.98
0.5	0.164059	0.164056	0.00	1.22
0.6	0.234887	0.234907	0.01	1.44
0.7	0.317525	0.317579	0.02	1.66
0.8	0.411579	0.411592	0.00	1.87
0.9	0.516270	0.516329	0.01	2.07
1.0	0.631223	0.631182	−0.01	2.25
		$P/P_e = 0.50$		
0.0	0.000000	0.000000	—	0.00
0.1	0.021039	0.021044	0.02	0.79
0.2	0.083962	0.083932	−0.04	1.57
0.3	0.187808	0.187828	0.01	2.33
0.4	0.331320	0.331511	0.06	3.07
0.5	0.513103	0.513077	0.00	3.76
0.6	0.730283	0.730400	0.02	4.40
0.7	0.980300	0.980618	0.03	5.01
0.8	1.260747	1.260810	0.01	5.52
0.9	1.566974	1.567304	0.02	6.01
1.0	1.896801	1.896542	−0.01	6.38
		$P/P_e = 0.75$		
0.0	0.000000	0.000000	—	0.00
0.1	0.062944	0.063015	0.11	2.37
0.2	0.250833	0.250858	0.01	4.68
0.3	0.559112	0.559534	0.08	6.91
0.4	0.981829	0.983259	0.15	9.03
0.5	1.512425	1.513218	0.05	10.97
0.6	2.137987	2.139785	0.08	12.68
0.7	2.847177	2.850330	0.11	14.23
0.8	3.629746	3.632429	0.07	15.41
0.9	4.466392	4.470819	0.10	16.44
1.0	5.348440	5.351315	0.05	17.04

[a]Comparisons based on results from 10-element models. [b]Differential solution employing an exact $\sin\phi$ formula. [c]% differences are with respect to integral solution.

Table 4 Comparison[a] of integral and differential[b] elastic solutions for various loads with $a/l = 0.5$

Transverse deflection (cm) from various solutions

$s = \bar{s}/l$	Integral	Differential	% diff[c]	Angle, deg
		$P/P_e = 0.25$		
0.0	0.000000	0.000000	—	0.00
0.1	0.006642	0.006645	0.00	0.25
0.2	0.026543	0.026538	−0.02	0.50
0.3	0.059548	0.059550	0.00	0.74
0.4	0.105461	0.105489	0.03	0.98
0.5	0.164059	0.164056	0.00	1.22
0.6	0.234887	0.234907	0.01	1.44
0.7	0.317525	0.317579	0.02	1.66
0.8	0.411579	0.411592	0.00	1.87
0.9	0.516270	0.516329	0.01	2.07
1.0	0.631223	0.631182	−0.01	2.25
		$P/P_e = 0.50$		
0.0	0.000000	0.000000	—	0.00
0.1	0.021039	0.021046	0.04	0.79
0.2	0.083962	0.083932	−0.04	1.57
0.3	0.187808	0.187830	0.01	2.33
0.4	0.331320	0.331511	0.06	3.07
0.5	0.513103	0.513080	0.00	3.76
0.6	0.730283	0.730402	0.02	4.40
0.7	0.980300	0.098620	0.03	5.01
0.8	1.260747	1.260813	0.01	5.52
0.9	1.566974	1.567307	0.02	6.01
1.0	1.896801	1.896547	−0.01	6.38
		$P/P_e = 0.75$		
0.0	0.000000	0.000000	—	0.00
0.1	0.062944	0.063017	0.12	2.37
0.2	0.250833	0.250868	0.01	4.68
0.3	0.559112	0.559559	0.08	6.91
0.4	0.981829	0.983305	0.15	9.03
0.5	1.512425	1.513286	0.06	10.97
0.6	2.137987	2.139881	0.09	12.68
0.7	2.847177	2.850459	0.12	14.23
0.8	3.629746	3.632594	0.08	15.41
0.9	4.466392	4.471020	0.10	16.44
1.0	5.348440	5.351554	0.06	17.04

[a]Comparisons based on results from 10-element models. [b]Differential solution employing an approximate $\sin\phi$ formula. [c]% differences are with respect to integral solution.

tensionality" of the integral model. These changes did produce a differential model with an effectively inextensional centroidal axis. It was anticipated that this would further improve the correlation between the differential and integral results. Unfortunately, such was not the case.

When the angle of rotation is very small, such as one that results from a low level of loading and minimal eccentricity, all formulations provide virtually identical predictions. Increases in the angle of rotation, however, due to increases in loading or eccentricity or both, cause the modified differential predictions to diverge from those of the others. This divergence between results increased with both load magnitude and eccentricity.

This behavior is attributed to the manner in which the modified numerical model handles the end deflection of the beam-column. In the modified model, the end of the beam-column effectively moves only in the vertical direction (see Fig. 1). The standard differential model as well as the integral model, however, include influences generated when the end can move both vertically and horizontally. Thus, for any given vertical deflection, the horizontal movement that occurs in the integral and unmodified differential models acts to increase the angle of rotation. This, in turn, reduces the magnitude of the applied moment [see Eq. (23)]. Therefore, at any particular given vertical deflection, the moment loading in the standard formulation model is lower than that in the modified version. Effectively, the moment decreases a greater amount in the un-

modified model than it does in the modified model at equivalent amounts of transverse deflection. This, in turn, implies that the beam-column of the unmodified model would not deflect as much as the one of the modified model would.

The implication is that the numerical modeling of the influence of deformation on loading is an important factor. This conclusion is consistent with the observations made concerning how the structure of the integral equation, Eq. (5), changes as a result of the interaction between loading and deflection. Additionally, it should be noted that neglecting centroidal axis strain in the differential technique does not necessarily provide an effect equivalent to the assumption of inextensionality in the integral techniques. This is attributed to the fact that the elimination of the centroidal axis strain in the differential formulation can be accomplished only at the expense of reducing the actual coupling between deformation and loading.

For both methods, the initial elastic deflection of the beam-column provides the initial condition for the viscoelastic deformation. Consequently, any differences in the initial elastic responses predicted by the two methods will only be accentuated during the subsequent period of time-dependent behavior. The comparisons discussed demonstrate that the two methods provide virtually identical predictions of initial elastic deformation. Table 6 provides a typical comparison for the integral and the differential (exact $\sin\phi$) method predictions for the viscoelastic deflection of the beam-column over a period of two

$s = \bar{s}/l$	Integral	Differential	% diff[c]	Angle, deg
		$P/P_e = 0.25$		
0.0	0.000000	0.000000	—	0.00
0.1	0.006642	0.006645	0.00	0.25
0.2	0.026543	0.026533	−0.04	0.50
0.3	0.059548	0.059548	0.00	0.74
0.4	0.105461	0.105479	0.02	0.98
0.5	0.164059	0.164048	−0.01	1.22
0.6	0.234887	0.234894	0.00	1.44
0.7	0.317525	0.317576	0.02	1.66
0.8	0.411579	0.411589	0.00	1.87
0.9	0.516270	0.516349	0.02	2.07
1.0	0.631223	0.631210	0.00	2.25
		$P/P_e = 0.50$		
0.0	0.000000	0.000000	—	0.00
0.1	0.021039	0.021067	0.13	0.79
0.2	0.083962	0.084005	0.05	1.57
0.3	0.187808	0.188041	0.12	2.33
0.4	0.331320	0.331889	0.17	3.07
0.5	0.513103	0.513776	0.13	3.76
0.6	0.730283	0.731457	0.16	4.40
0.7	0.980300	0.982246	0.20	5.01
0.8	1.260747	1.263051	0.18	5.52
0.9	1.566974	1.570406	0.22	6.01
1.0	1.896801	1.900517	0.20	6.38
		$P/P_e = 0.75$		
0.0	0.000000	0.000000	—	0.00
0.1	0.062944	0.064879	3.07	2.37
0.2	0.250833	0.258313	2.98	4.68
0.3	0.559112	0.576725	3.15	6.91
0.4	0.981829	0.014219	3.30	9.03
0.5	1.512425	1.562702	3.32	10.97
0.6	2.137987	2.212025	3.46	12.68
0.7	2.847177	2.950167	3.62	14.23
0.8	3.629746	3.763475	3.68	15.41
0.9	4.466392	4.636892	3.82	16.44
1.0	5.348440	5.554259	3.85	17.04

[a]Comparisons based on results from 10-element models. [b]Influences of centroidal axis strain terms suppressed. [c]% differences are with respect to integral solution.

$s = \bar{s}/l$	Integral	Differential	% diff[c]	Angle, deg
		at time $= 0$		
0.0	0.000000	0.000000	—	0.00
0.1	0.021039	0.021044	0.02	0.79
0.2	0.083962	0.083932	−0.04	1.57
0.3	0.187808	0.187828	0.01	2.33
0.4	0.331320	0.331511	0.06	3.07
0.5	0.513103	0.513077	0.02	3.76
0.6	0.730283	0.730400	0.02	4.40
0.7	0.980300	0.980618	0.03	5.01
0.8	1.260747	1.260810	0.01	5.52
0.9	1.566974	1.567304	0.02	6.01
1.0	1.896801	1.896542	−0.01	6.38
		at time $= \tau_0$		
0.0	0.000000	0.000000	—	0.00
0.1	0.038311	0.038326	0.04	1.44
0.2	0.152784	0.152725	−0.04	2.86
0.3	0.341170	0.341234	0.02	4.22
0.4	0.600532	0.600994	0.08	5.54
0.5	0.927608	0.927590	0.00	6.76
0.6	1.315809	1.316129	0.02	7.86
0.7	1.759290	1.760083	0.05	8.87
0.8	2.252647	2.252896	0.01	9.70
0.9	2.785532	2.786395	0.03	10.44
1.0	3.353191	3.352810	−0.01	10.95
		at time $= 2\tau_0$		
0.0	0.000000	0.000000	—	0.00
0.1	0.048583	0.048611	0.06	1.83
0.2	0.193685	0.193629	−0.03	3.62
0.3	0.432178	0.432313	0.03	5.34
0.4	0.759968	0.760689	0.09	7.00
0.5	1.172517	1.172627	0.01	8.52
0.6	1.660764	1.661396	0.04	9.88
0.7	2.216699	2.218045	0.06	11.13
0.8	2.832971	2.833680	0.03	12.12
0.9	3.495617	3.497252	0.05	12.99
1.0	4.198267	4.198371	0.00	13.55

[a]Comparisons based on results from 10-element models. [b]Differential solution employing an exact $\sin\phi$ formula. [c]% differences are with respect to integral solution.

material time constants. The viscoelastic model employed for these computations is the three-parameter "limited" creep material illustrated in Fig. 2. As noted previously, the material parameters were selected so that the material time constant τ_0 equals unity. The load and eccentricity ratios for this particular set of results were $P/P_e = 0.50$ and $a/l = 0.05$, respectively.

As demonstrated by this data, the high correlation between the integral and differential method predictions for the initial elastic deflections carries over directly to the viscoelastic analysis. The time-dependent deflection predicted by one technique is virtually indistinguishable from that predicted by the other. This indicates that the differential formulation methodology employed to account for the influence of viscoelastic strain provides the equivalent effect as the hereditary integral component of the integral formulation. As such, this lends high confidence to the differential solution methodology.

It should be noted that these particular numerical results are typical of other results obtained for higher, as well as lower, loads and eccentricities. Generally, the correlation between the solutions was not influenced by the magnitude of the loading or the amount of load eccentricity.

A minor, high-order-type influence was, however, noted. As the angle of rotation became very large, on the order of 45 deg, a small but distinct divergence in predicted deflections was observed. Typically, the rate of increase in deflection predicted by the differential formulation would begin to slightly exceed

that predicted by the integral method. Normally, this could be observed as time approached two material time constant for the highest loads (P/P_e approaching unity) and with extremely large eccentricities. Under some conditions, it also could be observed as time exceeded four to five material time constants.

These observed differences between the two sets of predictions were still very small. Generally, they were on the order of 0.10%. Thus, from a practical viewpoint, they are totally negligible with respect to normal accuracy requirements for engineering computation. It is mentioned here only to indicate that, under conditions such as these, the accumulation of numerical errors may begin to influence the results. A comparison between the integral and the approximate $\sin\phi$ differential solution results was not included because the differences between the exact and approximate differential solution results are again so small as to be negligible.

The final item meriting discussion is the length of the time increment used in each of the formulations. Unlike the prior results, some differences do exist between the maximum allowable time-step increments for the integral and differential formulations. Additionally, the allowable time-step increment for the integral formulation exhibits a higher dependence on the actual angle of rotation than does the differential formulation.

In general, a relatively small time step increment must be used with the integral solution methodology. For example, the results previously presented typically employed a 0.01-time-

step increment. As the length of this time step is increased, the accuracy of the solution decreases and tends to underpredict the deflection. This convergence "from below" is not surprising since the convolution integral is approximated as the sum of a finite number of terms.

In contrast, much larger time-step increments were used with the differential formulation. This is principally attributed to the high accuracy provided by the Runge-Kutta integration routine. Most of the results provided were developed using a 0.10 time step. The use of even larger time steps was also examined. It was found that time increments four to five times greater than 0.10 could be employed without significant changes in the calculated results. Additionally, the allowable length of this time-step increment tended to be rather insensitive to the angle of rotation. The allowable time step for the integral formulation, on the other hand, exhibited a high level of sensitivity to the angle of rotation. Larger angles of rotation required significantly shorter time steps for accurate results to be obtained.

These factors combine in a rather interesting manner with regard to which method of analysis is computationally more efficient. Typically, for the analysis of short periods of viscoelastic deformation, the integral solution method was two to three times faster than the differential method. This is attributed to two factors. The first is the comparitively slow Runge-Kutta integration procedure used in the differential formulation. For a short period of viscoelastic deformation, the calculation of the convolution integral of the integral formulation, requiring simple summation of a limited number of terms, can be performed much more rapidly.

The second factor is that the fixed-point iteration scheme of the integral formulation, although requiring more iterations than the Newton method, is also performed more rapidly since it is simply an algebraic operation. The Newton method, in contrast, requires inversion of the matrix, premultiplying the vector of trial function corrections, and then numerical evaluation through solution of the system of equations. Even for just a 10-element beam, this process is slow in comparison to the fixed-point iteration.

However, as the length of the period of viscoelastic deformation increases, this relative speed relationship reverses. Eventually, the differential formulation begins to generate solutions more rapidly than the integral method. In the example problem previously described, this generally occurred approximately between the second and third time constants. The reason for this change is directly related to the computation of the convolution integral of the integral technique. As time increases, the number of terms in the summation increases linearly. This, in turn, increases the number of algebraic operations that must be performed and therefore linearly increases the time need for each complete computation. In contrast, the speed of the Runge-Kutta integration routine is virtually independent of time. Thus, the continually increasing computational effort required in the integral technique eventually exceeds that need for the differential technique. This reverses the relative speed relationship.

Conclusions

Based on the results reported herein and elsewhere,[12] it is concluded that the differential formulation procedure presented can be employed for the analysis of quasistatic nonlinear one-dimensional viscoelastic problems. This conclusion is based directly on the high level of correlation between results developed using this formulation technique to those obtained with the previously published integral method for solution of such problems. Additionally, it is observed that both of these methods exhibit exceptionally similar accuracy characteristics with regard to the number of elements employed in the approximation. For both, a relatively low number of elements can be used without engendering any significant errors.

References

[1]Christensen, R. M., *Theory of Viscoelasticity, An Introduction*, Academic, New York, 1982.

[2]Rabotnov, Y. N., *Elements of Hereditary Solid Mechanics*, Mir Publications, Moscow, USSR, 1980.

[3]Schapery, R. A., "Approximate Methods of Transform Inversion for Viscoelastic Stress Analysis," *Proceedings of the 4th US National Congress on Applied Mechanics*, Vol. 2, 1962, pp. 1075–1085.

[4]Kraus, H., *Creep Analysis*, Wiley, New York, 1980.

[5]Libove, C., "Creep Buckling of Columns," *Journal of the Aeronautical Sciences*, Vol. 19, July, 1952, pp. 459–467.

[6]Zyczkowski, M., "Geometrically Non-Linear Buckling of Bars," *IUTAM Colloquium on Creep in Structures*, Academic, New York, 1962, pp. 307–325.

[7]Patel, S. A., "Buckling of Columns in the Presence of Creep," *The Aeronautical Quarterly*, Vol. 7, No. 2, April–June 1956, pp. 25–134.

[8]Hoff, N. J., "A Survey of the Theories of Creep Buckling," *Proceedings of the 3rd U.S. National Congress of Applied Mechanics*, 1958, pp. 29–49.

[9]Rogers, T. G. and Lee, E. H., "On the Finite Deflection of a Viscoelastic Cantilever," *Proceedings of the 4th U.S. National Congress on Applied Mechanics*, Vol. 2, 1962, pp. 977–987.

[10]Stubstad, J. M. and Simitses, G. J., "Bounding Solutions of Geometrically Nonlinear Viscoelastic Problems," *AIAA Journal*, Vol. 24, Dec. 1986, pp. 1843–1850.

[11]Thurston, G., "Newton's Method Applied to Problems in Nonlinear Mechanics," *Journal of Applied Mechanics*, Vol. 32, No. 2, 1965, pp. 383–388.

[12]Stubstad, J. M., "Nonlinear Thermoviscoelastic Analysis of Metallic Plane Curved Beams," Ph.D. Thesis, Georgia Inst. of Technology, Atlanta, GA, 1986.

[13]Vinogradov, A. M. "Nonlinear Effects in Creep Buckling Analysis of Columns," *Journal of Engineering Mechanics*, Vol. 111, No. 6, 1985, pp. 757–767.

[14]Vinogradov, A. M. and Wijewerra, H., "Theoretical and Experimental Studies on Creep Buckling," *Proceedings of the AIAA/ASME/ASCE/AHS 26th Structures, Structural Dynamics and Materials Conference*, AIAA, New York, 1985, Vol. 1, pp. 160–164.

[15]Tricomi, F. G., *Integral Equations*, Dover, New York, 1985, pp. 42–47.

CREEP ANALYSIS OF BEAMS AND ARCHES BASED ON A
HEREDITARY VISCO-ELASTIC-PLASTIC CONSTITUTIVE LAW

J. M. Stubstad and G. J. Simitses
Georgia Institute of Technology
Atlanta, Georgia

ABSTRACT

An analytic study of planar beams and arches subjected to signifi-
cant thermal cycling from ambient temperatures up to 800 °C is presented.
In the study, a recently developed unified nonlinear hereditary type of vis-
coelastoplastic constitutive law is employed to characterize the time- and
temperature-dependent properties of a typical aerospace alloy, Hastelloy X.

The results from this work demonstrate that a strong interaction
exists between the backstress variable of this particular constitutive law
,and the time-dependent stress distribution produced by the geometry of
the deformation. Effectively, this interaction tends to control, in a highly
nonlinear manner, the creep-ratchetting response of the beam and the arch.
An unexpected consequence of this is that temperature gradients in the
thickness direction, a factor normally neglected in most studies, tends to
exert an important influence on the response during thermal cycling.

NOMENCLATURE

a	load eccentricity
A	cross sectional area of beam or arch
b	width of beam or arch
c_{ij}	inelastic strain tensor
d	deformation vector for points on the centroidal axis
E	Young's Modulus
E_0, E_1, E_2	zero, first and second moments of the elastic modulus across a cross section, respectively
g_α, G_α	base vectors for undeformed and deformed configurations
$g_{\alpha\beta}, G_{\alpha\beta}$	metric components of the undeformed and deformed configurations
h	depth of beam or arch
k	$\kappa + \frac{\partial\phi}{\partial s}$
K	drag stress
K_1, K_2	constitutive law constants
n_1 thru n_7	constitutive law constants
m, n	constitutive law exponents

M, N	moment and force resultants
M_c, N_c	creep strain moment and force pseudo-resultants
M_θ, N_θ	thermal strain moment and force pseudo-resultants
p	pressure load
P, V	axial and transverse force resultants
$Q(t), \Upsilon(t)$	constitutive law functions
r, R	position vectors in undeformed and deformed configurations
s, η	coordinates along length and depth directions
s_{ij}	components of the deviator stress tensor
t, n, k	triad of unit vectors for the undeformed configuration
T, N, K	triad of unit vectors for the deformed configuration
t	time
u, w	axial and transverse displacement of the centroidal axis
α	coefficient of thermal expansion
ϵ_o	centroidal axis strain
ϵ_{ij}	strain tensor component
Θ	change in temperature
κ	initial curvature of the arch
λ, μ	Lamè constants
σ_{ij}	stress tensor component
ϕ	angle of rotation of cross section
Ω_{ij}	backstress

INTRODUCTION

It is well known that metal alloys can undergo transitions in behavior
as temperature increases. Commonly, for loading substantially below yield,
the elastic response observed at room temperature generally gives way to a
time-dependent viscoelastic response at somewhat elevated temperatures.
Further increases in temperature, however, introduces the potential for sud-
den "rapid" or plastic type deformation. Such transitions can significantly
shorten the useful life of the structural element and generate the possibil-
ity of a sudden unanticipated failure. Consequently, for many years the
aerospace and nuclear power industries, where elevated temperature oper-
ating environments abound, have had a continuing interest in predicting
the behavior of metallic structural elements subjected to such conditions.

Early investigators [1-3] generally focused their attention on the be-
havior of structural components subjected to conditions of constant load at

constant uniform elevated temperatures. Many of these studies employed simplified analyses to improve mathematical tractability. Additionally, "experimentally based equation of state" type constitutive laws were often used to express the nonlinear elevated temperature time-dependent behavior of the material. A summary of many of methods developed and key findings obtained is provided by Hoff [4].

These efforts answered many of the questions regarding elevated temperature creep buckling. However, they were not able to satisfactorily describe the creep ratchetting behavior resulting from thermal cycling at elevated temperatures. Consequently, it was not until Miller [5] and Edmunds and Beer [6], both of whom considered nuclear pressure vessels, that this particular form of behavior was specifically addressed. Subsequently, Bree [7,8] investigated basic factors which determine when this type of response could occur. These studies led to experimental investigations and other analytic studies to explore various aspects of the phenomena. The works of Conway et. al. [9], Corum [10,11] and Mukhejeree, Kumar and Chang [12] provide a representative sampling of these efforts.

However, the greatest concentration of effort has been directed toward improving the capability to predict the elevated temperature behavior of metals. The contributions of Hart [13,14], Pointer and Leckie [15], Pugh [16-18], Krempl [19], and Walker and Krempl [20], to name of few, provide a dramatic illustration of the intensity of these efforts to develop advanced constitutive models. Yet, as pointed out by Corum and Sartory [21], an equation of state approach to constitutive modeling is still generally used in design situations. However, as Pugh [18] has noted, the newer types of unified constitutive laws, where inelastic strain is not divided into distinct creep and plasticity components, can provide an alternate approach.

Consequently, one of the aims of this study is to examine the use of a typical unified constitutive model in an analysis of the behavior of structural elements subject to thermal cycling from an elevated ambient temperature. The specific law which was selected is one developed by Walker [22] to model the time- and temperature-dependent behavior of Hastelloy X, an alloy routinely used in the aerospace industry.

The study results indicate that, with this particular constitutive law and material, an implicit interaction exists between the stress in the member and the backstress of the constitutive law. This interaction strongly influences the ultimate response. This result is significant for two reasons. First, because saturation of the backstress of this constitutive law can lead to plastic response, it indicates that the ultimate reliability of any predicted results rests strongly upon the accuracy with which the backstress growth law parameters have been determined.

Additionally, this aspect produces the rather interesting result that, due to the strong temperature dependence of the material constants of the law, temperature variations in the thickness direction greatly influence predicted response. This is significant for any analysis since the influences of such temperature variations are generally neglected.

MATHEMATICAL FORMULATION

To focus principally upon the interaction between the response of the structural element and the prediction of thermal dependence of the material, the problem is formulated within the context of a simplified beam theory. Consequently, it is assumed that the beam or arch deforms in accordance with the Euler-Bernoulli hypotheses. As such, cross sectional planes normal to the centroidal axis in the undeformed geometry are assumed to remain plane and normal in the deformed state. Similarly, extensional straining in the thickness and depth directions are neglected. Thus, based on the geometry illustrated in Fig. 1, the position vectors r and R, where

$$r = r_o + \eta n \quad \text{and} \quad R = r_o + d + \eta N \qquad (1)$$

are employed to locate a typical point on an arbitrary cross section in the undeformed and deformed configurations, respectively. Note that η represents the coordinate in the normal direction. Also, lower case and upper case symbols are employed to denote quantities referred to the undeformed and deformed configurations, respectively.

Base vectors for the reference and current state, g_α and G_α, respectively, are defined by

$$g_\alpha = \frac{\partial r}{\partial \alpha} \quad \text{and} \quad G_\alpha = \frac{\partial R}{\partial \alpha} \quad \text{where} \quad \alpha = s, \eta \qquad (2)$$

Consequently, the deformation vector which translates a point from the undeformed to deformed configurations, denoted as d, can be expressed as

$$d + \eta N = (u + \eta \sin \phi)t + (w + \eta \cos \phi)n \qquad (3)$$

where u and w represent axial and transverse displacement functions for points on the centroidal axis, respectively. Substitution of Eqns. (1) and (3) into (2), followed by differentiation and subsequent employment of the Fernet-Serret formulae and the strain definition,

$$\gamma_{\alpha\beta} = \frac{1}{2}(G_{\alpha\beta} - g_{\alpha\beta}); \quad \text{where} \quad g_{\alpha\beta} = g_\alpha \bullet g_\beta, \quad G_{\alpha\beta} = G_\alpha \bullet G_\beta \qquad (4)$$

yields the strain expressions

$$\gamma_{ss} = \frac{1}{2}\left\{(1 + \frac{\partial u}{\partial s} + \kappa w + \eta k \cos \phi)^2 + (\frac{\partial w}{\partial s} - \kappa u - \eta k \sin \phi)^2 - (1 + \eta \kappa)^2\right\} \qquad (5a)$$

$$\gamma_{s\eta} = \frac{1}{2}\left\{(1 + \frac{\partial u}{\partial s} + \kappa w + \eta k \cos \phi) \sin \phi + (\frac{\partial w}{\partial s} - \kappa u - \eta k \sin \phi) \cos \phi\right\} \qquad (5b)$$

and

$$\gamma_{\eta\eta} = \frac{1}{2}\left\{\sin^2 \phi + \cos^2 \phi - 1\right\} = 0 \qquad (5c)$$

In these, $k = \kappa + \partial \phi/\partial s$, where κ denotes the initial constant curvature of the arch and ϕ represents the angle of rotation of the cross section.

From the Euler-Bernoulli hypotheses, the shear strains must vanish. Consequently, from this requirement Eqn. (5b) yields

$$\tan \phi = \frac{-(\frac{\partial w}{\partial s} - \kappa u)}{(1 + \frac{\partial u}{\partial s} + \kappa w)} \qquad (6)$$

Therefore, employing the definition

$$1 + 2\epsilon_o = (1 + \frac{\partial u}{\partial s} + \kappa w)^2 + (\frac{\partial w}{\partial s} - \kappa u)^2 \qquad (7)$$
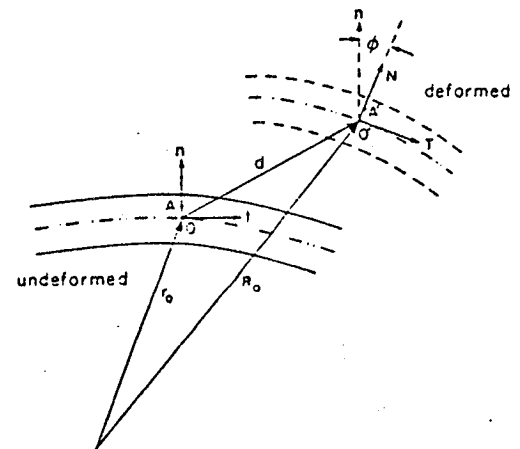

Figure 1. Geometry of Deformation.

43

and Eqn. (6) it is relatively easy to show that

$$\sin\phi = \frac{-(\frac{\partial w}{\partial s} - \kappa u)}{\sqrt{1 + 2\epsilon_o}} \quad \text{and} \quad \cos\phi = \frac{1 + \frac{\partial u}{\partial s} + \kappa w}{\sqrt{1 + 2\epsilon_o}} \quad (8)$$

Thus, expanding Eqn. (5a) and employing Eqns. (7) and (8) yields

$$\gamma_{ss} = \epsilon_o + \eta\{\kappa\sqrt{1 + 2\epsilon_o} - \kappa + \sqrt{1 + 2\epsilon_o}\frac{\partial \phi}{\partial s}\} + \eta^2\{\kappa + \frac{1}{2}\frac{\partial \phi}{\partial s}\}\frac{\partial \phi}{\partial s} \quad (9)$$

From the above it is clear that ϵ_o represents the strain induced along the centroidal axis. Since, for a thin arch or beam, the last term of Eqn. (9) should be small in comparison to the others, it may be neglected. Similarly, additional simplifications may be obtained for the case where the centroidal axis strain is sufficiently small so that it may be neglected in comparison to one. Based on these assumptions, Eqn. (9) simplifies to the standard form

$$\gamma_{ss} \approx \epsilon_o + \eta\frac{\partial \phi}{\partial s} \quad (10)$$

Equilibrium equations are obtained through application of the Principle of Virtual Work. Stress resultants, N and M, are defined such that

$$N = \int_A \sigma \, dA \quad \text{and} \quad M = \int_A \sigma\eta \, dA \quad (11)$$

Note that

$$\delta\phi = \frac{\partial \delta v_1}{\partial s} + k\delta v_2 \quad (12a)$$

$$\delta\epsilon = \frac{\partial \delta v_2}{\partial s} - k\delta v_1 \quad (12b)$$

where $\delta\phi$ and $\delta\epsilon$ denote the incremental changes in rotation and centroidal axis strain resulting from the deformed configuration axial and transverse displacement changes, δv_1 and δv_2, respectively.

Consequently, from the Principle of Virtual Work,

$$\delta W_{est} = [M\delta\phi + N\delta v_1 + Q\delta v_2]_1^2 + \int_1^2 -p^*\delta v_2 \, ds \quad (13)$$

Expressing the first term on the right hand side in terms of an integral over the length and then combining that result with the work term yields

$$\delta W_{est} = \int_1^2 \left[\frac{\partial M}{\partial s}\delta\phi + M\frac{\partial \delta\phi}{\partial s} + \frac{\partial N}{\partial s}\delta v_1 + N\frac{\partial \delta v_1}{\partial s} + \frac{\partial Q}{\partial s}\delta v_2 + Q\frac{\partial \delta v_2}{\partial s} - p^*\delta v_2\right] ds \quad (14)$$

Therefore, employing Eqns. (12) and noting that terms multiplying the virtual displacements δv_1, δv_2 and $\delta\phi$ must vanish identically yields, after eliminating the shear resultant, the equilibrium equations

$$kN - \frac{\partial^2 M}{\partial s^2} = p^* \quad \text{and} \quad \frac{\partial N}{\partial s} + k\frac{\partial M}{\partial s} = 0 \quad (15)$$

with the associated boundary conditions at $s = 0, l$

$$N = N^* \quad \text{or} \quad \delta v_1 = 0$$
$$\frac{\partial M}{\partial s} = -Q^* \quad \text{or} \quad \delta v_2 = 0 \quad (16)$$
$$M = M^* \quad \text{or} \quad \delta\phi = 0$$

where N^*, Q^*, and M^* denote the axial, shear and moment resultants applied at the ends of the arch, respectively.

Expressions for the force and moment resultants, N and M, respectively, are obtained from the constitutive law. A unified hereditary viscoelastic-plastic law developed by Walker [22] to characterize the time and temperature dependence of Hastelloy X is employed. The selection of
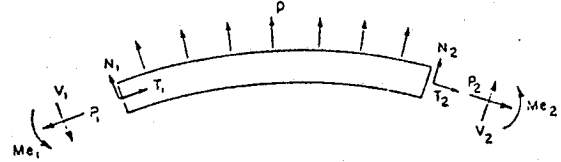

Figure 2 External Forces and Moments Acting on the Arch.

Walker's functional theory, a highly generalized representation for a three parameter viscoelastic solid, was based on three considerations. First, from a strictly practical point of view, a substantial body of experimental work [22-24] had been performed to establish the temperature dependence of the constitutive law parameters for a wide range of temperatures. These efforts included a validation which examined the predictive capability of the law through a comparison of analytical and experimental results for time variable thermo-mechanical load cycling of uniaxial specimens.

A second factor which favored selection of the Walker law was that it is able to reproduce forms of classical behavior as limiting cases. For example, saturation of the drag stress produces an effect equivalent to isotropic hardening of a material. Similarly, saturation of the backstress produces an effect equivalent to kinematic hardening. Finally, the associated laws which govern the evolution of the state variables provide for the opportunity to include effects related to both dynamic and static thermal recovery.

The final reason for selection of the Walker law is that it can be expressed in both differential and integral formats. For this particular study, the differential format of the law was found to be the most convenient. However, it was hoped that the availability of an integral format would provide, at a future date, the opportunity to extend some prior work involving kinematic bounding of nonlinear integral formulations [25] to also include some form of constitutive bounding.

The general integral form of Walker's functional theory has been provided in Appendix A. That appendix also contains a derivation of the differential form from the integral format. It should be noted that, in the modeling of the elevated temperature behavior of Hastelloy X, additional simplifications in the form of the law were possible. These simplifications resulted from the fact that, for Hastelloy X, a number of material constants are zero over the entire temperature range.

Due to these simplifications, the differential format of Walker's functional theory, for one-dimensional loading of Hastelloy X, has the form

$$\dot{\epsilon}_e = \text{sign}(\sigma - \Omega_{11})\left(\frac{\text{abs}(\sigma - \Omega_{11})}{K}\right)^n \quad (17a)$$

$$\dot{\Omega}_{11} = \dot{\Omega}_{11}^o + n_2\dot{\epsilon}_e - (\Omega_{11} - \Omega_{11}^o)(\dot{G} - \frac{1}{n_2}\frac{\partial n_2}{\partial \Theta}\dot{\Theta}) \quad (17b)$$

$$\dot{\Omega}_{11}^o = \frac{\Omega_{11}^o}{\Omega^o}\dot{\Theta} \quad (17c)$$

$$K = K_1 \quad (17d)$$

and

$$\dot{G} = n_3\text{abs}(\dot{\epsilon}_e) + n_6(\text{abs}\{\Omega_{11}\})^{m-1} \quad (17e)$$

Finally, since the time rate of change of temperature is relatively low in the sample problems, all terms where $\dot{\Theta}$ appeared were assumed to be insignificant and therefore neglected. Note that this provides some minor simplifications to Eqn. (17b) and makes the reference backstress, Ω_{11}^o, independent of the time rate of change in temperature.

The law is based on an additive decompostion of the strain into elastic, thermal and inelastic components, ϵ_e, ϵ_θ and ϵ_i, respectively. Thus,

$$\epsilon_o + \eta \frac{\partial \phi}{\partial s} = \epsilon_o + \epsilon_\phi + \epsilon_\epsilon \tag{18}$$

For the state of one-dimensional loading considered, this yields

$$\sigma = E(\epsilon_o + \eta \frac{\partial \phi}{\partial s} - \epsilon_\phi - \epsilon_\epsilon) \tag{19}$$

Therefore, integrating this expression over the cross section and employing the force resultant definition, Eqn. (11), yields

$$N = E_o \epsilon_o + E_1 \frac{\partial \phi}{\partial s} - N_\phi - N_\epsilon \tag{20}$$

where E_0 and E_1 denote the zero and first integrals of the elastic modulus over the cross section and N_ϕ and N_ϵ represent "pseudo-resultant" type quantities defined as

$$N_\phi = \int_A E\epsilon_\phi \, dA \quad \text{and} \quad N_\epsilon = \int_A E\epsilon_\epsilon \, dA \tag{21}$$

Note that the first integral of the elastic modulus over the cross section, E_1, does not necessarily vanish since the elastic modulus is a function of the temperature, which is not necessarily constant across a cross section. An interseting aspect of this is that it induces a form of bending-stretching coupling {see also Eqn. (22)} similar to that of a laminated composite material. Finally, it should be noted that, although the quantities defined by Eqn. (21) have the units of a force resultant, these definitions are merely employed to simplify subsequent expressions.

Multiplying Eqn. (19) by the coordinate, η, integrating over the cross section and employing the moment resultant definition, Eqn. (12), yields

$$M = E_1 \epsilon_o + E_2 \frac{\partial \phi}{\partial s} - M_\phi - M_\epsilon \tag{22}$$

where E_2 denotes the second integral of the elastic modulus over the cross section and the "pseudo-moment" resultants are defined by

$$M_\phi = \int_A \eta E\epsilon_\phi \, dA \quad \text{and} \quad M_\epsilon = \int_A \eta E\epsilon_\epsilon \, dA \tag{23}$$

Consequently, substituting Eqns. (20) and (22) into Eqns. (15) yields the general governing relations

$$kE_0\epsilon_o + kE_1 \frac{\partial \phi}{\partial s} - E_1 \frac{\partial^2 \epsilon_o}{\partial s^2} - E_2 \frac{\partial^3 \epsilon_o}{\partial s^3} = p^* + k(N_\epsilon + N_\phi) + \frac{\partial^2}{\partial s^2}(M_\epsilon + M_\phi) \tag{24}$$

and

$$(E_0 + kE_1)\frac{\partial \epsilon_o}{\partial s} + (E_1 + kE_2)\frac{\partial^2 \phi}{\partial s^2} = \frac{\partial}{\partial s}(N_\epsilon + N_\phi) + k(M_\epsilon + M_\phi) \tag{25}$$

In the development of these relationships, it is assumed that the moments of the elastic modulus, E_0, E_1 and E_2, are constant with respect to the axial coordinate. This implies that these quantities are independent of stress or strain and that the temperature is constant along the length direction.

Equations (24) and (25) represent a pair of interrelated spatially dependent nonlinear differential relationships which describe the deformation of the beam or arch. In their present form, they are stated in terms of the strain along the centroidal axis and the rotation of the cross section. These two quantities, in turn, are interrelated through the axial and transverse displacements of the centroidal axis. Substitution of the appropriate expressions for the centroidal axis strain and cross section rotation ultimately results in a set of equations, one of third order and the other of fourth order, in terms of these displacement functions.

Due to the significant nonlinearity of these equations, a numerical method of solution was selected. The particular method employed is an adaptation of Newton's method for the solution of nonlinear algebraic equations [26]. The basic approach is an iterative procedure where a "close" trial solution is directed towards the actual solution. Note that this method neither guarantees convergence to a solution nor that a solution is unique.

The basic methodology is to expand a nonlinear differential term such as $dX^m dY^n$, where dX and dY represent differentials of the functions X and Y and m and n represent integer exponents, into the sum and products of trial solutions $\bar{X}$ and $\bar{Y}$ and corrections of the form ΔX and ΔY. Consequently, substituting $X = \bar{X} + \Delta X$ and $Y = \bar{Y} + \Delta Y$ yields,

$$dX^m dY^n = d\bar{X}^m d\bar{Y}^n + m d\bar{X}^{m-1} d\bar{Y}^n d(\Delta X) + n d\bar{X}^m d\bar{Y}^{n-1} d(\Delta Y) + f(\bar{X}, \bar{Y}) O[\Delta X, \Delta Y] \tag{26}$$

where $f(\bar{X}, \bar{Y}) O[\Delta X, \Delta Y]$ represents a nonlinear function of $\bar{X}$ and $\bar{Y}$ of second and higher order terms in ΔX and ΔY. Provided the trial solution is close to the true solution, these higher order terms should be small in comparison to the linear terms and thus may be neglected. Consequently, the nonlinear term may be closely approximated by the linear form

$$dX^m dY^n \approx d\bar{X}^m d\bar{Y}^n + m d\bar{X}^{m-1} d\bar{Y}^n d(\Delta X) + n d\bar{X}^m d\bar{Y}^{n-1} d(\Delta Y) \tag{27}$$

With this technique, the nonlinear differential equations are approximated in terms of linear differential equations for the corrections to assumed trial functions. These coupled differential equations are then converted to a set of coupled algebraic relations through the use of central difference formulae to approximate the derivative terms for the corrections to the assumed deflections. Appendix B provides, for example, the general finite difference expressions developed for the initially circular arch.

A matrix iteration procedure is employed to refine an assumed trial solution. Each sucessive set of corrections is used to update the trial solution until convergence is obtained. Tests for such convergence included the consideration of the magnitude of each set of corrections as well as the overall accuracy for which each of the individual nodal equations was solved. In this regard it is noted that an equivalent degree of coupling did not exist between the in-plane and transverse equations of equilibrium. Typically, the accuracy of the solution of the transverse equation of equilibrium was strongly dependent upon the transverse deflection but only weakly influenced by the in-plane displacement. Conversely, the in-plane equation of equilibrium was strongly dependent upon both the transverse and in-plane deflections. Consequently, the rate of convergence of the transverse nodal equations was much more rapid than that of the in-plane ones.

In contrast to the treatment of the equations of equilibrium as a typical boundary value problem, the solution for the changes to the moment and force resultants between successive states of quasi-static equilibrium is handled as an initial value problem. As such, a fourth order Runge-Kutta integration routine was employed to integrate the constitutive law at a preselected set of points across the cross section for each axial node used in the finite difference mesh. In this process, it was assumed that the change in actual stress at each of these points could be approximated as a linear function of time over a given, reasonably short, time interval.

Once the "trial stresses" at the end of the time interval had been approximated, a Newton-Cotes quadrature formula was used to numerically approximate the force and moment resultants. These were then employed to compute the deflections for this new state of quasi-static equilibrium. From the deflection solution, a revised stress field could be calculated and compared with that which had been employed to integrate the constitutive law. The process was repeated if more than nominal differences existed between the assumed and computed changes in stress. For this, the linear approximating functions were adjusted based upon the computed stress distribution. Otherwise, the results were accepted and the analysis proceeded on to the next time increment.

This procedure was found to work very well after the first few time steps. Most of the computation effort was expended in the solution of the "boundary value" part of the problem and not in the iteration for material behavior. Principally, this was due to the fact that the rate of change in

actual stress was reasonably constant and was therefore easy to estimate between successive increments. This began to break down, however, when the behavior of the material began to resemble a plastic response. Under these conditions, the rate of change in actual stress would change rapidly even over very short time intervals. Consequently, accurately forecasting its rate of change was difficult. Thus, a greater number of iterations was needed to close the numerical loop.

NUMERICAL RESULTS

The problems considered are an eccentrically loaded cantilever beam-column and a simply supported pressure loaded shallow circular arch. In both cases, the behavior of the structural element is examined for constant loading at constant temperatures of 400, 600 and 800 °C and with sinusoidal variations about the temperatures of 400 and 600 °C. Simultaneous variations in loading and temperature are not examined. However, the potential influences of time-invariant temperature gradients in the depth direction are examined for both constant and variable temperatures.

The beam-column considered is 30.48 cm long having a square cross section of 1.27 cm depth and thickness. The eccentric load is applied 0.3048 cm below the centroidal axis yielding an eccentricity ratio of 0.01. The direction of the load is assumed to remain constant. Twelve axial nodes are used to model the beam-column. Additionally, a five point transverse grid is employed at each axial node to approximate variations in stress and strain across the cross section. One transverse grid point is located at each extreme surface of the cross section and one is positioned on the centroidal axis. The remaining two points are spaced equidistantly between these three points. It should be noted that the results from this "twelve axial node five grid" model compare favorably with results obtained using greater numbers of axial nodes and transverse grid points.

The circular arch examined is a 8.59 deg. segment of a circle. Physically, the arc length of the arch is 22.86 cm with an initial radius of curvature of 152.4 cm. For this relatively shallow arch, the rise of the centroidal axis is approximately 0.43 cm. Unlike the beam-column, the arch has a rectangular cross section 0.51 cm in width and 0.38 cm in depth. The arch is divided into fourteen segments for the numerical model. Again, a five point transverse grid is established at the location of each axial node. Similar to the beam-column, the results obtained with this "fourteen segment five transverse grid model" compare favorably with models employing greater numbers of both. Illustrations of the geometry of the beam-column and arch models are provided in Figs. 3 and 4.

Note that the dimensions selected for these sample problems are not based upon the consideration of "typical" structural elements. Instead, the dimensions are specifically chosen to accelerate the onset of time-dependent behavior. The purpose of this is to minimize the length of the initial "stable" response period thereby reducing the overall magnitude of the computational effort. In general, a "realistically" sized structural element would be appreciably stiffer and thus provide a much longer period of stable response. However, other than this extension of the "stable" useful life, the behavioral characteristics of such "realistic" structural elements would be highly similar to those of the example problems.

Finally, before proceeding with a detailed discussion of the numerical results, some introductory remarks on the principal factors which determine the form of the response merit consideration. Examination of Eqn. (17a), for instance, reveals that the inelastic strain rate is determined by the relative magnitudes of the actual stress and the backstress. The inelastic strain rate changes whenever the rate of change in actual stress varies from the rate of change of the backstress. In some situations, the rates of change of actual stress and backstress tend to equilibrate yielding a relatively constant difference. With this, the rate of inelastic straining tends to decrease to a nearly constant value. This behavior might be characterized as initial "primary creep" transitioning to "secondary" or "steady" creep .
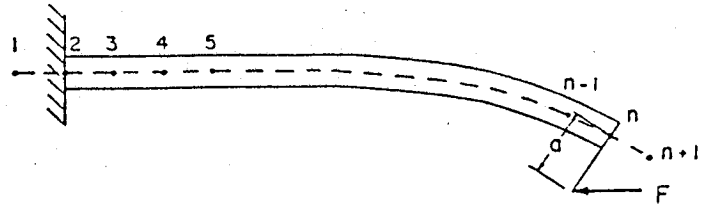

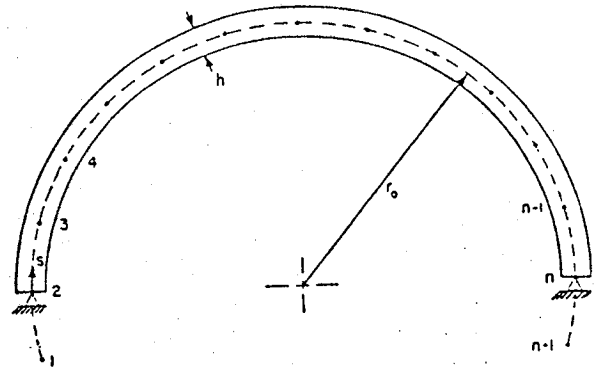Figure 3 Eccentrically Loaded Cantilever Beam-Column.

Figure 4 Axial Finite Difference Mesh for the Arch

In other cases, the rate of change in stress increases much more rapidly than the backstress. Provided the magnitude of the difference between them is not excessive, this produces a response akin to that of accelerating or "terciary" creep. The final possibility occurs when the difference between the actual stress and the backstress is very large. When this happens, the exponential nature of Eqn. (17a) creates a situation where inelastic strain rate tends to follow stress increment directly. Consequently, in the limit, the law exhibits a behavior similar to incremental plasticity.

Thus, it should be evident that the crucial factors in the analysis are those which determine how rapidly the actual stress and the backstress change with time. The most significant factors were found to be a geometrical effect related to the bending moment and the growth law for the backstress. Consequently, the overall response of the structural element was determined by the relative interaction between these effects.

The geometric effect occurs in both the beam-column and the arch. However, it is more easily visualized with respect to the beam-column geometry and therefore is described in that context. Essentially, the maximum (in magnitude) stresses in the beam-column are determined by the moment created by the end load. Transverse deflection of the beam-column, increasing the moment arm of the eccentric load, increases the magnitude of these stresses. However, tending to counterbalance this effect is the end rotation. Because the line of action of the load remains constant, end rotation reduces the effective moment arm created by the eccentricity of the load. Thus, this tends to reduce the magnitude of the end moment.

In a prior study [25] it was found that the relative significance of these two influences was related to the load eccentricity and the time-dependent characteristics of the material. For an eccentricity of the order employed in this study, these two opposing effects can approximately counterbalance one another only when beam deflection is relatively minor. Beyond this threshold, the transverse deflection effect predominates and the end moment inherently increases. Therefore, the magnitudes of the maximum stresses increase with deflection and thus also with time.

In contrast, for slowly varying temperature changes, allowing the $\dot\theta$ terms of Eqn. (17b) to be neglected, the evolution of the backstress is

46

governed by a relationship of the form

$$\dot{\Omega}_{11} = n_2 \dot{\epsilon}_e - (\Omega_{11} - \Omega_{11}^*) \dot{G} \qquad (28)$$

From Eqn. (17e), it should evident that $\dot{G}$ must be non-negative. Thus, the magnitude of the rate of change of backstress depends upon the signs and magnitudes of the inelastic strain rate and the difference between the current and reference backstress. Because the actual stress is only indirectly coupled to the backstress, through the deformation and the growth laws, an increase in actual stress does not necessarily generate an equivalent increase in backstress. Thus, the quantities in Eqn. (28) need not change in equivalent or proportional amounts. As such, the rate of change of backstress may increase, decrease or remain relatively constant, thereby providing a wide variety of possible results.

The Beam – Column at Constant Temperature

The time-dependent deflection of the beam-column at constant temperature provides the simplest demonstration of these effects. Figures 5, 6 and 7 illustrate the time-dependent end deflection of the beam-column under constant load at temperatures of 400, 600 and 800 °C, respectively. The loading is expressed in terms of the ratio of the applied load to the Euler load for a perfect configuration, P_e, where $P_e = \pi^2 EI/4L^2$. Note that the Euler load is a function of temperature due to the temperature dependence of the elastic modulus. Also note that the relative transverse deflection (i.e.: the vertical axis) represents the ratio of the time-dependent deflection to the initial elastic deflection. Thus, the results indicate the relative increase in deflection produced by inelastic straining.

Except for the lowest loading at 400 °C, the 400 and 600 °C beam-column results exhibit a short initial settling period followed by a virtually linear increase in transverse deflection with time. This type of behavior is synonomous with a response of primary creep transitioning to secondary creep. Not unexpectedly, the higher loadings produce the greater rates of increase. This infers that under these conditions, the difference between the actual stress and the backstress must remain nearly constant with the greater numerical differences occurring at the highest loadings.

This hypothesis is confirmed by in Fig. 8, which illustrates the difference between the maximum (in magnitude) actual stress and the backstress for the 400 °C case.† Note that, due to the combination of bending and axial loading, the maximum (in magnitude) actual stress occurs in the extreme fibers adjacent to the wall on the same side of the centroidal plane as the applied end load.

Except for some slight initial variations, the difference between the actual stress and backstress remains virtually constant. Thus, the right-hand side of Eqn. (17a) effectively is constant. This yields a constant relatively low rate of inelastic straining. Since this low rate of inelastic straining does not significantly alter the deflection of the beam-column, significant changes in the actual stresses do not occur. Concurrently, the low rate of inelastic straining yields a low the rate of change in backstress. Thus, the combination of these effects maintains an approximately constant difference between actual stress and backstress.

In contrast, virtually all levels of loading at an 800 °C temperature produce an accelerating rate of transverse deflection. Only the lowest load produces a steady creep response; all higher loadings produce an accelerating rate of deformation. At the two highest load levels, the beam-column deflects so rapidly it could be considered to have failed almost instantaneously. Of course, in comparing results between these different cases, the significant differences in the time scales should be kept in mind. At the lower temperatures, elapsed time can be expressed in hours. At the highest temperature, elapsed time must be indicated in seconds.

Why the 800 °C results are so different from those at the lower temperatures is directly attributable to the difference between the actual

---

† Results for the difference between the maximum (in magnitude) actual stress and the backstress at a 600 °C temperature are not included since they are virtually identical to those of Fig. 8 and are available elsewhere [27]. The difference tends to remain relatively constant following a short initial period with the greater differences at the higher loads.
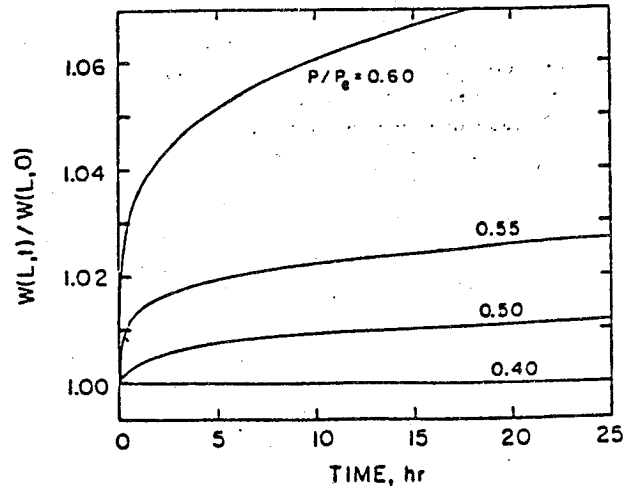

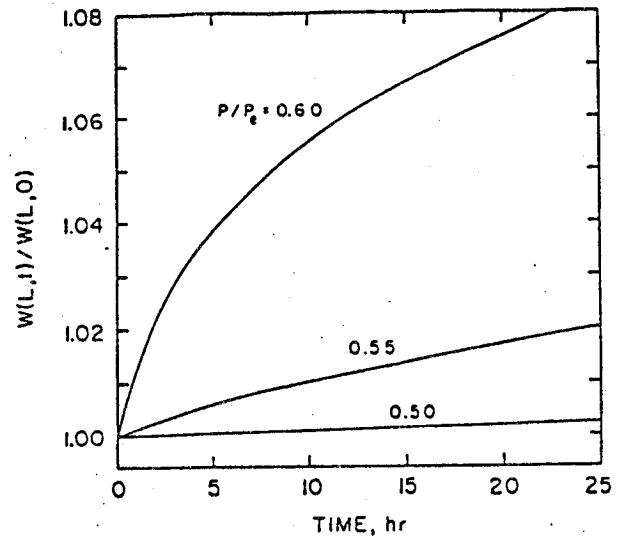Figure 5   Beam-Column Deflection at 400 °C.
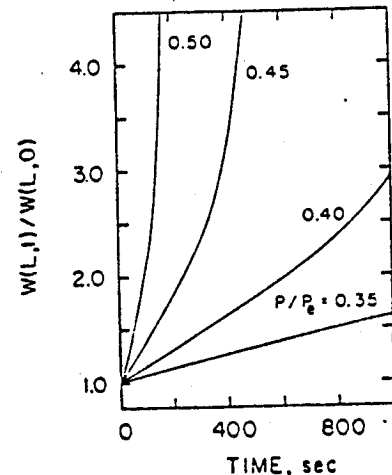

Figure 6   Beam-Column Deflection at 600 °C.

Figure 7   Beam-Column Deflection at 800 °C.

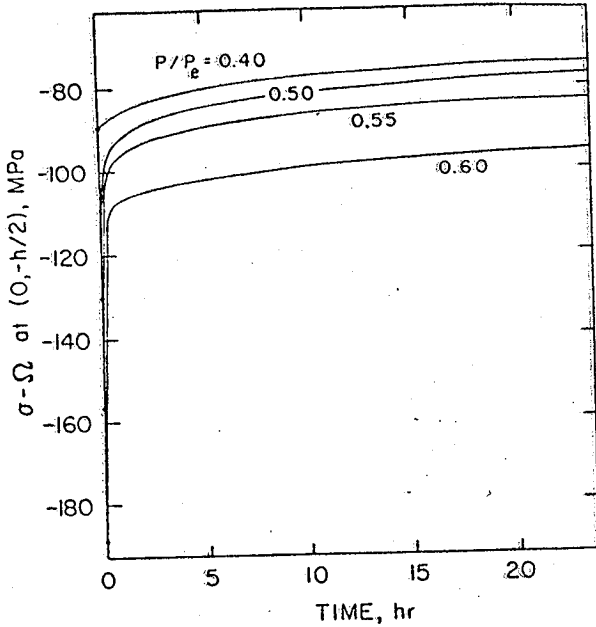Figure 8. Difference between actual stress and backstress for the 400° C beam-column.

One factor common to both temperatures is the sensitivity to load magnitude. Note that only a slight increase in pressure can substantially alter the character of the response. The reason is that in the arch, the centroidal axis stress is always significant due to the curvature and boundary conditions. Thus, it always influences behavior. This stressing induces a high rate of compressive inelastic straining along the centroidal axis "reducing" the nominal arc length of the arch. This geometric change tends to accomodate additional transverse deflection through reduction of both the "nominal" curvature and the "unloaded" arc length of the arch. Note also that, unlike the beam-column, where such an effect is localized near the wall, this centroidal axis straining occurs over most of the central section of the arch. Thus, the "failure" zone tends to be distributed and not
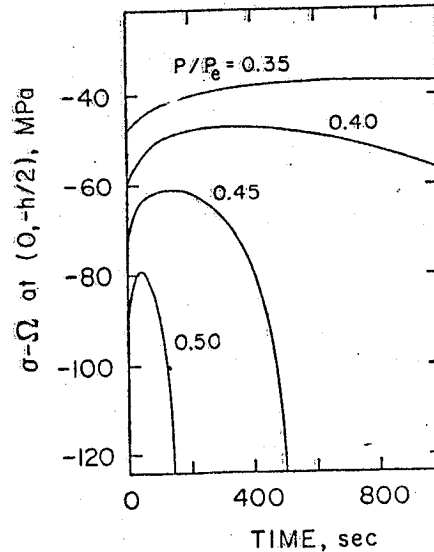

Figure 9. Difference between actual stress and backstress for the 800° C beam-column.

stress and the backstress, illustrated in Fig. 9. At the lowest load, the initial relaxation is followed by a period of constant difference between the actual stress and backstress. Thus, the increase in actual stress from transverse deflection is counterbalanced by the concurrent growth in the backstress. Higher levels of loading alter the relative rates of growth. At higher loads, the rate of increase in actual stress far exceeds that of the backstress. The inelastic strain rate increases thus increasing the rate of deflection which, in turn, further increases the rate of change of actual stress. Thus, the process reinforces itself accelerating the approach to failure.

Before proceeding to the arch, a few words concerning the initial relaxation are warranted. The "relaxation" process is a combination of effects. First, the inelastic deformation tends to limit the rate of increase in the stresses at the extreme fibers. To maintain equilibrium, load bearing responsibility is transfered toward the centroidal axis. Due to the relatively low initial magnitudes of these stresses, this normally does not produce any significant inelastic staining near the centroidal axis.

The exception occurs with the behavior demonstrated in the 800 ° C case. The rapid inelastic straining at the extreme fibers significantly increases the magnitudes of the stresses throughout the central core. Thus, appreciable inelastic straining occurs over the majority of the cross section. With this, inelastic straining along the centroidal axis also begins to strongly influence the overall response. In fact, the form of "failure" which results might be characterized as a viscoelastic analog to a "plastic hinge."

The Arch at Constant Temperature.

The behavior of the pressure loaded shallow arch at constant temperatures of 400, 600 and 800 ° C is generally similar to that of the beam-column. Figures 10 and 11 illustrate the transverse deflection at the center of the arch at 600 and 800 ° C. Note that the critical load for the arch is estimated to lie between 179 to 186 kPa (26 to 27 psi) for these temperatures.

Again, the temperature increase from 600 to 800 ° C reduces useful life by more than an order of magnitude. This is apparent from the significant difference in time scale between the figures. The differences between the actual stress and the backstress for these arch examples are similar to the those for the beam-column and thus have not been included.

localized. As such, the sudden rapid increase in transverse deflection which occurs with the beam-column is not as pronounced in the arch.

The Influence of Time — Invariant Temperature Gradients

The effects of a time-invariant, linear (in the depth direction) temperature gradient on the constant temperature response are considered next. This type of temperature gradient is associated with the steady state flow of heat through the depth. For simplicity, the gradient is assumed to remain constant with respect to the length of the element.

For bookkeeping purposes, gradients where the temperature is greatest at the upper surface and lowest at the bottom surface are considered to be "positive." Conversely, the case where the greatest temperature is at the bottom surface is denoted as a "negative" gradient. Note that all the gradients were established so that the temperature of the centroidal axis would remain at the nominal case temperature. Thus, a +10 ° C gradient for a 400 ° C beam-column implies that the upper, centroidal and lower surface temperatures are 405, 400 and 395 ° C, respectively.

This type of temperature gradient introduces two effects. First, due to the temperature dependence of the elastic modulus, the first integral of the elastic modulus over a cross section does not vanish. This produces a weak level of bending-stretching coupling. The second effect is that such gradients cause thermal bending of the element. Positive gradients cause downward bending thereby augmenting the mechanically induced deflection. Conversely, a negative gradient reduces the load induced bending.

It was found that neither of these exert a major influence on the con-

48

stant temperature behavior. Figure 12, for example, illustrates the typical relative increase in transverse deflection resulting from a depth direction temperature gradients for the 400 °C beam-column at a load ratio of 0.50. Note that a temperature difference of +10 or −10 °C through the 1.27 cm thick beam-column represents a gradient of ± 7.87 °C/cm. The largest temperature difference considered, namely ± 25 °C, corresponds to a heat flux through the depth on the order of 400 kW/m² °C.

As noted above, Fig. 12 provides the relative increase in deflection. This is the ratio of the time-dependent deflection for a given temperature difference to the initial elastic deflection of the uniform temperature beam-column. Thus, this ratio indicates the net amplification resulting from inelatic and thermo-elastic effects.

Temperature differences less than 5 °C had virtually no influence on the deflection of the constant temperature beam-columns. The +10 °C and larger temperature differences did, however, have some impact on transverse deflection. Gradients of these magnitudes generated observable increases in the deflection after several hours of loading. Figure 13 illustrates this with results obtained for a 600 °C beam-column with an applied load ratio of 0.50. The solid line represents the initial ratio of end deflection with a thermal gradient to that of the zero gradient case. The dashed lined provides the same ratio after 12.5 hours of loading. Note that although the deflection of the beam-column is modified due to the presence of the
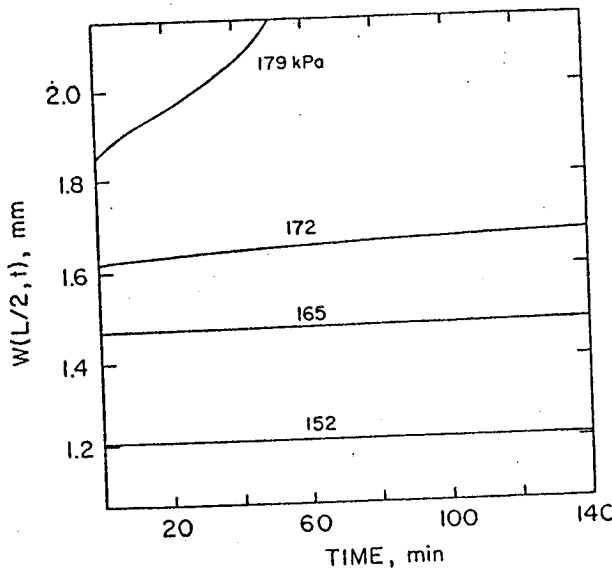

Figure 11. Center deflection for the 800°C arch.

Figure 10. Center deflection for the 600°C arch.

thermal gradient, the magnitude of this change is not sufficient to alter the occurance of the general behaviors illustrated in Figs. 8 through 11. These results are typical of the behavior observed for the other constant temperature beam-column and arch examples.

As mentioned above, the imposition of such thermal gradients also creates some weak bending-stretching coupling in the governing equations. This was found to be an insignificant effect. Specifically, a number of test cases were examined where the coupling term, E_1, was artificially set to zero. There was no appreciable difference in the results with respect to results obtained when the coupling term was retained. Consequently, it can be concluded that the potential bending-stretching coupling which might be induced by the temperature dependence of the elastic modulus is negligible.

Arch and Beam – Column Variable Temperature Behavior

The final aspect of behavior examined is the response of the arch and beam-column under sinusoidally varying temperatures. Results are
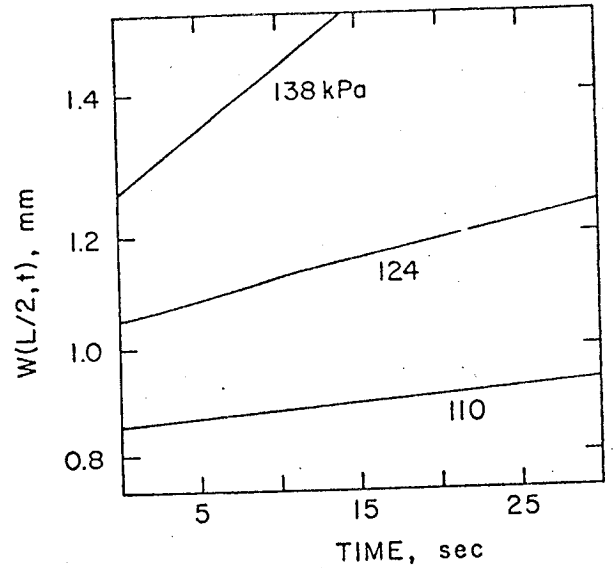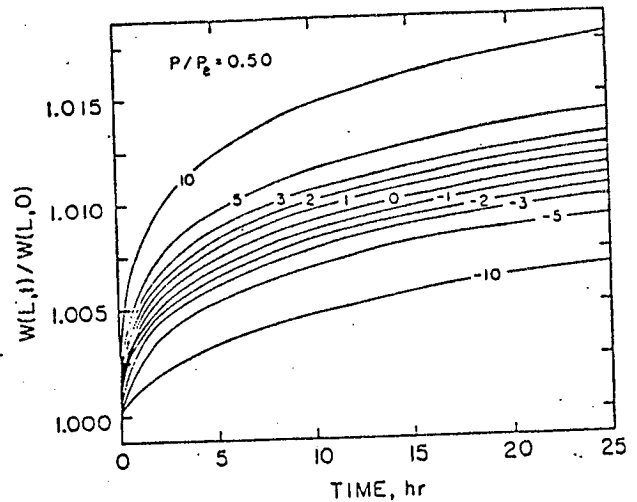

Figure 12. Influence of temperature difference on the deflection of the 400°C beam-column.

presented for both the arch and beam-column without a temperature gradient in the depth direction. The combined influences of sinusoidal temperature variations and a time-invariant depth direction thermal gradient are investigated only for the case of the beam-column.

In the cases examined, the temperature is assumed to vary in a sinusoidal manner about an elevated mean temperature of either 400 or 600 °C. Amplitudes of 50, 100 and 150 °C are employed. Also, in keeping with the use of a quasi-static analysis, 1200 and 1800 sec periods are employed for the sinusoids. Sinusoidal variations about the 800 °C temperature were not studied due to the extremely short life exhibited in the constant temperature cases.

Finally, the thermal model includes a slight initial delay between when the load is first applied and when the sinusoidal temperature variations commence. With some combinations of higher temperatures and higher loads, a step-like initial transient is generated-in the constitutive law state variables. Superimposing a sinusoidal temperature at the same time that this step-like increase in the state variables occurs forces the Runge-Kutta integration routine to employ exceptionally small time step
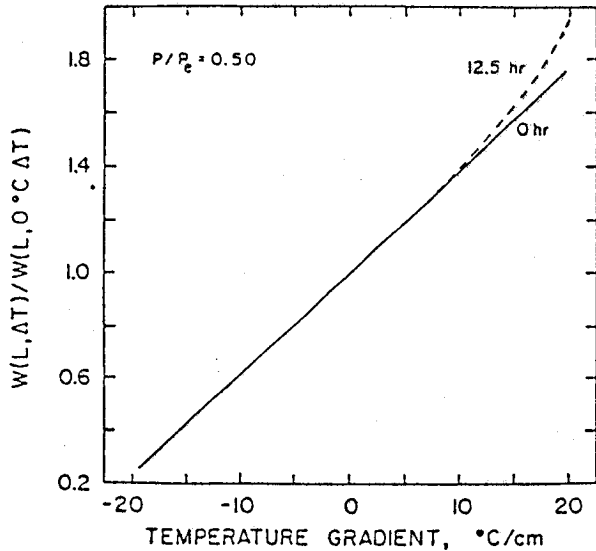
Figure 13. Transverse deflection as a function of temperature
gradient for the 600° C beam-column.

Figure 15. End deflection for the 600° C beam-column for 50
and 100° C sinusoidal temperature amplitudes.

increments to provide accurate results. However, the need to employ such small time step increments passes almost immediately once the load induced transient change has taken place. Thus, the short delay allows the integration routine to stabilize before the start of the temperature oscillations. Typically, a delay period on the order of 50 sec is employed. Based on a limited number of test cases, it was found that such a delay period has no appreciable impact on the overall results.

Figures 14 and 15 illustrate the time dependent deflection of the arch and the beam-column, respectively, for 50 and 100 ° C amplitude temperature oscillations about a 600 ° C temperature. Note that the loading employed in both of these cases would nominally produce a "stable" time-dependent response under constant temperature conditions. Several interesting features can be discerned. First, the shape of each deflection curve is a distorted sinusoid. The upper peaks tend to be exaggerated whereas the lower peaks are well rounded. Additionally, an underlying increasing trend in time-dependent deflection can be observed in both. Specifically, both the upper peak and lower peak deflections increase between each cycle.
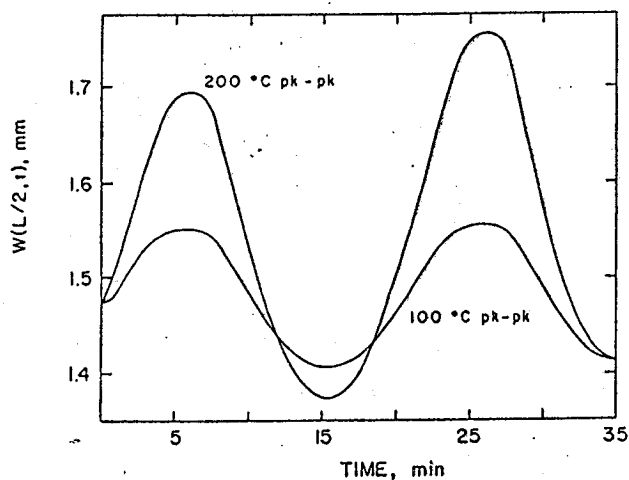
The distortion of the peaks from a true sinusoid is a result of the temperature dependence of the inelastic strain. During the higher temperature portion of the cycle, inelastic straining increases due to the temper^ture sensitivity of the constitutive law parameters. This results in a rapid increase in the deflection. Conversely, the inelastic strain rate is reduced at lower temperatures yielding less inelastic deformation during that part of the cycle. Thus, the behavior during the lower temperature portion of the cycle more closely approximates that of simple thermo-elastic deformation where deflection follows the thermal cycle exactly.

Tables I and II summarize these increasing trends for the arch and beam-column cases, respectively. Note that these tables present results obtained for a variety of temperature differences in the depth direction.

Table I.   Rate of Change of Arch Deflection for Sinusoidal
Temperature Variations

Pressure (kPa)	Sine Amplitude °C	Rate of Change (cm/sec)	
		1st to 2nd Upper Peak	1st to 2nd Lower Peak
165	25	3.18×10^{-7}	2.74×10^{-7}
165	50	3.84×10^{-7}	3.20×10^{-7}
165	100	4.98×10^{-6}	2.87×10^{-6}
152	100	7.87×10^{-7}	6.12×10^{-7}

As Table I illustrates, the magnitude of the increase in deflection between the first and second upper peaks appreciably exceeds that between the first and second lower peaks. Although not indicated in this or the following table, the increase in deflection at the cycle midpoint temperature falls between the values of the extremes. It should be noted that this unequal expansion of the thermal cycle deflection indicates that creep ratchetting is occurring.

This table also demonstrates the significant nonlinearity involved in this phenomena. The first doubling of the amplitude of the thermal cycle, from 25 to 50 ° C, results in only a modest increase in the peak to peak

Figure 14. Center deflection for the 600° C arch for 50 and
100° C sinusoidal temperature amplitudes.

50

deflections. However, a second doubling, from 50 to 100 °C, increases the peak to peak deflection by slightly more than an order of magnitude. Table II illustrates that a similar effect for the beam-column. Note that except for the 50 °C amplitude with no gradient, increasing the amplitude of the thermal cycle increases the change in peak to peak deflection in a nonlinear manner.

Table II also demonstrates that the increase between consecutive peaks has an overall decreasing trend. The absolute increase in deflection decreases as the number of cycles increases. The cause of this decreasing trend is attributed to the growth in backstress. Generally, the maximum stresses do not change significantly between consecutive peaks of the thermal cycle because they are principally determined by the thermo-elastic deformation. The accumulated inelastic deformation does not significantly alter this stress distribution. However, the amount of inelastic strain is sufficient to create an increase in the backstress between consecutive peaks, one which exceeds that of the actual stress. Thus, the difference between the actual stress and the backstress decreases. In turn, this reduces the rate of inelastic straining. Of course, this effect becomes less significant as the backstress approaches saturation.

Table II. Rate of Change of Beam-Column Deflection for Sinusoidal Temperature Variations

| Sine Ampl. °C | Temp. Diff. °C | Rate of Change (cm/sec) | | | |
| | | Upper Peaks | | Lower Peaks | |
		1st to 2nd	2nd to 3rd	1st to 2nd	2nd to 3rd
50	0	1.48×10^{-8}	1.27×10^{-8}	1.48×10^{-8}	1.27×10^{-8}
50	+10	8.46×10^{-8}	8.26×10^{-8}	8.05×10^{-8}	7.82×10^{-8}
50	+20	4.29×10^{-7}	4.06×10^{-7}	4.01×10^{-7}	3.84×10^{-7}
100	0	1.07×10^{-6}	1.03×10^{-6}	9.83×10^{-7}	9.45×10^{-7}
100	+10	2.21×10^{-6}	2.06×10^{-6}	2.01×10^{-6}	1.88×10^{-6}
100	+20	4.72×10^{-6}	4.27×10^{-6}	4.24×10^{-6}	3.86×10^{-6}
150	0	1.87×10^{-5}	1.66×10^{-5}	1.61×10^{-5}	1.45×10^{-5}
150	+10	3.22×10^{-5}	2.91×10^{-5}	2.77×10^{-5}	2.52×10^{-5}
150	+20	5.41×10^{-5}	4.93×10^{-5}	4.67×10^{-5}	4.32×10^{-5}

The remaining influence illustrated by the data of Table II is the effect of a time-invariant depth direction temperature gradient on the inelastic response. In general, the change in peak to peak deflection is significantly greater in the presence of the time-invariant temperature gradient. Typically, almost an order of magnitude increase in peak to peak change in deflection occurs for the lowest temperature cycle amplitude. Interestingly, the effect of the depth direction gradient becomes less significant as the amplitude of the thermal cycle increases.

The ultimate significance of this is whether or not temperature gradients in the depth direction are truly negligible. The data of this table tend to indicate that the gradient may not be a negligible factor when the magnitude of the gradient is of the same relative magnitude as the thermal cycle. In such cases, the thermal gradient does appear to exert an appreciable influence on the overall response. Obviously, this also tends to imply that the impact of the depth direction gradient is potentially very significant in transient cases where the magnitude of the temperature difference through the depth can easily approach that of the gross transient change in temperature.

CONCLUSIONS

The elevated temperature behavior of generic types of structural elements fabricated from a typical aerospace alloy have been studied analytically using a nonlinear kinematic analysis and employing a recently developed nonlinear unified hereditary constitutive law to express the time-temperature dependence for the material. The study results demonstrate

that, due to the specific format of the constitutive law, the behavioral response of the structural element is determined principally by the difference between the actual stress in the element and the backstress variable of the constitutive law. The first of these, the actual stress in the element, is basically controlled by the geometry of deformation. However, the second factor, the backstress, is governed by the appropriate growth rules of the constitutive law.

This implies that accurate results for such an analysis can be obtained only if the form of the backstress growth law and the numerical values employed therein have been established to a reasonably high degree of certainty. Otherwise, the prediction of the conditions under which the response of the structural element may change from that of a "steady" form of creep to a rapid approach to failure could not be established with any degree of reliability. For entirely similar reasons, the actual stresses in the structural element needs to be established accurately to ensure that reliable results ensue.

The specific results obtained from the sample problems indicate that a constitutive law of the type proposed by Walker has the capability to model various forms of creep behavior. Under various constant load and temperature conditions, it has been shown that the predicted response may vary from simple primary creep-secondary creep to almost instantaneous terciary creep. Additionally, under varying temperature conditions, the Walker law has demonstrated the capability to predict the development of the type of inelastic strain biasing which can produce creep ratchetting.

Assuming the Walker law and associated constants provide an accurate representation of the elevated temperature response of a material such as Hastelloy X, the sample problem results indicate that the existence of a depth direction temperature gradient in a thin section may not always be negligible. Specifically, under constant temperature conditions, the results indicate that such temperature gradients do not appear to exert any significant influence on behavioral response. However, such gradients do have a significant impact when the overall temperature of the element is not constant. The existence of this type of gradient can appreciably accelerate the overall rate of creep. It is indicated that this specific effect is most pronounced when the magnitude of the temperature difference through the depth of the element is on the order of the amplitude of the gross variation in temperature of the element. Consequently, in addition to when such conditions may exist in a "quasi-steady state" situation, this implies that such gradients may exert considerable influence in transient thermal problems.

ACKNOWLEDGEMENT

REFERENCES

1. Hilton, H.H., "Creep Collapse of Viscoelastic Columns With Initial Curvature," Journal of the Aeronautical Sciences, Vol. 19, No. 12, 1952, pp. 844-846.

2. Libove, C. "Creep Buckling of Columns," Jounal of the Aeronautical Sciences, Vol. 19, No. 7, 1952, pp. 459-467.

3. Odqvist, F.K.G., "Influence of Primary Creep on Column Buckling," Journal of Applied Mechanics, Vol. 21, No. 3, 1954, pp 295.

4. Hoff, N.J., "Creep Buckling," The Aeronautical Quarterly, Vol. 7, No. 1, 1956, pp. 1-20.

5. Miller, D.R., "Thermal Stress Ratchet Mechanism in Pressure Ves-

sels," ASME Journal of Basic Engineering, Vol. 81, 1959, pp. 190–196.

6. Edmunds, H.G. and Beer, F.J., "Notes on Incremental Collapse in Pressure Vessels," Journal of Mechanics and Engineering Science, Vol. 5, 1961, pp. 187–199.

7. Bree, J. "Elastic Plastic Behavior of Thin Tubes Subjected to Internal Pressure and Intermittent High Heat Fluxes," Journal of Strain Analysis, Vol. 2, 1967, pp. 226–238.

8. Bree, J., "Incremental Growth Due to Creep and Plastic Yielding of Thin Tubes Subjected to Internal Pressure and Cyclic Thermal Stresses," Journal of Strain Analysis, Vol. 3, 1968, pp. 122–127.

9. Conway, J.B., Berling, J.T., Stentz, R.H., Pugh, C.E. and Anderson, W.F., "Thermal Ratchetting Studies of Type 304 Stainless Steel - An Evaluation of a New Test Procedure," Symposium on Structural Materials for Service at Elevated Temperatures in Nuclear Power Generation, ASME 1975 Winter Annual Meeting, Houston, Texas, pp. 247–281.

10. Corum, J.M., Young, H.C. and Grindell, A.G., "Thermal Ratchetting in Pipes Subjected to Intermittent Thermal Downshocks at Elevated Temperature," Oak Ridge National Laboratory, Tennessee, 1974.

11. Corum J.M., Richardson, M. and Clinard, J.A., "Elevated-Temperature Benchmark Tests of Simply Supported Circular Plates Subjected to Time-Varying Loadings," Oak Ridge National Laboratory, Tennessee, 1977

12. Mukherjee, S., Kumar, V., and Chang, K.J., "Elevated Temperature Inelastic Analysis of Metallic Media Under Time Varying Loads Using State Variable Theories," International Journal of Solids and Structures, Vol. 14, 1978, pp. 663–679.

13. Hart, E.W., "Constitutive Relations for the Inelastic Deformation of Metals," Journal of Engineering Materials and Technology, Vol. 98, 1976, pp. 193–202.

14. Hart, E.W., "A Micromechanical Basis for Constitutive Equations with Internal Variables," Journal of Engineering Materials and Technology, Vol. 106, 1984, pp. 322–325.

15. Pointer, A.R.S. and Leckie, F.A., "Constitutive Relationships for the Time Dependent Deformation of Metals," Journal of Engineering Materials and Technology, Vol. 98, 1976, pp. 47–51.

16. Pugh, C.E. and Robinson, D.N., "Some Trends in Constitutive Equation Model Development for High-Temperature Behavior of Fast-Reactor Structural Alloys," Nuclear Engineering Design, 1978, pp. 269–276.

17. Pugh, C.E. and Robinson, D.N., "Constitutive Equations for Meeting Elevated-Temperature-Design Needs," ASME Pressure Vessel and Piping Conference, Denver, Colorado, 1981.

18. Pugh, C.E., "Progress in Developing Constitutive Equations for Inelastic Design Analysis," Journal of Pressure Vessel Technology, Vol. 105, 1983, pp. 273–276.

19. Krempl, E., "On the Interaction of Rate and History Dependence in Structural Metals," Acta Mechanica, Vol. 22, 1975, pp. 53–90.

20. Walker, K.P. and Krempl. E., "An Implicit Functional Theory of Viscoplasticity," Mechanics Research Communications, Vol. 5, No. 4, 1978, pp. 179–184.

21. Corum, J.M. and Sartory, W.K., "Assessment of Current High-Temperature Design Methodology Based on Structural Failure Tests," Journal of Pressure Vessel Technology, Vol. 109, 1987, pp. 160–168.

22. Walker, K.P., "Research and Development Program for Nonlinear Structural Modeling with Advanced Time-Temperature Dependent Constitutive Relationships," United Technologies Research Center, NASA Contract Report NASA-CR-165533, 1981.

23. Moreno, V., "Development of a Simplified Analytic Method for Representing Material Cyclic Response," United Technologies Research Center, NASA Contract Report NASA-CR-168100, 1983.

24. Moreno, V., "Combustor Durability Analysis," United Technologies Research Center, NASA Contract Report NASA-CR-165250, 1981.

25. Stubstad, J.M. and Simitses, G.J., "Bounding Solutions for Geometrically Nonlinear Viscoelastic Problems," AIAA Journal, Vol. 24, No. 11, 1986, pp. 1843–1850.

26. Thurston, G., "Newton's Method Applied to Problems in Nonlinear Mechanics," Journal of Applied Mechanics, Vol. 22, 1965, pp. 383–388.

27. Stubstad, J.M., "Nonlinear Thermoviscoelastic Analysis of Metallic Plane Curved Beams," PhD Dissertation submitted in partial fulfillment of the requirements for the degree of Doctor of Philosophy, Georgia Institute of Technology, 1986.

APPENDIX A CONSTITUTIVE LAW

In its most general integral form, Walker's functional theory has the format:

$$\sigma_{ij}(t) = \frac{2}{3}\Omega_{ij}(t) + \delta_{ij} \int_0^t \left(\lambda[\Theta(\xi)] + \frac{2}{3}\mu[\Theta(\xi)]\right) \left(\frac{\partial \epsilon_{kk}}{\partial \xi} - 3\alpha[\Theta(\xi)]\frac{\partial \Theta}{\partial \xi}\right) d\xi$$
$$+ \int_0^t e^{-(Q(t)-Q(\xi))} \left(2\mu[\Theta(\xi)]\frac{\partial \epsilon_{ij}}{\partial \xi} - \frac{2}{3}\delta_{ij}\mu[\Theta(\xi)]\frac{\partial \epsilon_{kk}}{\partial \xi} - \frac{2}{3}\frac{\partial \Omega_{ij}}{\partial \xi}\right) d\xi, \tag{A-1a}$$

$$\Omega_{ij}(t) = \Omega_{ij}^o(t) + n_1[\Theta(t)]c_{ij}(t) + n_2[\Theta(t)] \int_0^t e^{-(G(t)-G(\xi))}\frac{\partial c_{ij}}{\partial \xi} d\xi, \tag{A-1b}$$

$$K(t) = K_1[\Theta(t)] - K_2[\Theta(t)]e^{-n_7[\Theta(t)]W(t)}, \tag{A-1c}$$

$$c_{ij} = \int_0^t \frac{1}{2\mu}\left(\delta_{ij}\lambda[\Theta(\xi)]\frac{\partial \epsilon_{kk}}{\partial \xi} + 2\mu[\Theta(\xi)]\frac{\partial \epsilon_{ij}}{\partial \xi} - \frac{\partial \sigma_{ij}}{\partial \xi}\right.$$
$$\left. - \delta_{ij}\alpha[\Theta(\xi)](3\lambda[\Theta(\xi)] + 2\mu[\Theta(\xi)])\frac{\partial \Theta}{\partial \xi}\right) d\xi, \tag{A-1d}$$

$$\Omega_{ij}^o = -\Omega^o[\Theta(t)]\left(\delta_{ij} - 3\frac{c_{ik}(t)c_{kj}(t)}{c_{pq}(t)c_{pq}(t)}\right), \tag{A-1e}$$

$$Q(t) = \int_0^t \frac{3\mu[\Theta(\xi)]}{K(\xi)}\left(\frac{\partial W}{\partial \xi}\right)^{1-1/n[\Theta(t)]} d\xi, \tag{A-1f}$$

$$G(t) = \int_0^t \left\{ (n_3[\Theta(\xi)] + n_4[\Theta(\xi)]e^{-n_5[\Theta(t)]W(t)})\frac{\partial W}{\partial \xi} \right.$$
$$\left. + n_6[\Theta(\xi)](\frac{2}{3}\Omega_{ij}(\xi)\Omega_{ij}(\xi))^{(m[\Theta(t)]-1)/2}\right\} d\xi, \tag{A-1g}$$

and

$$W(t) = \int_0^t \sqrt{\frac{2}{3}\frac{\partial c_{ij}}{\partial \xi}\frac{\partial c_{ij}}{\partial \xi}} d\xi. \tag{A-1h}$$

Square bracket terms, of the form $\mu[\Theta(t)]$, are used to denote the dependence of the material constants λ, μ, Ω^*, n, m, n_1, n_2, n_3, n_4, n_5, n_6, n_7, K_1, and K_2 on the temperature, Θ. However, for clarity, the indication of the explicit dependence on temperature will be suppressed in the following development.

The differential format for Walker's functional theory is obtained through differentiating the above relations with respect to time. Employing

Leibniz's rule, differential formats for Eqns. (A-1d), (A-1f), (A-1g) and (A-1h) are readily obtained. A somewhat simplified differential format for Eqn. (A-1b) may be obtained in the following manner. Differentiating Eqn. (A-1b) with respect to time and using Leibniz's rule, after rearranging, yields

$$\dot{\Omega}_{ij} = \dot{\Omega}^{\circ}_{ij} + (n_1 + n_2)\dot{c}_{ij} + c_{ij}\frac{\partial n_1}{\partial \Theta}\dot{\Theta} + \left[\frac{\partial n_2}{\partial \Theta}\dot{\Theta} - n_2\dot{G}\right]\int_{o}^{t}e^{-\{G(t)-G(\xi)\}}\frac{\partial c_{ij}}{\partial \xi}. \qquad (A-2)$$

The integral which appears in the above is identical to the integral of Eqn. (A-1b). Consequently, solving Eqn. (A-1b) for the integral and substituting into Eqn. (A-2) yields the differential format given by Eqn. (A-6b).

With some manipulation, the differential form of Eqn. (A-1a) may be stated in a "power law" type format. First, Eqn. (A-1a) is differentiated with respect to time and then simplified using the deviatoric stress tensor to yield

$$\frac{2}{3}\left(\frac{3}{2}\dot{s}_{ij} - \dot{\Omega}_{ij}\right) = \int_{o}^{t}e^{-\{Q(t)-Q(\xi)\}}\left[2\mu\frac{\partial \epsilon_{ij}}{\partial \xi} - \frac{2}{3}\mu\delta_{ij}\frac{\partial \epsilon_{kk}}{\partial \xi} - \frac{2}{3}\frac{\partial \Omega_{ij}}{\partial \xi}\right]d\xi. \qquad (A-3)$$

Note that to establish the above it is necessary to show that $\Omega_{kk} = \Omega^{\circ}_{kk} = 0$. These, however, follow directly from Eqns. (A-1b) and (A-1e) provided the inelastic portion of the deformation may be treated as, at least, approximately incompressible (i.e., $c_{kk} \approx 0$).

Therefore, substituting Eqn. (A-3) into Eqn. (A-2) and using the differential form of Eqn. (A-1d) yields:

$$2\mu\dot{c}_{ij} = \frac{2}{3}\dot{Q}\left(\frac{3}{2}s_{ij} - \Omega_{ij}\right). \qquad (A-4)$$

The $\dot{Q}$ term can be replaced with the aid of the differential forms of Eqns. (A-1f) and (A-1h). After some algebraic manipulation and minor rearranging this yields:

$$\dot{W} = \left(\frac{\sqrt{\frac{2}{3}\left(\frac{3}{2}s_{ij} - \Omega_{ij}\right)\left(\frac{3}{2}s_{ij} - \Omega_{ij}\right)}}{K}\right)^{n} \qquad (A-5)$$

Consequently, substituting Eqn. (A-5) back into the differential form of Eqn. (A-1f) and using Eqn. (A-4) yields, after some algebra, the differential power law of Eqn. (A-1a). Thus, the complete set of differential relations for Walker's functional theory are:

$$\dot{c}_{ij} = \left(\frac{\sqrt{\frac{2}{3}\left(\frac{3}{2}s_{kl} - \Omega_{kl}\right)\left(\frac{3}{2}s_{kl} - \Omega_{kl}\right)}}{K}\right)^{n}\frac{\left(\frac{3}{2}s_{ij} - \Omega_{ij}\right)}{\sqrt{\frac{2}{3}\left(\frac{3}{2}s_{mn} - \Omega_{mn}\right)\left(\frac{3}{2}s_{mn} - \Omega_{mn}\right)}}, \qquad (A-6a)$$

$$\dot{\Omega}_{ij} = \dot{\Omega}^{\circ}_{ij} + (n_1 + n_2)\dot{c}_{ij} + c_{ij}\frac{\partial n_1}{\partial \Theta}\dot{\Theta} - (\Omega_{ij} - \Omega^{\circ}_{ij} - n_1 c_{ij})\left(\dot{G} - \frac{1}{n_2}\frac{\partial n_2}{\partial \Theta}\dot{\Theta}\right), \qquad (A-6b)$$

$$K = K_1 - K_2 e^{-n_r W}, \qquad (A-6c)$$

$$2\mu\dot{c}_{ij} = \delta_{ij}\lambda\dot{\epsilon}_{kk} + 2\mu\dot{\epsilon}_{ij} - \dot{\sigma}_{ij} - \delta_{ij}(3\lambda + 2\mu)\alpha\dot{\Theta}, \qquad (A-6d)$$

$$\dot{\Omega}^{\circ}_{ij} = \frac{\Omega^{\circ}_{ij}}{\Omega^{\bullet}}\frac{\partial \Omega^{\bullet}}{\partial \Theta}\dot{\Theta} + \frac{3\Omega^{\bullet}}{(c_{pq}c_{pq})^2}\left[\dot{c}_{ik}c_{kj}c_{pq}c_{pq} + c_{ik}\dot{c}_{kj}c_{pq}c_{pq} - 2c_{ik}c_{kj}c_{pq}\dot{c}_{pq}\right], \qquad (A-6e)$$

$$\dot{G} = (n_3 + n_4 e^{-n_s W})\dot{W} + n_6\left(\frac{2}{3}\Omega_{ij}\Omega_{ij}\right)^{(m-1)/2}, \qquad (A-6f)$$

and

$$\dot{W} = \sqrt{\frac{2}{3}\dot{c}_{ij}\dot{c}_{ij}}. \qquad (A-6g)$$

Note that a differential form for the function Q is not required since it does not appear in any of the other expressions.

Numerical constants for the law were established [22-24] from uniaxial bar specimens tested under fully reversed, strain-rate controlled cyclic stress-strain tests. These tests were conducted for a variety of temperatures and strain rates. The testing conditions were sufficiently rigorous to cause plastic deformation during the loading cycle. The creep and relaxation properties were deduced from observation of the behavior of the samples when the cyclic loading was "held" at various points on the "steady-state" hysteresis loop. Appendix Figs. A-1 through A-7 illustrate the temperature dependent parametric values established under that work. Note that the material constants K_2, n_1, n_4, n_5, and n are zero over the enitre temperature range considered. This results in additional simplifications to the constitutive law.

APPENDIX B FINITE DIFFERENCE EQUATIONS

Solutions for the governing nonlinear differential equations are obtained using a Newton type method for nonlinear differential equations. It is assumed that trial solutions for the transverse and axial deflection functions, denoted as $\tilde{w}$ and $\tilde{u}$, respectively, exist. From these, trial values for centroidal axis strain and cross section rotation, $\tilde{\epsilon}_o$ and $\tilde{\phi}$, respectively, are determined. Then, using the approximations $\epsilon_o = \tilde{\epsilon}_o + \Delta\epsilon_o$ and $\phi = \tilde{\phi} + \Delta\phi$ to substitute into Eqns. (16) yields

$$\tilde{k}\left(E_0\Delta\epsilon_o + E_1\frac{\partial \Delta\phi}{\partial s}\right) - \frac{\partial^2 \Delta M}{\partial s^2} = p^{\bullet} - \tilde{k}\tilde{N} + \frac{\partial^2 \tilde{M}}{\partial s^2}, \qquad (B-1a)$$

$$(E_0 + \tilde{k}E_1)\frac{\partial \Delta\epsilon_o}{\partial s} + (E_1 + \tilde{k}E_2)\frac{\partial^2 \Delta\phi}{\partial s^2} = -\frac{\partial \tilde{N}}{\partial s} - \tilde{k}\frac{\partial \tilde{M}}{\partial s}. \qquad (B-1b)$$

The terms $\tilde{N}$ and $\tilde{M}$ are evaluated by substituting $\tilde{\epsilon}_o$ and $\tilde{\phi}$ into Eqns. (11). Numerical methods are used to approximate the derivative terms on the
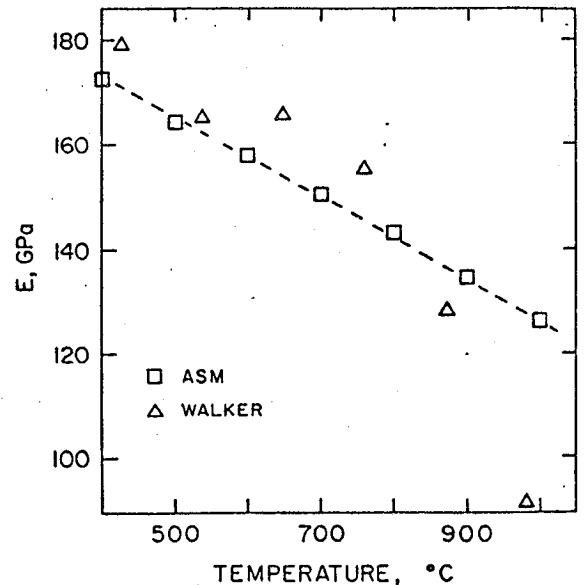

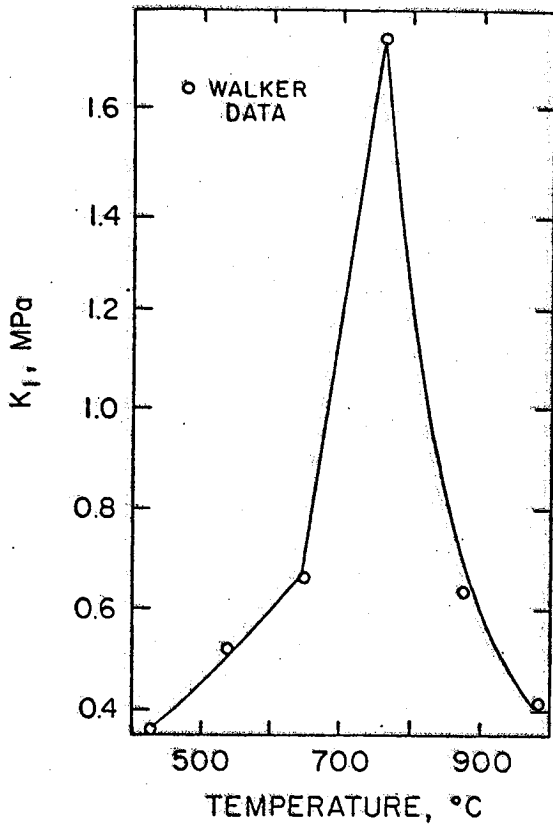Figure A-1. Young's modulus as a function of temperature

53

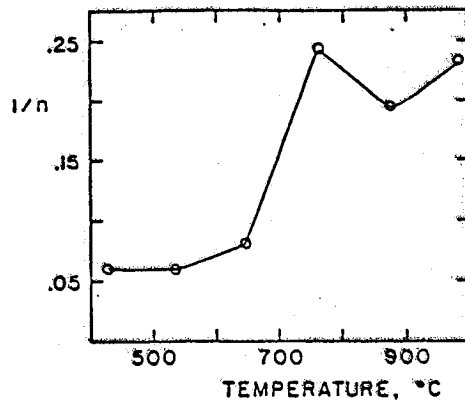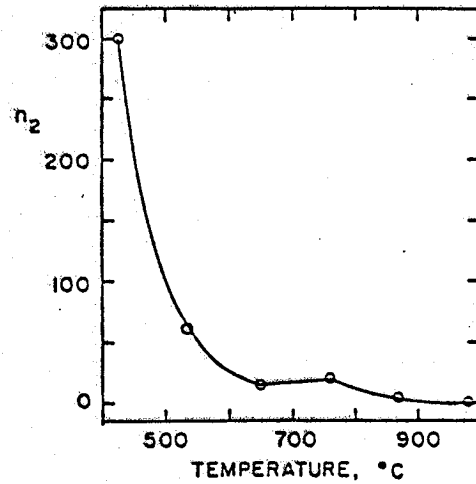Figure A-2. K_1 as a function of temperature.

Figure A-3 n^{-1} as a Function of Temperature

right-hand side of Eqns (B-1). The second derivative of the moment correction, which appears on the left-hand side of Eqn. (B-1a), also is evaluated numerically. This avoids the numerical problems which can result in approximating fourth derivatives directly.

Assuming $w = \bar{w} + \Delta w$ and a similar expansion for u, upon substitution into Eqn. (7) and neglecting terms of order $(\Delta w)^2$ and higher, yields

$$\Delta \epsilon_o = A(\frac{\partial \Delta u}{\partial s} + \kappa \Delta w) + B(\frac{\partial \Delta w}{\partial s} - \kappa \Delta u) \qquad (B - 2)$$

where the factors A and B are defined as:

Figure A-4 n_2 as a Function of Temperature
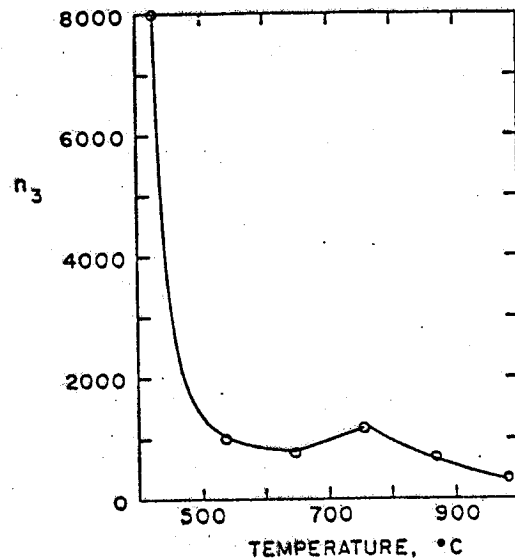
Figure A-5 n_3 as a Function of Temperature
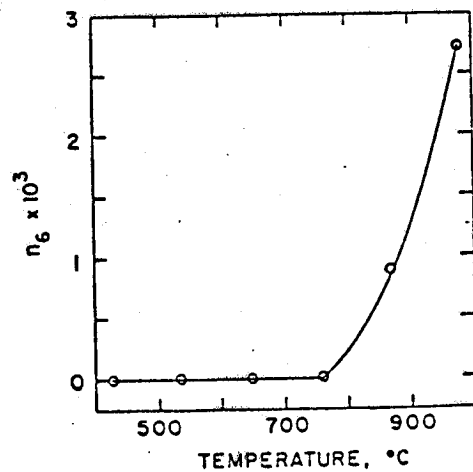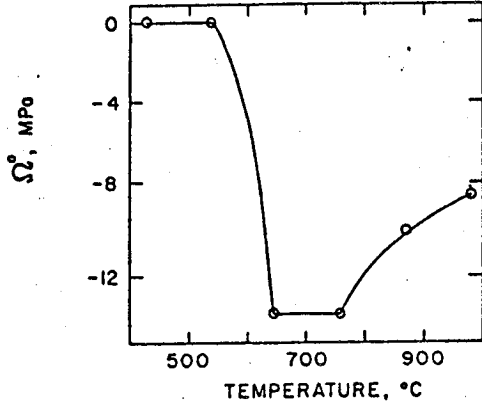

Figure A-6 n_6 as a Function of Temperature

54

Figure A-7. Reference backstress, Ω°, as a function of temperature.

$$A = 1 + \frac{\partial \bar{u}}{\partial s} + \kappa \bar{w} \quad \text{and} \quad B = \frac{\partial \bar{w}}{\partial s} - \kappa \bar{u}. \qquad (B-3a,b)$$

Differentiating Eqn. (B-2) with respect to s yields, after rearranging,

$$\frac{\partial \Delta \epsilon_o}{\partial s} = A \frac{\partial^2 \Delta u}{\partial s^2} + (C - \kappa B)\frac{\partial \Delta u}{\partial s} - \kappa D \Delta u,$$

$$+ B \frac{\partial^2 \Delta w}{\partial s^2} + (D + \kappa A)\frac{\partial \Delta w}{\partial s} + \kappa C \Delta w \qquad (B-4)$$

where C and D are given by

$$C = \frac{\partial^2 \bar{u}}{\partial s^2} + \kappa \frac{\partial \bar{w}}{\partial s} \quad \text{and} \quad D = \frac{\partial^2 \bar{w}}{\partial s^2} - \kappa \frac{\partial \bar{u}}{\partial s}. \qquad (B-5a,b)$$

Developing an expression for $\Delta \phi$ is accomplished by using Eqn. (8). Since it is assumed that $\phi = \bar{\phi} + \Delta \phi$, substitution into Eqn. (8) yields

$$\sin(\bar{\phi} + \Delta \phi) \approx \sin \bar{\phi} + \Delta \phi \cos \phi \approx \frac{-\frac{\partial \bar{w}}{\partial s} + \kappa \bar{u}}{\sqrt{1 + 2\bar{\epsilon}_o + 2\Delta \epsilon_o}} + \frac{-\frac{\partial \Delta w}{\partial s} + \kappa \Delta u}{\sqrt{1 + 2\bar{\epsilon}_o + 2\Delta \epsilon_o}} \qquad (B-6)$$

where the approximations $\sin \Delta \phi \approx \Delta \phi$ and $\cos \Delta \phi \approx 1$ have been used. For small $\bar{\epsilon}_o$ it is reasonable to assume that $\Delta \epsilon_o < \bar{\epsilon}_o$, thus allowing the $\Delta \epsilon_o$ term to be neglected. Thus, since the first term on the left-hand side, according to Eqn. (8), is equal to the first term of the right-hand side, this implies that

$$\Delta \phi \cos \phi \approx \frac{-\frac{\partial \Delta w}{\partial s} + \kappa \Delta u}{\sqrt{1 + 2\bar{\epsilon}_o}}. \qquad (B-7)$$

Therefore, combining Eqns. (8) and (B-7) yields

$$\Delta \phi \approx \frac{1}{A}(-\frac{\partial \Delta w}{\partial s} + \kappa \Delta u). \qquad (B-8)$$

Derivatives of $\Delta \phi$ are obtained from Eqn. (B-8). In this, it is assumed that the term 1/A may be treated as an approximate constant and thus need not be differentiated. This provides significant simplifications without engendering any substantial inaccuracies since the correction terms become

negligible as the exact solution is approached. Consequently, differentiating Eqn. (B-8) with respect to s yields:

$$\frac{\partial \Delta \phi}{\partial s} \approx \frac{1}{A}(-\frac{\partial^2 \Delta w}{\partial s^2} + \kappa \frac{\partial \Delta u}{\partial s}), \qquad (B-9a)$$

and

$$\frac{\partial^2 \Delta \phi}{\partial s^2} \approx \frac{1}{A}(-\frac{\partial^3 \Delta w}{\partial s^3} + \kappa \frac{\partial^2 \Delta u}{\partial s^2}). \qquad (B-9b)$$

Central difference formulae are used to approximate the derivative terms. However, prior to substituting into Eqns. (B-1) it is useful to establish the following definitions:

$$a_i = \bar{k}_i E_0 + \frac{2E_1}{\Delta s^2}, \qquad b_i = \bar{k}_i E_1 + \bar{N}_i + \frac{2E_2}{\Delta s^2}, \qquad (B-10a,b)$$

$$c_i = E_0 + \bar{k}_i E_1 \quad \text{and} \quad d_i = E_1 + \bar{k}_i E_2. \qquad (B-10c,d)$$

Thus, substituting the various expressions given above into Eqns. (B-1) yields, after rearranging, the general finite difference nodal equations

$$\left(\frac{E_1 A_{i-1}}{2\Delta s^3} + \frac{\kappa E_2}{2A_{i-1}\Delta s^3}\right)\Delta u_{i-2} + \left(\frac{\kappa E_1 B_{i-1}}{\Delta s^2} - \frac{a_i A_i}{2\Delta s} - \frac{\kappa b_i}{2A_i \Delta s}\right)\Delta u_{i-1}$$

$$+ \left(-\frac{E_1}{2\Delta s^3}(A_{i-1} - A_{i+1}) - \kappa a_i B_i - \frac{\kappa E_2}{2\Delta s^3}(\frac{1}{A_{i-1}} - \frac{1}{A_{i+1}})\right)\Delta u_i$$

$$+ \left(\frac{a_i A_i}{2\Delta s} + \frac{\kappa E_1 B_{i+1}}{\Delta s^2} + \frac{\kappa b_i}{2\Delta s A_i}\right)\Delta u_{i+1} - \left(\frac{E_1 A_{i+1}}{2\Delta s^3} + \frac{\kappa E_2}{2A_{i+1}\Delta s^3}\right)\Delta u_{i+2}$$

$$+ \left(\frac{E_1 B_{i-1}}{2\Delta s^3} + \frac{E_2}{A_{i-1}\Delta s^4}\right)\Delta w_{i-2}$$

$$- \left(\frac{\kappa E_1 A_{i-1}}{\Delta s^2} + \frac{a_i B_i}{2\Delta s} + \frac{2E_2}{A_{i-1}\Delta s^4} + \frac{b_i}{A_i \Delta s^2}\right)\Delta w_{i-1}$$

$$- \left(\frac{E_1}{2\Delta s^3}(B_{i-1} - B_{i+1}) - \kappa a_i A_i - \frac{E_2}{\Delta s^4}(\frac{1}{A_{i-1}} + \frac{1}{A_{i+1}}) - \frac{2b_i}{A_i \Delta s^2}\right)\Delta w_i$$

$$+ \left(\frac{a_i B_i}{2\Delta s} - \frac{\kappa E_1 A_{i+1}}{\Delta s^2} - \frac{b_i}{A_i \Delta s^2} - \frac{2E_2}{A_{i+1}\Delta s^4}\right)\Delta w_{i+1}$$

$$- \left(\frac{E_1 B_{i+1}}{2\Delta s^3} - \frac{E_2}{A_{i+1}\Delta s^4}\right)\Delta w_{i+2} = p^\circ + \frac{\partial^2 \bar{M}_i}{\partial s^2} - \bar{k}_i - \bar{N}_i \qquad (B-11)$$

and

$$\left(\frac{c_i A_i}{\Delta s^2} + \frac{c_i(C_i - \kappa B_i)}{2\Delta s} + \frac{\kappa d_i}{A_i \Delta s^2}\right)\Delta u_{i+1} - \left(\frac{2c_i A_i}{\Delta s^2} + \kappa c_i D_i + \frac{2\kappa d_i}{A_i \Delta s^2}\right)\Delta u_i$$

$$+ \left(\frac{c_i A_i}{\Delta s^2} - \frac{c_i(C_i - \kappa B_i)}{2\Delta s} + \frac{\kappa d_i}{A_i \Delta s^2}\right)\Delta u_{i-1} + \left(\frac{d_i}{2A_i \Delta s^3}\right)\Delta w_{i+2}$$

$$+ \left(\frac{c_i B_i}{\Delta s^2} + \frac{c_i(D_i + \kappa A_i)}{2\Delta s} - \frac{d_i}{A_i \Delta s^3}\right)\Delta w_{i+1} + \left(-\frac{2c_i B_i}{\Delta s^2} + \kappa c_i C_i\right)\Delta w_i$$

$$+ \left(\frac{c_i B_i}{\Delta s^2} - \frac{c_i(D_i + \kappa A_i)}{2\Delta s} + \frac{d_i}{A_i \Delta s^3}\right)\Delta w_{i-1} - \left(\frac{d_i}{2A_i \Delta s^3}\right)\Delta w_{i-2}$$

$$= -\frac{\partial \bar{N}_i}{\partial s} - \bar{k}_i \frac{\partial \bar{M}_i}{\partial s}. \qquad (B-12)$$

55

These two equations provide the finite-difference approximation for the deflection of the internal nodes of the beam, that is for the subscript i over the range $3 \leq i \leq n - 1$, (see Fig. 4). Therefore, for an arch of $n + 1$ total nodes, they provide a system of $2n - 6$ equations in $2n + 2$ unknowns. Thus, eight additional equations are required to provide a unique solution for the problem. Six of these equations are obtained by using the boundary condition. These provide two sets of three equations, one set applicable to node 1 and the other set for node $n + 1$.

As evidenced above, the boundary conditions do not provide a sufficient number of relations to enable unique solution. This, in part, results from the inherent coupling generated by the assumption of Euler-Bernoulli bending when both axial and transverse deflections are possible. Note that the deflection functions are not only related to one another, but they also appear in the same functional format in both expressions. The derivative of one is added to (subtracted from) the other multiplied by the curvature. This, in turn, indicates that a form of implicit coupling exists between the two generalized displacements, centroidal axis strain and rotation. Ideally, the generalized displacements should be completely independent.

A number of approaches can be employed to generate the two additional equations needed for unique solution. The one used in this study is to require the "centroidal axis" strain in the wall to vanish. Mathematically, this is equivalent to appending, to the existing system of equations, the two additional equations:

$$\Delta \epsilon_{ol} = -\bar{\epsilon}_{ol} \qquad \text{and} \qquad \Delta \epsilon_{or} = -\bar{\epsilon}_{or}, \qquad (B - 14a, b)$$

where ϵ_{ol} and ϵ_{or} represent the strain in the left and right extensions, respectively. No condition is established for the "rotations" which might occur in the wall sections. This is not felt to be significant since the nodal mesh, at least for the equilibrium problem, is a centroidal mesh.

Using the boundary conditions and the two "wall strain" relations it is possible to eliminate the transverse and axial displacement components for nodes 1, 2, n, and $n + 1$ from the general finite-difference equations. This leaves a system of exactly $2n - 6$ equations in the same number of unknowns. If the coefficients of these equations are arranged in matrix form, the result is a banded matrix with a bandwidth of six.

APPENDIX B

Novel Approach Papers

Thermodynamically Consistent Constitutive Equations for Nonisothermal Large-Strain, Elastoplastic, Creep Behavior

Richard Riff,* Robert L. Carlson,† and George J. Simitses‡
Georgia Institute of Technology, Atlanta, Georgia

The paper is concerned with the development of constitutive relations for large nonisothermal elastic-viscoplastic deformations for metals. The kinematics of elastic-plastic deformation, valid for finite strains and rotations, is presented. The resulting elastic-plastic uncoupled equations for the deformation rate combined with use of the incremental elasticity law permits a precise and purely deductive development of elastic-viscoplastic theory. It is shown that a phenomenological thermodynamic theory in which the elastic deformation and the temperature are state variables, including few internal variables, can be utilized to construct elastic-viscoplastic constitutive equations appropriate for metals. The limiting case of inviscid plasticity is examined.

Nomenclature

da	= element of area
ds	= material line element
d_{rs}	= deformation rate
$\dot{E}_{\omega J}$	= strain rate
F	= yield function
f^A_α, F^r_α	= deformation gradients
g_r, G^A	= base vectors
g^{rs}, G^{AB}	= metric tensors
J	= absolute determinant of the deformation gradient
$k, \alpha^A_C, A^{AB}_{CD}$	= internal variables
n	= normal to the surface
P	= force
q	= specific applied heat
s	= entropy
T	= temperature
t	= fraction sector
t	= time
u	= specific internal energy
V	= volume
v^r	= velocity
w	= specific mechanical work
W_{rs}	= spin tensor
x^i	= inertial coordinate system
x^a	= material coordinate system
x^A	= convected coordinate system
ρ	= density
σ	= Cauchy stress tensor
τ	= Kirchhoff stress tensor
ϕ	= specific free energy
$\overset{\triangledown}{\sigma}$	= Jauman stress rate
$\dot{\sigma}$	= time derivative

Introduction

THE prediction of inelastic behavior of metallic materials at elevated temperature has increased in importance in recent years. Many important engineering applications involve the use of metals subjected to cyclic thermomechanical loads, e.g., hot section components of turbine engines, nuclear reactor components, etc. These materials exhibit substantial complexity in their thermomechanical constitution. In fact, so complex is their material response that it could be argued that without useful a priori information, experimental characterization is futile. It is, therefore, important to be able to model accurately the nonelastic behavior of metals under cyclic mechanical and thermal loading at temperature levels for which creep and recovery introduce significant response phenomena.

Under this kind of severe loading conditions, the real world of structural behavior is highly nonlinear due to the combined action of geometrical and physical nonlinearities. On one side, finite deformation (in a stressed structure) introduce nonlinear geometric effects. On the other side, physical nonlinearities arise even in small strain regimes, whereby inelastic phenomena play a particularly important role. From a theoretical standpoint nonlinear constitutive equations should be applied only in connection with nonlinear deformation measures. However, in engineering practice, the two sources of nonlinearities are separated for practical reasons, yielding at one end of the spectrum large displacement and large rotation problems and on the other end inelastic analysis in the presence of small strain.

Constitutive models for small strain in engineering literature may generally be grouped into three categories: classical plasticity, nonlinear viscoelasticity, and theories based on microstructural phenomena. Each group can be further separated into "unified" and "uncoupled" theories, where the two differ in their approach to the treatment of rate-independent and rate-dependent inelastic deformation. The uncoupled theories decompose the inelastic strain rate into a time-independent plastic strain rate and a time-dependent creep rate with independent constitutive relations describing plastic and creep behavior. Such uncoupling of the strain components provides for simpler theories to be developed, but precludes any creep/plasticity interaction. Recognizing that cyclic plasticity, creep, and recovery are not independent phenomena but rather are very interdependent, a number of "unified" models for inherently time-dependent nonelastic deformation have been developed recently.

Classical incremental plasticity theories are macro-phenomenological because they base the derivation of state variables purely on experimental results without direct reference to the microstructure of the material. Most incremental plasticity theories have four major components: 1) a stress-elastic strain relation, 2) a yield function describing the onset of plastic deformation, 3) a hardening rule that prescribes the strain hardening of the material and the modification of the yield surface during plastic flow, and 4) a flow rule that defines the components of strain that is plastic or nonrecoverable. Research in this area is voluminous. For example, Zienkiewicz and Cormeau[1] developed a rate-dependent unified theory that allows for nonassociative plasticity and strain softening, but does not model the Bauschinger effect or temperature dependence. Extensions of classical plasticity to model both rate and temperature effects were presented recently by Allen and Haisler,[2] Haisler and Cronenworth,[3] and Yamada and Sakurai.[4]

In the nonlinear viscoelastic approach, the constitutive relation is expressed as a single integral or convoluted form. This type of constitutive model employs the thermodynamic laws along with physical constraints to complete the formulation. A detailed review of several existing theories is presented by Walker.[5] Walker's theory is based on a unified viscoplastic integral developed by modifying the constitutive relations for a linear three-parameter viscoelastic solid. The theory contains clearly defined material parameters, a rate-dependent equilibrium stress, and a proposed multiaxial model. An important shortcoming of Walker's theory is its failure to model transient temperature conditions. Many other nonlinear viscoelastic theories have been proposed, including those by Cernocky and Krempl,[6] Valanis,[7] and Chabache.[8]

The microphenomenological theories attempt to represent the response of polycrystalline materials in terms of various micromechanisms of deformation and failure. Various dislocation theories have been developed to predict plastic deformation in terms of dislocation interaction, slip, glide, density, etc. Most of the material models developed to date depend primarily on the number of state variables used and their growth or evolutionary laws. Many of the recent "unified" microphenomenological theories have been discussed and evaluated by Walker[9] and Chan et al.[10]

One example of a microphysically based constitutive law is an elastic-viscoplastic theory based on two internal state variables as proposed by Bodner et al.[11] These authors demonstrate the ability of the constitutive equations to represent the principal features of cyclic loading behavior, including softening upon stress reversal, cyclic hardening or softening, cyclic saturation, cyclic relaxation, and cyclic creep. One limitation of the formulation though is that the computed stress-strain curves are independent of the strain amplitude and therefore too "flat" or "square."

Miller[12] has reported research on the modeling of cyclic plasticity with "unified" constitutive equations. He also recognizes the shortcomings of many theories in predicting hysteresis loops that are oversquare in comparison to observed experimental behavior. Improvement is accomplished by making the kinematic work-hardening coefficient depend on the back stress and the sign of the nonelastic strain term. Theories that are similar in format to Miller's have been proposed by Krieg et al.[13] and Hart.[14] The models use two internal state variables to reflect current microstructure state and are based upon models for dislocation processes in pure metals. All of these constitutive theories were formulated without the use of a yield criterion. Since these models do not contain a completely elastic regime, the function that describes the inelastic strain rate should be such that the inelastic strain rate is very small for low stress levels. Theories with a yield function and a full elastic regime have been developed for the case of isotropic hardening by Robinson[15] and Lee and Zavrel[16] for both isotropic and directional hardening.

As previously noted, the quantities utilized in the small strain theory of viscoplasticity (stress, strain, stress rate, and strain rate) are defined only within the assumption of "small strains." Yet the precise definition of what constitutes "small strain" is always left unstated. Whether or not the stresses for a given case are "small" cannot be determined a priori by geometric considerations. In general, one cannot know in advance whether, for a given loading of a material, the "small-strain" assumption (always left undefined) will hold or not. The question of whether the small-strain approximations are valid is always avoided in the "small-strain" literature. Furthermore, as Hill[17] points out, the really typical plastic problems involve changes in geometry that cannot be disregarded. In many cases, for example, it is sufficient to take into account finite plastic strains and small elastic strains or vice versa. From the theoretical viewpoint, it is desirable in all cases to have a theory that intrinsically allows for both the elastic and plastic strains to be large. Such a theory, of course, must reduce to the earlier mentioned special cases, as limiting cases. Furthermore, such theories provide a check for those obtained by generalizing small-strain theories.

The mathematical theories of deformation and flow of matter deal essentially with the gross properties of a medium. Heat and mechanical work are considered as additional causes for a change of the state of the medium. The resulting phenomena in any particular material are not unrelated. Therefore, a thermodynamical treatment of the foundation of the theory of flow and deformation is appropriate and, indeed, the obvious approach. Two very different main approaches to a thermodynamic theory of a continuum can be identified. These differ from each other in the fundamental postulates upon which the theories are based. An essential controversy (a good survey of this controversy is given in Ref. 18) can be traced through the whole discussion of the thermodynamic aspects of continuum mechanics. None of these approaches is concerned with the atomic structure of the material. Therefore, they represent purely phenomenological approximations. Both theories are characterized by the same fundamental requirement that the results should be obtained without having recourse to statical or kinetic methods.

Within each of these approaches, there are two distinct methods of describing history and dissipative effects: the functional theory[19] in which all dependent variables are assumed to depend on the entire history of the independent variables and the internal variable approach[20] wherein history dependence is postulated to appear implicitly in a set of internal variables. For experimental as well as analytical reasons,[21,22] the use of internal variables in modeling inelastic solids is gaining widespread usage in current research. The main differences among the various modern theories lie in the choice of these internal variables.

Therefore, the predictive value of an elastic-viscoplastic material model for nonisothermal, large-deformation analyses depends on three basic elements: 1) the nonlinear kinematic description of the elastic-plastic deformation, 2) thermodynamic considerations, and 3) the choice of external and internal thermodynamic variables. The objective of this paper is to examine each of these elements, illustrate their interaction, and extend these considerations to model the large, nonisothermal, elastic-viscoplastic deformation behavior of metals.

Moreover, the paper deals with the phenomenological theory of elastic-viscoplastic bodies. The process inside the lattice and at the border of the crystal grains is taken as the physical background, without considering its connection to the macroscopic behavior of the material at the present.

Kinematic and Fundamental Considerations

Consider body of volume V that occupies a finite region of Euclidean space. When subjected to prescribed body

forces, surface tractions, surface temperature, and surface velocities, the body undergoes motion characterized by $x^i = \chi^i(X^\alpha, t)$. The material particles of the body are identified by coordinates X^α, which are referred to as material coordinates. The relation of the material particles to the material coordinates X^α does not change in time. The places in space that the particles occupy during the motion are identified by the coordinates x^i. Functions χ^i describe the motion of the particles X^α through space. The place occupied by the body at $t = 0$ is taken as the initial configuration. In this configuration the body is assumed to be strain-free, but not necessarily stress-free.

A third coordinate system is defined by the material coordinates as they deform with the body. This system will be denoted by X^A, which are referred to as convected coordinates. The current configuration of the body with spatial coordinates x^i and convected coordinates X^A and the initial configuration of the body with material coordinates X^α will be employed in what follows. For the spatial coordinates x^i, the covariant base vectors g_r, the contravariant base vector g^r, the metric g_{rs}, and its dual g^{rs} are used. Similarly, for the convected coordinates X^A, the covariant base vectors G_A, the contravariant base vectors G^A, the metric tensor G_{AB}, and its dual G^{AB} are used. With regard to the initial configuration, the covariant base vectors $G\alpha$, the contravariant base vectors G^α, the metric tensor $G_{\alpha\beta}$, and it dual $G^{\alpha\beta}$ are used for the material coordinates X^α.

For a second-order tensor A with components A^{rs} in the spatial coordinates and components A^{AB} in the convected coordinates, the following is true:

$$A = A^{rs} g_r g_s = A^{AB} G_A G_B \qquad (1)$$

The two sets of components are related to each other through

$$A^{rs} = x^r_{,A} x^s_{,B} A^{AB} \qquad (2)$$

where $X^r_{,A}$ denotes the partial derivative $\partial \chi^r(X^B, t)/\partial X^A$.

For the motion, characterized by $\chi^r(X^A, t) = \chi^r(X^\alpha, t)$, we have

$$G_A = x^r_{,A} g_r \qquad G_{AB} + X^r_{,A} x^s_{,B} g_{rs} \qquad (3)$$

From Eq. (3), it is seen that $\dot{G}_{AB} = 0$, where the dot denotes time material derivative. The tensor transformation equations (1) and (2) will be used extensively in what follows.

A material line element $ds = dX^\alpha G^\alpha$ in the initial configuration when subjected to motion $\chi^r(X^\alpha, t)$ is deformed into $ds = dx^r g_r$ in the current configuration. The line element dx^r is related to the line element dX^α through the deformation gradient F^r_α by $dx^r = F^r_\alpha dX^\alpha$ where

$$F^r_\alpha = \frac{\partial x^r}{\partial x^\alpha}(x^\beta, t) \qquad (4)$$

The mapping defined by the deformation gradient $F = F^r_\alpha g_r G^\alpha$ allows one to shift quantities from the current configuration to equivalent, but alternate, quantities in the initial configuration. For example, the right Caushy-Green tensor $C = C_{\alpha\beta} G^\alpha G^\beta$ and the Green-St. Venant strain tensor $E = E_{\alpha\beta} G^\alpha G^\beta$, in the initial configuration are

$$ds = dS = g_{rs} dx^r dx^s - G_{\alpha\beta} dX^\alpha dX^\beta$$

$$= (g_{rs} F^r_\alpha F^s_\beta - G_{\alpha\beta}) dX^\alpha dX^\beta$$

$$= (C_{\alpha\beta} - G_{\alpha\beta}) dX^\alpha dX^\beta = 2E_{\alpha\beta} dX^\alpha dX^\beta \qquad (5)$$

The components of the deformation gradient, which relate a deformed line element dX^A in the convected coordinates to the undeformed line element dX^α in the initial configuration,

are given by f^A_α,

$$F^r_\alpha = x^r_{,A} f^A_\alpha \qquad (6)$$

Equation (6) places in a single expression the easily confused but distinct ideas of the transformation of tensor components under a change of coordinates and a shift between the current configuration and the initial configuration as a setting for the governing equations. Truesdell and Toupin[23] and Truesdell and Noll[24] emphasizes the current configuration with the spatial coordinates and an initial configuration with material coordinates. As a result, the deformation gradient plays a prominent role in their work. Only in isolated spots do they mention convected coordinates and, then, as indirectly as possible. On the other hand, Green and Adkins[25] and Sedov[26] rely heavily on convected coordinates. Our intention here is only to tie the two together for the purpose of discussing elementary assumptions. Recently, Mendelssohn and Baruch[27] review this same point as well as additional material relevant to sound numerical formulation of finite deformation problems.

The velocity $v = v^r g_r$ of a particle X^n is defined by

$$v^r = \frac{\partial x^r}{\partial t}(X^\alpha, t) \qquad (7)$$

From the spatial gradient of the velocity, the deformation rate

$$d = d_{rs} g^r g^s = d_{AB} G^A G^B \qquad (8)$$

is defined as

$$d_{rs} = \tfrac{1}{2}(V_{r,s} + V_{s,r}) \qquad (9)$$

The spin

$$W = W_{rs} g^r g^s = W^{AB} G_A G_B \qquad (10)$$

is defined as

$$W_{rs} = \tfrac{1}{2}(V_{r,s} - V_{s,r}) \qquad (11)$$

In the initial configuration, the Green-St. Venant strain rate is the shifted deformation rate,

$$\dot{E}_{\alpha\beta} = F^r_\alpha F^s_\beta d_{rs} = f^A_\alpha f^B_\beta d_{AB} \qquad (12)$$

Basic to most of the postulated models of large elastic-plastic deformation behavior is the additive decomposition of d_{rs} and $E_{\alpha\beta}$ into elastic and plastic parts,[28]

$$d_{rs} = \overset{E}{d}_{rs} + \overset{P}{d}_{rs}, \qquad \dot{E}_{\alpha\beta} = \overset{E}{\dot{E}}_{\alpha\beta} + \overset{P}{\dot{E}}_{\alpha\beta} \qquad (13)$$

The validity of this additive decomposition in the case of finite elastic-plastic strains has been questioned by Lee and his associates.[29-32] Lee's[29] approach is based on the total purely elastic unloading from the current state to an intermediate unstressed plasticity deformed configuration, without any reverse or other kind of plastic flow. The major point in his theory is to decouple the total elastically induced distortion and measure it from a relaxed unstressed state, which is only plastically deformed from the initial to the intermediate configuration. Accordingly, the deformation gradient F is decomposed in the form

$$F = \overset{E}{F} \overset{P}{F} \qquad (14)$$

where $\overset{P}{F}$ transforms a line element from the initial configuration to the intermediate configuration and $\overset{E}{F}$ from the latter

to the current configuration. The intermediate configuration is chosen in such a way so that $\overset{P}{F}$ is unaffected by the presence of rigid-body motion. The deformation rate tensors d_r, and d_Λ are then defined. After some manipulations, Lee shows the following relation:

$$d_\Lambda = \overset{E}{d^r} + \overset{E}{F_{r\kappa}}\overset{P}{d_{kl}}\overset{E}{F_\Lambda^{-1}}\Big|_s + \overset{E}{F_{r\kappa}}\overset{P}{W_{r\lambda}}F_\Lambda^{-1}\Big|_s \quad (15)$$

where the subscripts s denote the symmetric parts. Generalization of Lee's theory for anisotropic elasticity was given by Mandel.[13]

Lee's theory is based on the assumption that the elastic law does not change with the history of deformation and, hence, a total elastic unloading can take place. However, it has been shown[34] that after a fair amount of plastic flow has taken place, reverse plastic deformation will result soon upon unloading, even for small strains. Therefore, a total elastic unloading cannot have any physical significance. In view of this, the theory of Lee appears as a special case of the theory of Green and Naghdi.[35] Although not as general as the theory of Green and Naghdi, Lee's theory has the advantage of being more easily fitted with the physical property of invariance of elasticity with respect to plastic deformation. In particular, Mandel[33] has pointed out that the Green-Naghdi theory is not convenient if one wants to include anisotropic elasticity effects. All this can be avoided by the use of the convected coordinates, as proposed by Sedov[26] and Lehmann.[36] The formulation presented herein will follow the work of Lehmann.

All quantities from here on will be related to the metric of the coordinate system X^Λ in the deformed state. Hence,

$$f_c^a = G^{aJ}G_{BC}$$
$$(f^{-1})_\gamma^\Lambda = G^{\Lambda B}G_{J\gamma} \quad (16)$$

and the deformation rate is

$$d_r^\Lambda = \tfrac{1}{2}G^{\Lambda B}\dot{G}_{J\gamma} = -\tfrac{1}{2}G_{CB}\dot{G}^{J\alpha}$$
$$= \tfrac{1}{2}(f^{-1})_J^\Lambda(\dot{f})_\gamma^J = -\tfrac{1}{2}(f^{-1})_{,B}^\Lambda f_\gamma^B \quad (17)$$

The deformation gradient may be split into its elastic and its plastic components in the following manner:

$$f_c^\kappa = \underbrace{G^{aJ}\,G_{Jr}}_{\overset{P}{F^\kappa_\Gamma}}\,\underbrace{G^{\Gamma D}G_{DC}}_{\overset{E}{f_c^\Gamma}}$$
$$(f^{-1})_\gamma^\Lambda = \underbrace{G^{\Lambda B}\,G_{BT}}_{\overset{E}{(f^{-1})_\Gamma^\Lambda}}\,\underbrace{G^{\Gamma \delta}\,G_{\delta\gamma}}_{\overset{P}{(f^{-1})_\gamma^\Gamma}} \quad (18)$$

The use of capital greek subscripts and superscripts (G_{JT}) denotes parameters belonging to a fictitious intermediate state, which is in general incompatible. The circumstance of the noncontinuous configuration in the unstressed state has been observed by Sedov,[26] who points out that convected coordinates, as used herein, become non-Euclidean in this configuration.

This multiplicative splitting of the metric change in the convected coordinates leads to an additive splitting of the deformation rate according to

$$d_C^\Lambda = \text{sym}\tfrac{1}{2}\{\overset{E}{(f^{-1})_\Gamma^\Lambda}(\overset{E}{f})_C^\Gamma\} + \text{sym}\tfrac{1}{2}\{\overset{E}{(f^{-1})_\delta^\Lambda}(\overset{P}{f})_\Gamma^\delta\overset{E}{f_C^\Gamma}\}$$

$$= \text{sym}\tfrac{1}{2}\{\overset{E}{(f^{-1})_\Gamma^\Lambda}f_C^\Gamma\} - \text{sym}\tfrac{1}{2}\{\overset{E}{(f^{-1})_\Gamma^\Lambda}\overset{P}{(f^{-1})_\delta^\Lambda}\Gamma_r f_C^\delta\} \quad (19)$$

$$= \qquad \overset{E}{d_C^\Lambda} \qquad + \qquad \overset{P}{d_C^\Lambda}$$

In the current configuration of the body V, consider an element of area da on the surface of $\mathcal{S}$ with an outward normal $n = n_r g^r = n_A G^A$. If the force $dP = dP^r g_r = dP^A G_A$ is acting on this element, the fraction vector is $t = dP/da$. The Caushy stress,

$$\sigma = \sigma^{rs}g_r g_s = \sigma^{AB}G_A G_B \quad (20)$$

defined, such that $t = \sigma \cdot n$, which in component form (in terms of spatial coordinates) is $t^r = \sigma^{rs}n_s$. In the convected coordinates, it is $t^A = \sigma^{AB}n_B$.

It is convenient to work with the Kirchhoff stress tensor τ in the current configuration, obtained from the Cauchy stress by scaling

$$\tau_B^A = \frac{\rho_0}{\rho}\sigma_B^A J\sigma_B^A \quad (21)$$

where ρ denotes the current mass density, ρ_0 the mass density in the initial state, and J the absolute determinant of the deformation gradient at the current configuration.

The time derivative of a tensor such as stress, which is associated with the current configuration, admits infinitely many definitions, depending upon the coordinate system employed in the computation of such time derivatives. For a correct large-strain, large-rotation elastic-plastic model, the notion of "invariant stress fluxes" and "objectivity" must be introduced. A good treatment requires more space than is available here.[23] The corotational stress rate, also referred to as Jauman stress rate, will suffice for the purpose of the present discussion. Hence, in convected coordinates,

$$\overset{\triangledown}{\sigma_B^A} = \dot{\sigma}_{,B}^A + d_C^A\sigma_B^C - d_B^C\sigma_C^A$$

$$\overset{\triangledown}{\tau_B^A} = \dot{\tau}_B^A + d_C^A\tau_B^C - d_B^C\tau_C^A \quad (22)$$

From Eq. (21), the following relations between the various rates of Kirchoff stress and Cauchy stress are obtained:

$$\dot{\tau}_B^A = \frac{\rho_0}{\rho}\dot{\sigma}_B^A + Jd_{,C}^C\sigma_B^A$$

$$\overset{\triangledown}{\tau_B^A} = \frac{\rho_0}{\rho}\overset{\triangledown}{\sigma_B^A} + Jd_{,C}^C\sigma_B^A \quad (23)$$

If a rate constitutive law is postulated between $\dot{\sigma}$ and d in finite inelasticity theories, then a potential does not exist, which is necessary in the variational or thermodynamics-based formulation of the problem. The basic difficulty lies with the $d_{,C}^C$ term. This is remedied by postulating a constitutive law between $\dot{\tau}$ and d.

The Elastic Deformations

The present study is concerned with the structure of the constitutive relation of an elastic-viscoplastic (elastic-plastic) medium. The term elastic-viscoplastic means that the viscosity does not intervene in the elastic domain whose boundary, in particular, is well defined at every stage of the deforma-

61

tion. For simplicity, we assume further that the thermoelastic behavior of the body is isotropic and unaffected by inelastic deformation in the sense that the material constants characterizing the thermoelastic behavior are independent of inelastic deformation. Thus, we can obtain a unique relation between the elastic deformations represented by $\overset{E}{f_C^A}$, the Kirchhoff stresses τ_C^A, and the temperature T,[35,36]

$$\overset{E}{f_C^A} = \overset{E}{f_C^A}(\tau_C^A, T); \qquad \tau_C^A = \tau_C^A(\overset{E}{f_D^B}, T); \qquad T = T(\tau_C^A, f_D^B) \qquad (24)$$

This function may be transformed into an incremental relation by differentiation with respect to time. This leads to a general expression of the form

$$\overset{E}{d_C^A} = \overset{E}{d_C^A}\{\tau_C^A, \overset{\triangledown}{\tau_C^A}, T, \dot{T}, G_{AC}, d_C^A\} \qquad (25)$$

From Eq. (24) we see that the total deformation rate enters the incremental form of the thermoelastic stress-strain relations. Therefore, the thermoelastic deformation is not independent of the inelastic deformation occurring at the same time. This follows from the fact that in the integrated form of the thermoelastic stress-strain relations Eq. (24), the stresses and the strains are referred to the deformed state of the body.

In view of the present discussion and the discussion in the previous section, the hyperelastic behavior described by Eqs. (24) and (25) will be replaced by a hypoelastic law. The hypoelastic law is a path-dependent material law, since it cannot be expressed in terms of an initial and a final state; it depends on the path connecting these states. Otherwise, if we did not make such a change, it would be necessary to retain the finite deformation measure in the constitutive law. For small elastic strains, there is practically no difference between hypoelastic and hyperelastic laws, as shown, for example, by Lehmann.[36]

The above could be illustrated by the following example. From the frequently used elastic stress-strain relation,

$$\epsilon_C^A = \tfrac{1}{2}\left\{\delta_C^A - \overset{E}{(f^{-1})_C^A}\right\} = \frac{1}{2G}\left\{\tau_C^A - \frac{\nu}{1+\nu}\tau_B^B\delta_C^A\right\}$$

$$+ \alpha(T - T_0)\delta_C^A \qquad (26)$$

we get

$$\overset{E}{d_C^A} = \frac{1}{2G}\left\{\text{sym}\left[\overset{E}{f_C^D}(\dot{\ })_D^A\right] - \frac{\nu}{1+\nu}\overset{E}{f_C^A}(\dot{\tau}_B^B)\right\} + \alpha\dot{T}f_C^A \qquad (27)$$

which may be replaced by

$$\overset{E}{d_C^A} = \frac{1}{2G}\left\{\overset{\triangledown}{\tau_C^A} - \frac{\nu}{1+\nu}\overset{\triangledown}{\tau_B^B}\delta_C^A\right\} + \alpha\dot{T}\delta_C^A + \alpha T\delta_C^A \qquad (28)$$

We assume that inelastic deformation occurs if and only if

$$F(\tau_C^A, T, k, \ldots, \alpha_C^A, \ldots, A_{CD}^{AB}, \ldots) = 0 \qquad (29a)$$

$$\frac{\partial F}{\partial \tau_C^A}\overset{\triangledown}{\tau_C^A} + \frac{\partial F}{\partial T}\dot{T} > 0 \qquad (29b)$$

or, for elastic-plastic material,

$$F(\tau_C^A, T, k, \ldots, \alpha_C^A, \ldots, A_{CD}^{AB}, \ldots) > 0 \qquad (30)$$

for an elastic-viscoplastic material. The function F represents the yield condition that bounds the domain of pure thermoelastic behavior in the ten-dimensional space of stress and

temperature. The inequality given by Eq. (29b) is the loading condition. The actual form of the yield condition for a given material is determined by a set of so-called internal parameters, which are scalars and/or tensors of even order. The current values of the internal parameters depend on the initial state of the material and the history of the thermomechanical process.

Thermodynamic Processes

In the treatment of elastic-plastic or elastic-viscoplastic deformations, we have to distinguish between the description as a thermomechanical process and the corresponding one by means of thermodynamic state equations. It is sometimes assumed that, in the case of processes which proceed through nonequilibrium states, it is fundamentally necessary to start with a description of the process.[19,24,37] Alternatively, it has been proposed that one might assume local equilibrium for the elements of a body and therefore describe the state of the elements, in general, by state equations.[38-40] The consequences of adopting these two approaches become particularly clear when considering the influence of entropy. In the description of the process, entropy is a derived quantity and in principle we can proceed without introducing it. In the description by state equations, it is, on the contrary, a necessary state value that, at least in principle, can be immediately determined. When restricting ourselves to homogeneous, quasistatical thermomechanical processes, the description by state equations can be reviewed as equivalent to that by processes.[37,41] The controversial issues will, thus, not be discussed further.

Restricting ourselves to elementary processes, we need not analyze whether the applied heat arises from heat conduction or from heat sources. For the same reason, it is not necessary, in our case, to introduce the temperature gradient in addition to the temperature or the body forces in addition to the stresses.

The first law states, under our simplifying assumptions, that the rate of the specific internal energy $\dot{u}$ is the sum of the rates of the specific mechanical work $\dot{w}$ and the specific applied heat $\dot{q}$,

$$\dot{u} = \dot{w} + \dot{q} \qquad (31)$$

The rate of mechanical work is given by

$$\dot{W} = \frac{1}{\rho_0}\tau_C^A d_A^C \qquad (32)$$

and may be split into an elastic and an inelastic part according to Eq. (19),

$$\dot{W} = \frac{1}{\rho_0}\tau_C^A\overset{E}{d_A^C} + \frac{1}{\rho_0}\tau_C^A\overset{P}{d_A^C} = \overset{E}{\dot{W}} + \overset{I}{\dot{W}} \qquad (33)$$

The rate of inelastic work must also be split into a part $\overset{D}{\dot{W}}$, which is dissipated at once, and into another part $\overset{S}{\dot{W}}$, which represents changes in the internal state. Thus,

$$\overset{I}{\dot{W}} = \frac{1}{\rho_0}\tau_C^A\overset{P}{d_A^C} = \overset{S}{\dot{W}} + \overset{D}{\dot{W}} \qquad (34)$$

Only $\overset{D}{\dot{W}}$ enters the entropy production

$$T\dot{S} = \dot{q} + \overset{D}{\dot{W}} \qquad (35)$$

The second law of thermodynamics requires

$$\overset{D}{\dot{W}} \geq 0 \qquad (36)$$

We use as thermodynamic state variables the elastic strain, represented by $f_C^{\overset{E}{A}}$, the absolute temperature T, and a number of other internal state variables $(k,...,\alpha_C^A,...,A_{CD}^{AB},...)$ that may be scalars and tensors of even order. The choice of $f_C^{\overset{E}{A}}$ and T as state variables is based on the fact that in pure thermoelastic deformations, both quantities form a suitable set of thermodynamic state variables. The plastic strain and the total strain are unsuitable as state variables because, in general, they do not uniquely define the state of the material. A conflicting point of view has been expressed in Refs. 42–44. The remaining state variables are added for the sake of the description of the changes of the internal structure of the material.

The specific free energy (Helmholtz function) ϕ given by

$$\phi = u - Ts \tag{37}$$

must be a unique function of the thermodynamic state variables

$$\phi = \phi(f_C^{\overset{e}{A}}, T, k, \alpha_C^A,...,A_{CD}^{AB},...) \tag{38}$$

Since the elastic part of the deformation, according to our assumptions, does not depend on the plastic deformation, we may divide the free energy into two different components, as

$$\phi = \overset{E}{\phi}(f_C^{\overset{E}{A}}, T) + \overset{S}{\phi}(T, k,...,\alpha_C^A,...,A_{CD}^{AB},...) \tag{39}$$

where the first component $\overset{E}{\phi}$ refers to the elastic deformation and the second $\overset{S}{\phi}$ to the changes of the internal state.

From Eqs. (31), (33–35), and (37) we derive

$$\dot{\phi} = -s\dot{T} + \overset{E}{W} + \overset{S}{W} \tag{40}$$

Also, we obtain from Eq. (39)

$$\dot{\phi} = \frac{\partial \overset{E}{\phi}}{\partial f_C^A} \overset{\overset{E}{\nabla}}{f_C^A} + \frac{\partial(\overset{E}{\phi}+\overset{S}{\phi})}{\partial T}\dot{T}$$

$$+ \frac{\partial \overset{S}{\phi}}{\partial k}\dot{k} + ... + \frac{\partial \overset{S}{\phi}}{\partial \alpha_C^A}\overset{\nabla}{\alpha_C^A} + ... + \frac{\partial \overset{S}{\phi}}{\partial A_{CD}^{AB}}\overset{\nabla}{A_{CD}^{AB}} + ... \tag{41}$$

By comparison of Eqs. (40) and (41), we may conclude that

$$S = -\frac{\partial(\overset{E}{\phi}+\overset{S}{\phi})}{\partial T} \tag{*}$$

$$\overset{S}{W} = \frac{\partial \overset{S}{\phi}}{\partial k}\dot{k} + ... + \frac{\partial \overset{S}{\phi}}{\partial \alpha_C^A}\overset{\nabla}{\alpha_C^A} + ... + \frac{\partial \overset{S}{\phi}}{\partial A_{CD}^{AB}}\overset{\nabla}{A_{CD}^{AB}} ...$$

$$\tau_C^A = \rho_0 f_C^{\overset{E}{B}}\frac{\partial \overset{E}{\phi}}{\partial f_B^{\overset{E}{A}}} \tag{42}$$

For irreversible processes, this scheme of description has to be completed by some statements about the dependence of entropy production on the thermomechanical process. Under our assumption, we need deal only with entropy production by dissipated mechanical work, in connection with inelastic

deformation. Thus, we assume, in general

$$\overset{D}{W} = C_{CD}^{AB}\tau_A^C d_B^{\overset{I}{D}} > 0 \tag{43}$$

where

$$C_{CD}^{AB} = C_{CD}^{AB}(f_C^{\overset{E}{A}}, T, k,...,\alpha_C^A,...,A_{CD}^{AB}) \tag{44}$$

Equations (42) and (43) are the governing equations for nonisothermal, elastic-inelastic elementary processes. The specific free energy ϕ, which determines the nondissipated work of the thermomechanical process and the quantity C_{CD}^{AB}, which governs the entropy production, must be specified according to the material behavior.

Elastic-Viscoplastic Model

Thermomechanical processes in elastic-viscoplastic bodies cannot be considered as a sequence of equilibrium states, even in the case of the elementary processes considered here. Elastic-viscoplastic deformations are associated with non-equilibrium states. One consequence of this fact is that we may get a continuation of a process without any change in the independent process variables. This occurs, for example, in the case of creep with constant stress and temperature or in the case of an adiabatic stress relaxation under constant strain. In such cases, the body moves from a nonequilibrium state to an equilibrium state.

In order to establish the constitutive relations for elastic-viscoplastic bodies, which in the limiting case becoming elastic-inviscidly plastic, we adopt the usual assumption that the stresses, which produce the inelastic deformation, may be expressed as the sum of the so-called athermal or inviscid stresses, τ_C^A and the viscous overstresses $\overset{*}{\tau}_C^A$

$$\tau_C^A = \overset{I}{\tau}_C^A = \overset{*}{\tau}_C^A + (\tau_C^A - \overset{*}{\tau}_C^A) \tag{45}$$

This assumption by no means detracts from the "unified" concept. The rate-independent limit of viscoplastic constitutive relation was recently discussed by Travnicek and Kratochvil.[45] Hence, the total work rate can be partitioned in the following way:

$$\overset{}{W} = \overset{E}{W} + \overset{P}{W} + \overset{V}{W} = \underbrace{\frac{1}{\rho_0}\overset{E}{\tau}_C^A d_A^C + \frac{1}{\rho_0}\overset{P}{\tau}_C^A d_A^C}_{\overset{I}{W}} + \frac{1}{\rho_0}\overset{*}{\tau}_C^A d_A^{\overset{P}{C}} \tag{46}$$

The viscous part of the work is completely dissipated. Thus, we may write

$$\overset{V}{W} = \overset{D_v}{W} \tag{47}$$

Regarding the plastic work, we have already stated that one part is used for changing the internal state and only the remaining part can be considered to be dissipated. Therefore, we must write

$$\overset{P}{W} = \overset{S}{W} + \overset{D_p}{W} \tag{48}$$

So, we finally obtain

$$\overset{}{W} = \overset{E}{W} + \overset{S}{W} + \underbrace{\overset{D_p}{W} + \overset{D_v}{W}}_{\overset{D}{W}} \tag{49}$$

We have assumed that the changes of the internal state of the material can be regarded as a sequence of equilibrium states. Then, the specific energy is well defined in each state of the process and we may take the usual overall statement concerning the specific free energy. In so doing, however, we must be aware of the fact that into the part $\overset{S}{W}$ of the plastic work rate $\overset{P}{W}$ only the athermal stress $\hat{\tau}_C^A$ enter, since only these stresses are involved in the plastic mechanism. For the same reason, we can introduce only the athermal stresses $\hat{\tau}_C^A$ into the statement concerning the dissipated plastic work $\overset{D_p}{W}$. On the other hand, we have to add the dissipated viscous work $\overset{D_v}{W}$ to $\overset{D_p}{W}$ in order to obtain the total rate of dissipation. The different mechanisms for determining the total dissipation and their coupling have been discussed by Perzyna.[46]

We now consider an example in which the specific free energy has the following form:

$$\phi = \overset{E}{\phi}(\overset{E}{f_C^A}, T) + \overset{S}{\phi}(T, k, \alpha_C^A) = \overset{E}{\phi}(\overset{E}{f_C^A}, T) + k + f(T) + k\alpha_C^A\alpha_A^C \tag{50}$$

In this equation, h denotes a constant with the dimension of a specific energy like the variable k and the function $f(T)$.

Furthermore, we assume that the dissipation is given by

$$\overset{D_p}{W} = \frac{1}{\rho_0}\xi(\hat{\tau}_C^A - c\rho_0 h\alpha_C^A)\overset{P}{d_A^C}$$

$$\overset{D_v}{W} = \frac{1}{\rho_0}(\tau_C^A - \hat{\tau}_C^A)\overset{P}{d_A^C} \tag{51}$$

where $\xi < 1$ and c denotes constant numbers. This leads to

$$\overset{D}{W} = \overset{D_p}{W} + \overset{D_v}{W} = (\xi-1)\overset{P}{W} - \xi ch\alpha_C^A\overset{P}{d_A^C} + \overset{I}{W} \tag{52}$$

Hence, we obtain

$$\overset{S}{W} = \overset{I}{W} - \overset{D}{W} = (1-\xi)\overset{P}{W} + \xi ch\alpha_C^A\overset{P}{d_A^C} \tag{53}$$

On the other hand, from Eqs. (42) and (50) we have

$$\overset{S}{W} = \dot{k} + 2h\alpha_C^A\overset{\triangledown}{\alpha_A^C} \tag{54}$$

Equations (53) and (54) are compatible, for instance, if we put

$$\dot{k} = (1-\xi)\overset{P}{W} \tag{55}$$

and

$$\overset{\triangledown}{\alpha_A^C} = \tfrac{1}{2}c\xi\overset{P}{d_A^C} \tag{56}$$

From Eq. (55) it follows that, in our case, the plastic work $\overset{P}{W}$ is equivalent to the thermodynamic state variable k. This is still true if we take ξ as a function of k. But it does not hold in the general case when ξ also depends on the other state variables T and α_C^A. Equation (56) shows that only in a very special case, a very unrealistic one, the state variable α_C^A is equivalent to the plastic deformation.

From the thermodynamical considerations, it follows then that we may introduce the quantities k and α_C^A, defined by Eqs. (55) and (56) or any other equivalent set $(\overset{P}{W}, c\rho_0 h\alpha_C^A)$,

as internal variables into the corresponding constitutive equations of the process description.

The constitutive equations themselves are not yet determined completely by Eqs. (50), (51), (55), and (56). These given only the restrictive frame for the formulation of these equations. We may derive a complete set of constitutive equations, which is compatible with this frame, by the further assumptions:

1) The introduction of a yield condition of the form,

$$F = (\hat{t}_C^A - c\rho_0 h\alpha_C^A)(\hat{t}_C^A - c\rho_0 h\alpha_C^A) - g^2(\overset{P}{W}, T) = 0 \tag{57}$$

where $\hat{t}_C^A$ denotes the deviator of the Kirchhoff stresses $\hat{\tau}_C^A$.

2) The plastic deformation obeys the so-called normality rule,

$$\overset{P}{d_C^A} = \lambda\frac{dF}{d\hat{\tau}_C^A} \tag{58}$$

3) The relations between the viscous stresses and the inelastic deformation rate are of the form,

$$\overset{P}{d_C^A} = \frac{1}{2\eta}\dot{\hat{t}}_C^A = \frac{1}{2\eta}(t_C^A - \hat{t}_C^A) \tag{59}$$

4) The quantities ξ and c are constant.

We can eliminate the athermal stresses $\hat{\tau}_C^A$ (which are not state variables) from the equations of evolution by considering that the inelastic deformation can be expressed in two different ways. In one, the plastic mechanism is considered and the viscous mechanism in the second. From Eq. (57), we then obtain

$$\overset{P}{d_C^A} = 2\lambda(\hat{t}_C^A - c\rho_0 h\alpha_C^A) \tag{60}$$

while from Eq. (59), we have

$$\overset{P}{d_C^A} = \frac{1}{2\eta}(t_C^A - \hat{t}_C^A)$$

$$= \frac{1}{2\eta}\{t_C^A - c\rho_0 h\alpha_C^A - (\hat{t}_C^A - c\rho_0 h\alpha_C^A)\} \tag{61}$$

By comparing these equations for $\overset{P}{d_C^A}$, we get

$$\lambda = \frac{1}{4\eta}\left\{\left(\frac{(t_C^A - c\rho_0 h\alpha_C^A)(t_C^A - c\rho_0 h\alpha_C^A)}{g^2}\right)^{1/2} - 1\right\} \tag{62}$$

Following the course of the process in each state, the internal parameters $\overset{P}{W}$ and α_C^A and, therefore, also $k^2 = k^2(\overset{P}{W}, \alpha_C^A)$ are known. Thus, we may calculate λ from Eq. (62) and then all the other needed quantities such as $\hat{t}_C^A$ and $\overset{P}{d_C^A}$.

Discussion

Many thermodynamic considerations of nonisothermal, elastic-viscoplastic deformations refer essentially to the general fundamentals that must be observed in describing such phenomena as thermomechanical processes and then discuss what particular restrictions follow from the second law of thermodynamics. Only a few papers attempt to describe completely such processes by state equations. Most of these papers introduce plastic strains as thermodynamic state variables. But one may conclude from the consideration of the phenomena in the crystal lattice (dislocations, for example, that have completely passed through the crystal produce plastic strains but no changes of state) as well as from phenomenological observations (different states of hardening

64

can belong to the same plastic strains) that plastic strains in general cannot be regarded as state variables. Furthermore, all these papers consider the plastic work as completely dissipated. However, this is in contradiction with experimental results, from which it emerges that one part of plastic work is used for producing states of residual stresses in the lattice, which, when phenomenologically considered, cause hardening.

The results in work presented here can be extended to more complex constitutive equations by introducing more internal parameters or state variables. We may extend our approach to more general, anisotropic hardening materials by assuming [see Eq. (50)], for example, that

$$\overset{E}{\phi} = \overset{E}{\phi}(f_C^A, T) + \overset{S}{\phi}(T, k, \alpha_C^A, A_{CD}^{AB})$$

$$\overset{E}{=} \overset{E}{\phi}(f_C^A, T) + k + f(T) + A_{CD}^{AB} \alpha_A^C \alpha_B^D \qquad (63)$$

Also, it may be more advantageous to replace the assumption in Eq. (58) for the plastic deformation rate by

$$\overset{P}{d_C^A} = \lambda \frac{\partial F}{\partial \tau_C^A} + B_{CD}^{AB} \overset{\triangledown}{\tau_B^D} \qquad (64)$$

This form of this model appears to be more suitable for representing some experimental results in which second-order effects and some deviations from the normality rule have been observed. Sometimes, the normality rule is considered as a fundamental law based on an entropy production principle. But we should keep in mind that, since not all of the plastic work is dissipated, we cannot expect the total plastic deformation rate to obey the theory of plastic potential even though the mentioned principles of entropy production are correct.

References

[1] Zienkiewicz, O. C., and Cormeau, I. C., "Visco-plasticity—Plasticity and Creep in Elastic Solids—A Unified Numerical Approach," *International Journal for Numerical Methods in Engineering*, Vol. 8, 1974, pp. 821-845.

[2] Allen, D. H. and Haisler, W. E., "A Theory for Analysis of Thermoplastic Materials," *Computer and Structures*, Vol. 13, 1981, pp. 129-135.

[3] Haisler, W. E. and Cronenworth, J., "An Uncoupled Viscoplastic Constitutive Model for Metals at Elevated Temperature," AIAA Paper 83-1016, 1983.

[4] Yamada, Y. and Sakurai, T., "Basic Formulation and a Computer Program for Large Deformation Analysis," *Pressure Vessel Technology*, Pt. I, ASME, New York, 1977, pp. 342-352.

[5] Walker, K. P., "Representation of Hastelloy-X Behavior at Elevated Temperature with a Functional Theory of Viscoplasticity," Paper presented at ASME Pressure Vessels Conference, San Francisco, Aug. 1980.

[6] Cernocky, E. P. and Krempl, E., "A Nonlinear Uniaxial Integral Constitutive Equation Incorporating Rate Effects, Creep and Relaxation," *International Journal of Nonlinear Mechanics*, Vol. 14, 1979, pp. 183-203.

[7] Valanis, K. D., "Some Recent Developments in the Endochronic Theory of Plasticity—The Concept of Internal Barriers," *Constitutive Equations in Viscoplasticity: Phenomenological and Physical Aspects*, AMD Vol. 21, 1976, pp. 15-32.

[8] Chaboche, J. L., "Thermodynamic and Phenomenological Description of Cyclic Viscoplasticity with Damage," European Space Agency Technical Translation Service, Pub. ESA-TT-548, May 1979.

[9] Walker, K. P., NASA CR 165533, 1981.

[10] Chan, K. S., Bodner, S. R., Walker, K. P., and Lindholm, U.S., "A Survey of Unified Constitutive Theories," NASA CR 23925, 1984.

[11] Bodner, S. R., Partom, I., and Partom, Y., "Uniaxial Cyclic Loading of Elastic-Viscoplastic Materials," *Journal of Applied Mechanics*, Vol. 46, 1979, pp. 805-810.

[12] Miller, A. K., "Modeling a Cyclic Plasticity with Unified Constitutive Equations: Improvements in Simulating Normal and Anomalous Bauschinger Effects," *Journal of Engineering Materials and Technology*, Vol. 102, 1980, pp. 215-222.

[13] Krieg, R. D., Swearengen, J. C., and Rodhe, R. W., "A Physically-Based Internal Variable Model for Rate-Dependent Plasticity," *Proceedings of ASME/CSME PVP Conference*, ASME, New York, 1978, pp. 15-27.

[14] Hart, E. W., "Constitutive Relations for the Nonelastic Deformation of Metals," *ASME Journal Engineering Material and Technology*, Vol. 98, 1976, pp. 193-202.

[15] Robinson, D. N, ORNL Rept. TM-5969, 1978.

[16] Lee, D. and Zaverl, F. Jr., "A Generalized Strain Rate Constitutive Equation for Anisotropic Metals," *Acta Metallurgica*, Vol. 26, 1978, pp. 1771-1780.

[17] Hill, R., "A General Theory of Uniqueness and Stability in Elastic-Plastic Solids," *Journal of the Mechanics and Physics of Solids*, Vol. 6, 1958, pp. 236-249.

[18] Parkus, H. and Sedov, L. I. (eds.), *Irreversible Aspects of Continuum Mechanics and Transfer of Physical Characteristics in Moving Fluids*, Springer-Verlag, NY, IUTAM 1966 Symposium, 1968.

[19] Coleman, B. D., "Thermodynamics of Material with Memory," *Archive for Rational Mechanics and Analysis*, Vol. 17, 1966, pp. 1-46.

[20] Coleman, B. D. and Gurtin, M. E., "Thermodynamics with Internal State Variables," *Journal of Chemical Physics*, Vol. 47, 1967, pp. 597-613.

[21] Lubliner, J., "On the Thermodynamic Foundation of Non-Linear Solid Mechanics," *International Journal of Non-Linear Mechanics*, Vol. 7, 1972, pp. 237-254.

[22] Perzyna, P., "Internal Variable Description of Plasticity," *Problems of Plasticity*, edited by A. Sawczuk, Noordhoff International Publishing, Leyden, 1974, pp. 145-176.

[23] Truesdell, C. and Toupin, R. A., "The Classical Field Theories," *Encyclopedia of Physics*, Vol. II, No. 1, edited by S. Flugge, Springer, Berlin, 1960, pp. 226-793.

[24] Truesdell, C. and Noll, W., "The Non-Linear Field Theories of Mechanics," *Encyclopedia of Physics*, Vol. 3, No. 3, edited by S. Flugge, Springer, Berlin, 1965.

[25] Green, A. E. and Adkins, J. E., *Large Elastic Deformation*, Oxford University Press, London, 1970.

[26] Sedov, L. I., *Foundation of the Non-Linear Mechanics of Continua* (translated from the Russian), Pergamon Press, New York, 1966.

[27] Mendelssohn, E. and Baruch, M., "Development of Rate Tensor Operators in Conjunction with the Principles of Solid Mechanics," Technion, Haifa, Israel, Rept. TAE 415, 1980.

[28] Nemat-Nasser, S., "On Finite Deformation Elasto-Plasticity," *International Journal of Solids and Structures*, Vol. 18, 1982, pp. 857-872.

[29] Lee, E. H., "Elastic-Plastic Deformation at Finite Strain," *Journal of Applied Mechanics*, Vol. 36, 1969, pp. 1-6.

[30] Lubarda, V. A. and Lee, E. H., "A Correct Definition of Elastic and Plastic Deformation and its Computational Significance," *Journal of Mechanics*, Vol. 48, 1981, pp. 35-40.

[31] Lee, E. H. and McMeeking, R. M., "Concerning Elastic and Plastic Components of Deformation," *International Journal of Solids and Structures*, Vol. 16, 1980, pp. 715-721.

[32] Lee, E. H., "Finite Deformation Theory with Nonlinear Kinematics," *Plasticity of Metals at Finite Strain: Theory, Experiment and Computation*, University Press, Stanford, CA, 1981, pp. 107-120.

[33] Mandel, J., "Director Vectors and Constitutive Equations for Plastic and Visco-plastic Media," *Problems of Plasticity*, edited by A. Sawczuk, Noozdhoff, Groningen, the Netherlands, 1974, pp. 135-144.

[34] Hutchinson, J. W., "Elastic-Plastic Behavior of Polycrystalline Metals and Composites," *Proceeding of the Royal Society of London*, Vol. A319, 1970, pp. 247-272.

[35]Green, A. E. and Naghdi, P. M., "A Thermodynamic Development of Elastic-Plastic Continua," *Irreversible Aspects of Continuum Mechanics and Transfer of Physical Characteristics in Moving Fluids*, edited by H. Parkus and L. I. Sedov, Springer-Verlag, NY, 1968, pp. 117-131.

[36]Lehmann, Th., "On Large Elastic-Plastic Deformation," *Proceedings of Symposium on Foundation of Plasticity*, edited by A. Sawczuk, Noozdhoff, Groningen, the Netherlands, 1973, pp. 57-85.

[37]Lehmann, Th., "Some Thermodynamic Considerations of Phenomenological Theory of Non-Isothermal Elastic-Plastic Deformations," *Archives of Mechanics*, Vol. 24, 1972, pp. 975-989.

[38]Kestin, J., "On the Application of the Principles of Thermodynamics to Strained Materials," *Irreversible Aspects of Continuum Mechanics and Transfer of Physical Characteristics in Moving Fluids*, edited by H. Parkus and L. I. Sedov, 1968, pp. 177-212.

[39]Perzyna, P., "Thermodynamic Theory of Viscoplasticity," *Advances in Applied Mechanics*, Vol. 11, 1971, pp. 313-354.

[40]Rice, J. R., "Continuum Mechanics and Thermodynamics of Plasticity in Relation to Microscale Deformation Mechanics," *Constitutive Equations in Plasticity*, edited by A. S. Argon, M.I.T. Press, Cambridge, MA, 1975, pp. 23-75.

[41]Lehmann, Th. and Zander, G., "Non-Isothermic Large Elastic-Plastic Deformations," *Archives of Mechanics*, Vol. 27, 1975, pp. 759-772.

[42]Perzyna, P. and Wojno, W., "Thermodynamics of a Rate Sensitive Plastic Material," *Archives of Mechanics*, Vol. 20, 1968, pp. 499.

[43]Kratochvil, J. and Dillon, O. W., "Thermodynamics of Crystalline Elastic-Viscoplastic Material," *Journal of Applied Physics*, Vol. 41, 1970, pp., 1470.

[44]Kratochvil, J., "On Finite Strain Theory of Elastic-Inelastic Materials," *Acta Mechanica*, Vol. 16, 1973, pp. 127-142.

[45]Travnicek, L. and Kratochvil, J., "On the Rate-Independent Limit of Viscoplastic Constitutive Equations," *Archives of Mechanics*, Vol. 32, 1980, pp. 101-110.

[46]Perzyna, P., "Coupling of Dissipate Mechanisms of Viscoplastic Flow," *Archives of Mechanics*, Vol. 29, 1977, pp. 607-624.

Nonisothermal Elastoviscoplastic Snap-Through and Creep Buckling of Shallow Arches

R. Riff*

Georgia Institute of Technology, Atlanta, Georgia

The problem of buckling of shallow arches under transient thermomechanical loads is investigated. The analysis is based on nonlinear geometric and constitutive relations and is expressed in a rate form. The material constitutive equations are capable of reproducing all nonisothermal, elastoviscoplastic characteristics. The solution scheme is capable of predicting response that includes pre- and postbuckling with creep and plastic effects. The solution procedure is demonstrated through several examples that include both creep and snap-through behavior.

Introduction

ELASTIC snap-through of low arches under quasistatic loads has been the subject of several investigations. The significance of the problem, insofar as it illustrates certain important features in more complicated buckling problems of plates and shells, was pointed out by Marguerre,[1] who constructed a simplified mechanical model to demonstrate these features. Timoshenko[2] obtained an approximate solution to the problem of a low arch under a uniformly distributed load. Biezeno[3] considered the problem of a low-parabolic arch loaded laterally at the midpoint with a concentrated load. He also investigated snap-through buckling of a shallow spherical cap, pinned along its circular boundary, under the action of a concentrated load applied along the axis of rotational symmetry. He presented his approximate solutions by means of load-deflection curves and equations from which the critical load could be calculated.

In 1952, Fung and Kaplan[4] investigated the problem of low-pinned arches of various initial shapes and spatial distributions of the lateral load. Their results show that a very shallow arch snap through symmetrically, whereas a higher arch buckles asymmetrically. They also ran a limited number of experimental tests, and their experimental data are in good agreement with their theoretical results. About the same time, Hoff and Bruce,[5] in investigating the possibility of snap-through buckling of a low-pinned arch with a half-sine-wave initial shape under a half-sine-wave distributed dynamic load (suddenly applied with infinite duration), obtained results for the quasistatic load case that are identical to those obtained by Fung and Kaplan for the same problem.

In 1962, Gjelsvik and Bodner[5] obtained an approximate solution to the problem of a low-circular arch with a concentrated load at the midpoint of the arch and clamped boundary conditions. They also reported on experimental results. Schreyer and Masur[7] obtained an exact solution to their problem (and for the load case uniform pressure), and they showed that for the concentrated load case, the arch snaps through symmetrically regardless of the value of the rise parameter. Masur and Lo[8] presented a general discussion of the behavior of the shallow circular arch regarding buckling, postbuckling,

and imperfection sensitivity. Snapping of low-pinned arches resting on an elastic foundation has been investigated by Simitses.[9] This system exhibits all forms of experimentally observed buckling phenomena (smooth and violent) and of theoretically predicted responses (limit point, bifurcation with stable branching, and bifurcation with unstable branching), and it is presented with sufficient detail in Ref. 10. Experimental results have also been reported by Roorda.[11]

The effects of inelastic material behavior found their way into the literature since the 1960's. Onat and Shu[12] considered the behavior to be one of rigid-perfectly plastic. Fromciosi, Augusti, and Sparacio[13] discussed the collapse of arches under repeated loads with inelastic material behavior. Studies of inelastic snap-through buckling of shallow arches also were reported by Lee and Murphy.[14] In addition, Augusti[15] investigated plastic buckling of a model of a three-hinged arch in 1968, and a more complete analysis of the same model was provided by Batterman[16] in 1971. Finally, the reader who is interested in the ultimate strength of parabolic steel arches with bracing system is referred to Komatsu,[17] who considers inelastic in-plane and out-of-plane instabilities and provides design formula for each case.

Creep buckling of shallow arches has been investigated by Huang and Nachbar,[18] Krajcinovic,[19] and Botros and Bienek.[20] The elastic response of arches under sudden (dynamic) application of the external loads has been reported by Hoff and Bruce,[5] Hsu,[21,22] and Lock.[23] For a more complete bibliography see Ref. 24. As far as the authors know, no work has been reported on the nonisothermal elastoviscoplastic behavior of shallow arches. The purpose of this paper is to demonstrate the effect of highly nonlinear material behavior on the snap through and creep buckling of shallow arches.

Elastothermoviscoplastic Constitutive Relations

The prediction of buckling loads and postbuckling behavior of structural components, like shallow arches, made of a realistic metallic material and subjected to nonisothermal thermomechanical loads has increased in importance in recent years.

Under this kind of severe loading conditions, the structural behavior is highly nonlinear due to the combined action of geometrical and material nonlinearities. On one side, finite deformation in a stressed structure introduces nonlinear geometric effects. On the other side, physical nonlinearities arise even in small strain regimes, whereby inelastic phenomena play a particularly important role. From a theoretical standpoint, nonlinear constitutive equations should be applied only in connection with nonlinear transformation measures (mea-

ing both deformation and rotations). However, in almost all of the works in this area,[25] the two identified sources of nonlinearities are always separated. The separation yields, at one end of the spectrum, problems of large response, whereas at the other end problems of viscous and/or nonisothermal behavior in the presence of small strain.

The classical theories in which the material response is characterized as a combination of distinct elastic, thermal, time-independent inelastic (plastic) and time-dependent inelastic (creep) deformation components cannot explain some phenomena that can be observed in complex thermomechanical loading histories. This is particularly true when high-temperature nonisothermal processes must be taken into account. There is a sizeable body of literature[25,26] on phenomenological constitutive equations for the rate and temperature-dependent plastic deformation behavior of metallic materials. However, almost all of these new "unified" theories are based on small strain theories, and several suffer from some thermodynamic inconsistencies.

In a previous paper,[27] the authors have presented a complete set of constitutive relations for nonisothermal, large strain, elastoviscoplastic behavior of metals. It was shown there[27] that the metric tensor in the convected (material) coordinate system can be linearly decomposed into elastic and (visco) plastic parts. So a yield function was assumed, which is dependent on the rate of change of stress on the metric, on the temperature, and on a set of internal variables. Moreover, a hypoelastic law was chosen to describe the thermoelastic part of the deformation.

A time- and temperature-dependent viscoplasticity model was formulated in this convected material system to account for finite strains and rotations. The history and temperature dependence were incorporated through the introduction of internal variables. The choice of these variables and their evolution were motivated by thermodynamic considerations.

The nonisothermal elastoviscoplastic deformation process was described completely by "thermodynamic state" equations. Most investigators[25,26] (in the area of viscoplasticity) employ plastic strains as state variables. The authors' previous study[27] shows that, in general, use of plastic strains as state variables may lead to inconsistencies with regard to thermodynamic considerations. Furthermore, the approach and formulation employed in previous works lead to the condition that all of the plastic work is completely dissipated. This, however, is in contradiction with experimental evidence, from which it emerges that part of the plastic work is used for producing residual stresses in the lattice that, when phenomenologically considered, causes hardening. Both limitations were excluded from this[27] formulation. Accuracy of the formulation was checked on a wide range of examples.[28]

The constitutive relation will be rephrased here in some different form. For brevity we compile only some notations and fundamental relations that are used in the formulation of the intended constitutive law. For details see Refs. 27 and 28.

Concerning the formulation of constitutive laws, it is advantageous to use a material (convected) coordinate system. The transformation from the underformed state (metric $\overset{\ast}{g}_{ik}$) to the deformed state g_{ik} can be represented by the tensor

$$f_k^i = g^{ir} \overset{\ast}{g}_{rk} \tag{1a}$$

or

$$(f^{-1})_k^i = g^{ir} \overset{\ast}{g}_{rk} \tag{1b}$$

The total deformation rate is defined by

$$d_k^i = \tfrac{1}{2} g^{ir} \dot{g}_{rk} = -\tfrac{1}{2} g_{ir} \dot{g}^{rk} = \tfrac{1}{2}(f^{-1})_r^i (\dot{f})_k^r = -\tfrac{1}{2}(f^{-1})_r^i \dot{f}_k^r \tag{2}$$

Here ($\dot{}$) denotes time material derivative. The rate of change of the metric tensor is given by

$$\dot{g}_{ik} = v_{i,k} + v_{k,i}$$

and $v_{i,k}$ are the material velocities gradients. Hence,

$$d_{ik} = \tfrac{1}{2}(v_{i,k} + v_{k,i}) \tag{4}$$

The expression

$$\overset{\triangledown}{f}_k^i = (\dot{f})_k^i - d_r^i f_k^r - d_r^k f_r^i = \text{sym}[(\dot{f})_k^i] \tag{5}$$

represents the symmetric part of $(\dot{f})_k^i$ or the covariant derivative with respect to time, also called the convected derivation, which is due to Zaremba and Jaumann.

The total deformation can be decomposed according to

$$f_k^i = g^{im} \overset{\ast}{g}_{mr} \overset{\ast}{g}_{sk} = \overset{(i)}{f_r^i} \overset{(r)}{f_k^r} \tag{6}$$

where the superscript (*) relates to a fictitious configuration defined by a fictitious reversible process with frozen internal variables. The decomposition of Eq. (6) leads to an additive decomposition of the deformation rate

$$d_k^i = \overset{(r)}{d_k^i} + \overset{(i)}{d_k^i} \tag{7}$$

$\overset{(r)}{d_k^i}$ is related to the reversible deformations, whereas $\overset{(i)}{d_k^i}$ denotes the remaining part of the deformation rate.

For the description of the stress state, we introduce the Kirchoff stress tensor s_k^i, which is connected with the real Cauchy stress tensor σ_k^i by the relation

$$s_k^i = (\overset{\ast}{\rho}/\rho)\sigma_k^i \tag{8}$$

Assuming that the elastic behavior is not affected essentially by inelastic deformations, the following hypoelastic incremental law was chosen[27]:

$$\overset{(r)}{d_k^i} = \frac{1}{2G} \overset{\triangledown}{t}_k^i + \left[\frac{1}{9K}\overset{\triangledown}{s}_r^r + \alpha \dot{T}\right]\delta_k^i \tag{9}$$

where t_k^i is the weighted stress deviator, G the shear modulus, K the bulk modulus, and α the coefficient of thermal expansion.

The following constitutive relations were established[27] for the inelastic behavior. Yield condition:

$$F = (t_k^i - c\overset{\ast}{\rho}g\beta_k^i)(t_i^k - c\overset{\ast}{\rho}g\beta_i^k) - k^2(A, T) = f^2 - k^2 > 0 \tag{10}$$

Accompanying equilibrium state:

$$\bar{F} = (\bar{t}_k^i - c\overset{\ast}{\rho}g\beta_k^i)(\bar{t}_i^k - c\overset{\ast}{\rho}g\beta_i^k) - k^2(A, T) = \bar{f}^2 - k^2 = 0 \tag{11}$$

Evolution law for inelastic deformations:

$$\overset{(i)}{d_k^i} = 2\lambda(\bar{t}_k^i - c\overset{\ast}{\rho}g\beta_k^i) \tag{12}$$

with

$$\lambda = \frac{1}{4\eta}\left(\sqrt{\frac{(t_k^i - c\overset{\ast}{\rho}g\beta_k^i)(t_i^k - c\overset{\ast}{\rho}g\beta_i^k)}{k^2}} - 1\right) \tag{13}$$

$$\bar{t}_k^i = \frac{1}{1 + 4\eta\lambda}(t_k^i - c\overset{\ast}{\rho}g\beta_k^i) + c\overset{\ast}{\rho}g\beta_k^i \tag{14}$$

Evolution laws for the internal variables:

$$\dot{A} = \frac{1}{\rho}\bar{t}_k^i \overset{(i)}{d_k^i} \tag{15}$$

$$\overset{\triangledown}{\beta}_k^i = \xi \overset{(i)}{d_k^i} \tag{16}$$

68

If

$$F = 0 \text{ and } \frac{\partial F}{\partial s_k^i}\overset{\triangledown}{s}_k^i + \frac{\partial F}{\partial T}\dot{T} > 0 \qquad (17)$$

then

$$d_k^i = \overset{(r)}{d}_k^i \qquad (18)$$

$$\overset{(i)}{d}_k^i = 0 \text{ and } \overset{\triangledown}{d}_k^i = 2\ddot{\lambda}(t_k^i - c\dot{\rho}g\beta_k^i) \qquad (19)$$

with

$$\ddot{\lambda} = \frac{1}{8\eta k^2}\left[2(t_k^i - c\dot{\rho}g\beta_k^i)\,\overset{\triangledown}{t}_i^k - \frac{\partial k^2}{\partial T}\dot{T}\right] \qquad (20)$$

If

$$F = 0 \text{ and } \frac{\partial F}{\partial s_k^i}\overset{\triangledown}{s}_k^i - \frac{\partial F}{\partial T}\dot{T} \le 0 \qquad (21)$$

or

$$F < 0 \qquad (22)$$

$$d_k^i = \overset{(r)}{d}_k^i \qquad (23a)$$

$$\dot{A} = 0 \qquad (23b)$$

$$\overset{\triangledown}{\beta}_k^i = 0 \qquad (23c)$$

Within the developed frame, the elastoviscoplastic behavior is governed by the scalar material functions $c(s_k^i,T,A,\beta_k^i)$, $k^2(A,T)$, $g(s_k^i,R,\beta_k^i)$, $\xi(A,R,\beta_k^i)$, and $\eta(A,T,\beta_k^i)$. These material functions can be determined from a series of monotonic and cyclic processes with proportional and nonproportional paths at different temperature levels.[28]

General Formulation and Solution Schemes

The rate form of the constitutive equations suggests that a rate approach be taken toward the entire problem so that flow is viewed as history-dependent process rather than an event. For this purpose, a complete true ab-initio rate theory of kinematics and kinetics for continuum and curved thin structures, without any restriction on the magnitude of the transformation, was presented in Ref. 28. It is implemented with respect to a body-fixed system of convected coordinates, and it is valid for finite strains and finite rotations. The time dependence and large strain behavior are incorporated through the introduction of the time rates of change of the metric and of the curvature.

The constitutive law may be applied to the conservation of momentum via an appropriate variational principle. The principle of virtual power (or of virtual velocities) reads

$$\int_V \sigma^{ij}\delta v_{j,i}\,dV - \int_V v\rho f^j \delta v_j\,dV - \int_A vT^j\delta v_j\,dA = 0 \qquad (24)$$

where δv_j are the virtual velocities, f^j the body forces per unit mass, and vT^j the surface tractions. Total differentiation of Eq. (24) yields

$$\int_V \left(\frac{d\sigma^{ij}}{dt} + \sigma^{ij}d_k^k - v_{,k}^i\sigma^{kj}\right)\delta v_{j,i}\,dV - \int_V v\rho\frac{df^j}{dt}\delta v_j\,dV$$

$$- \int_A v\frac{dT^j}{dt}\delta v_j\,dA + \int_V \sigma^{ij}\left(\frac{d\delta v_j}{dt}\right)_{,i}dV - \int_V \rho f^j\frac{d\delta v_j}{dt}\,dV$$

$$- \int_A vT^j\frac{d\delta v_j}{dt}\,dA = 0 \qquad (25)$$

At any instant Eq. (25) must be satisfied. The virtual velocity and its time derivative are then independent. Moreover, the last three terms of Eq. (25) are equivalent to Eq. (24). Hence, the principle of the rate of virtual power may be obtained in its concise form. For further classifiations, the total derivative of the stress components will be represented by the Jauman derivative, and the following integrals are defined by

$$I_e = \int_V \overset{\triangledown}{\sigma^{ij}}\delta v_{j,i}\,dV \qquad (26)$$

$$I_d = \int_V (\sigma^{ij}d_c^k - \sigma^{kj}d_{,k}^i)\delta v_{j,i}\,dV \qquad (27)$$

$$I_r = \int_V \omega_{,k}^j\sigma^{kj}\delta v_{j,i}\,dV \qquad (28)$$

Then, substitution in Eqs. (23) yields the final form of the principle of the rate of virtual power:

$$I = I_e + I_c + I_r = \int_V \rho\frac{df^i}{dt}\delta v_i\,dV + \int_A v\frac{dT^j}{dt}\delta v_j\,dA \qquad (29)$$

The quasilinear nature of the principle of the rate of virtual power suggests the adoption of an incremental approach to numerical integration with respect to time. The availability of the field formulation provides assurance of the completeness of the incremental equations and allows the use of any convenient procedure for spatial integration over the domain V. In the present instance, the choice has been made in favor of a simple first-order expansion in time for the construction of incremental solutions from the results of finite-element spatial integration of the governing equations.

The procedure employed permits the rates of the field formulation to be interpreted as increments in the numerical solution. This is particularly convenient for the construction of incremental boundary condition histories.

The finite-element method for spatial discretization has been well documented (see, e.g., the books by Zienkiewicz[29] or Oden[30]) and will not be detailed here. The algebraic counterpart of Eq. (29) After the finite-element discretization (for detail see Ref. 28) is the well-known stiffness expression

$$[K]\{V\} = \{\dot{P}\} - \{\dot{F}\} \qquad (30)$$

with the tangent stiffness matrix $[K]$, the vector of the incremental velocities $\{V\}$, and the vector out-of-balance force rates, external force rates $\{\dot{P}\}$ minus internal force rates $\{\dot{F}\}$. The homogenous case of Eq. (30) indicates either the non-uniqueness of the equilibrium path at a stable or unstable bifurcation point or the unique but unstable situation at a limit point. Hence, this criterion may be evaluated by a determinant check or supplementary eigenvalue analysis for the load parameter parallel to the loading process.

Even under the condition of static external loads and slowly growing creep effects, the presence of snap-through buckling makes the inertia effects significant. In dynamic analyses, the applied body forces include inertia forces. Assuming that the mass of the body considered is preserved, the mass matrix can be evaluated prior to the time integration using the initial configuration.

Finite-element solution of any boundary-value problem involves the solution of the equilibrium equation (global) together with the constitutive equation (local). Both equations are solved simultaneously in a step by step manner. The incremental form of the global and local equations can be achieved by taking the integration over the incremental time step $\Delta t = t_{j-1} - t_j$. The rectangular rule has been applied to execute the resulting time integration.

Clearly, the numerical solution involves iteration. A simplified version[1] of Riks Wempner constant-arch-length method
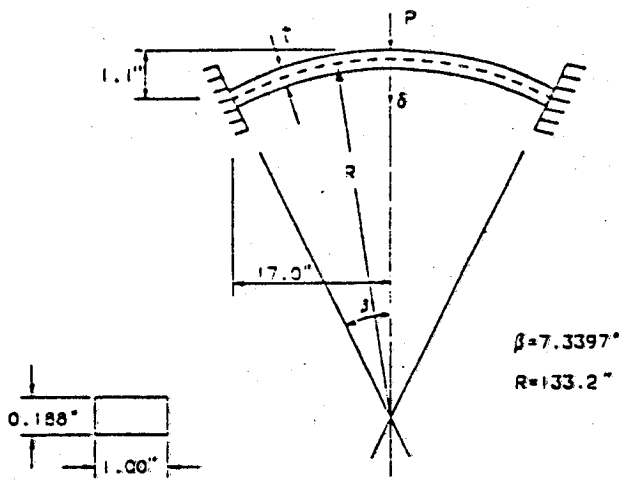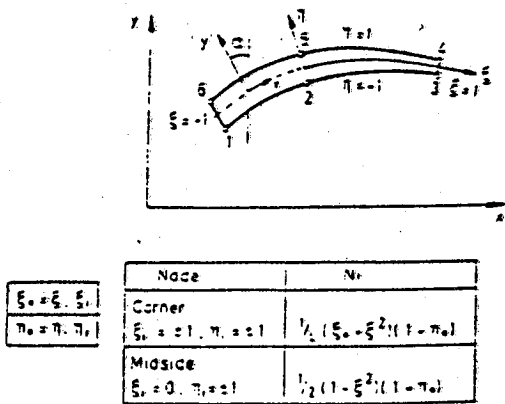
Fig. 1 Clamped circular arch.

$\beta = 7.3397°$

$R = 133.2°$

Fig. 2 Paralinear isoparametric element.

Fig. 3 Arch response.

Fig. 4 Deflection time history.

has been used. This iteration procedure, which is a generalization of the displacement control method, also allows to trace the nonlinear response beyond bifurcation points. In contrast to the conventional Newton-Raphson techniques, the iteration of the method takes place in the velocity and load rate space. The load step of the first solution in each increment is limited by controlling the length ds of the tangent. Either the length is kept constant in each step, or it is adapted to the characteristics of the solution. In each step the triangular-sized stiffness matrix has to be checked for negative diagonal terms, indicating that a critical point is reached.

Shallow Circular Clamped Arch

The theory and computational procedures described in the proceeding sections have been applied to the creep buckling analysis of a shallow circular clamped arch. The problem of the clamped arch, besides being of some practical interest, contains a number of similarities to that of the uniformly loaded spherical cap. The trend of results of the arch problem serves as a good indicator to the behavior of the latter.

The shallow circular clamped arch subjected to a single central concentrated load, as shown in Fig. 1, is analyzed. The material chosen for the numerical experimentation is the carbon steel C-45 (DIN 1720) with $E = 10^7$ psi, $\nu = 0.3$, and $\sigma_y = 2.7 \times 10^4$ psi at room temperature. The viscoplastic properties (the scalar material functions) were obtained in Ref. 28.

The analysis is performed with the aid of 24 paralinear isoparametric elements (Fig. 2). The paralinear isoparametric element is intended for the analysis of oriented structures where the geometry is such that the thickness is small compared to other dimensions. The characteristics of the element are defined by the geometry and interpolation functions, which are linear in the thickness direction and parabolic in the longitudinal direction (see Fig. 2). Consequently, the element
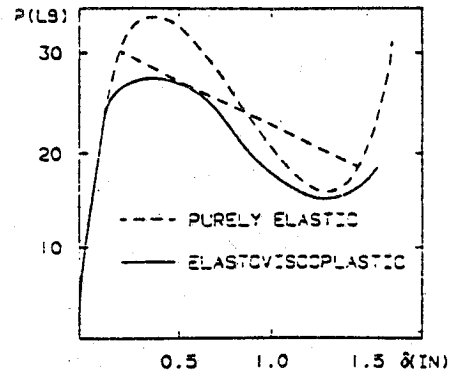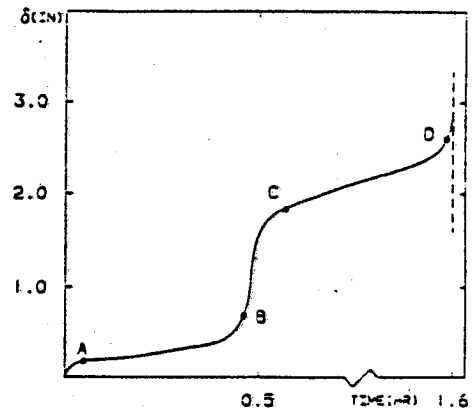
allows for shear strain energy, since normals to a midsurface before deformation remain straight but not necessarily normal to the midsurface after deformation.

The elastic behavior, corresponding to both axisymmetric and asymmetric response, is shown on Fig. 3. These curves are in complete agreement with those produced by Gjelsvik and Bodner,[6] only because the Young's modulus and Poisson's ratio values used are virtually the same (carbon steel C-45 here and 2024-T4 aluminum alloy in Ref. 6). Note that these elastic response curves are hypothetical for our material but true for the 2024-T4 alloy. The true behavior for our material is elastoviscoplastic, and it is labeled as such on Fig. 3. Note that this curve represents quasistatic (steady-state) elastoviscoplastic response, as described by the chosen constitutive law. According to this, snapping occurs at a load of 26.20 lb, primarily because of the low-yield strength. Then, the postlimit point behavior seems to be primarily driven by viscoplastic behavior.

It is expected here that if loads up to approximately 14 lb are reached quasistatically and left applied for a long time, the primary response will be creep, and the critical creep collapse time will be extremely large. On the other hand, for loads between 14 and 26.2 lb (especially for the higher range), the behavior will be a combination of creep and snap-through buckling. This is best demonstrated by the curve on Fig. 4. The applied load is reached quasistatically in 13 min, and then it is kept constant. The curve of Fig. 4 depicts the behavior of the arch in terms of midpoint deflection vs time. Creep, initially, is very slow; then snap-through takes place in 32 min, curve BC, and then the creep behavior continues until a critical time to creep (creep buckling occurs) is reached after a total time 97 min. Note that for this loading condition, the critical time to creep in 97 min. Creep buckling and critical time to creep are based on the phenomenon that the deflection increased very rapidly. For loads higher than 26.2 lb, it is expected that snapping will occur early during quasistatic loading, and then the creep behavior will be similar to that shown on Fig. 4, past point c.
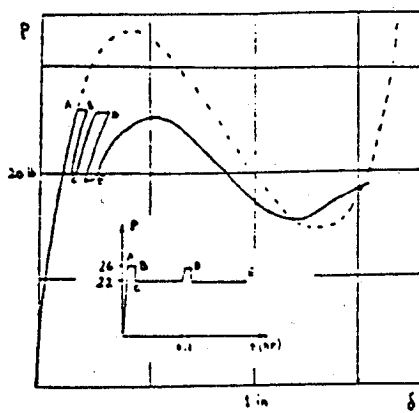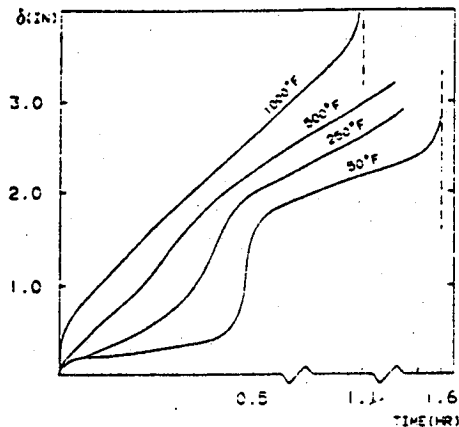
Fig. 5 Multicycle arch response.

Fig. 6 Influence of temperature raise.

The next example considers the influence of cyclic loading on the response. Figure 5 illustrates the load deflection behavior of the arch under a cyclically applied external load. The load is increased, quasistatically, from zero to 26 lb in 5 min, then it is held constant for 2.5 min, after that it is reduced to 20 lbs and held constant for 50 min, then raised to 25.5 lb for 2.5 min, and finally it is reduced back to 20 lb held constant.

The steady-state response under this type of loading exhibits several relative maxima points, which may imply that snapping is imminent shortly after the load reaches the value of 26 lb (between points A and B on Fig. 5). The dashed curve corresponds to the hypothetical elastic static response, and it is only shown for comparison purposes.

The last example presented in Fig. 6 considers the influence of temperature on the arch behavior. The loading history is the same on the one shown on Fig. 4. The curve corresponding to $T = 50°F$ was discussed previously (Fig. 4), and it is used here as a basis for comparison. When the temperature is raised to 200°F (after this, the loading is applied), the time to snap is reduced to 26 min, whereas the critical creep collapse time is not appreciably affected. On the other hand, at the highest temperature $T = 1000°F$ for which results are shown, the critical creep collapse time is reduced to 62 min, and the steady-state response does not show a clear snap-through behavior. Different values of α were used for the different temperature in the elastic range.

Discussion

As noted earlier, the main thrust of this work has been to demonstrate the effect of highly nonlinear material behavior on the snap-through and creep buckling of shallow arches. It is evident that in the presence of both elastic and viscoplastic deformation the process of buckling assumes an entirely new character. Buckling develops as a time-temperature-dependent deformation process under constant or variable loads of magnitudes smaller than the elastic critical values. In arches under loads below the critical values the structure initially deforms quasistatically, with the thermoviscous terms manifesting themselves in the form of increasing displacement under, say, a constant load. When the magnitude of the displacements reaches a certain threshold state, the arch snaps dynamically into the postbuckling configuration and then continues quasistatic deformation again.

The material constitutive relation has been proven to be capable of reproducing the main characteristics of viscoplastic deformations. The modified Riks/Wempner iteration scheme has been found to be a versatile technique in the pre- and postcritical range.

The influence of thermomechanical coupling can become very large in stability problems. Such processes are always connected with a rapid growth of inhomogeneity of the state. Thorough investigation of such problems, however, must be performed with the necessary detail.

References

[1]Marrguerre. K., "Die Durchschlagskraft eines Schwach Gekrummten Balken," *Sitz. Berlin Math. Gess.*, Vol. 37, 1938, pp. 92–108.

[2]Timoshenko, S. P., "Buckling of Curved Bars with Small Curvature," *Journal of Applied Mechanics*, Vol. 2, No. 1, March 1935, pp. 17–23.

[3]Biezeno, C. B., "Das Durchschlagen eines Schwach Gekrummten Stabes," *Zeitschrift Ange. Math. und Mekh*, Vol. 18, 1938, pp. 21–29.

[4]Fung, Y. C. and Kaplan, A ., "Buckling of Low Arches or Curved Beams of Small Curvature," NACA TN-2840, 1952.

[5]Hoff, N. J. and Bruce. V. G., "Dynamic Analysis of the Buckling of Laterally Loaded Flat Arches," *Journal of Mathematics and Physics*, Vol. 32, No. 4, Jan. 1954, pp. 276–288.

[6]Gjelsvik, A. and Bodner, S. R., "The Energy Criterion and Snap Buckling of Arches," *J. Eng. Mech.*, Div. ASCE. Vol. 88, EM5, May 1962, pp. 87–108.

[7]Schreyer, H. L. and Masur, E. F.,"Buckling of Shallow Arches," *J. Eng. Mech.*, Div. ASCE, Vol. 92, EM4, April 1966, pp. 1–17.

[8]Masur, E. F. and Lo, D. L. C., "The Shallow Arch-General Buckling, Post Buckling, and Imperfection Analysis," *Journal of Structural Mechanics*, Vol. 1, No. 1, 1972, pp. 91–107.

[9]Simitses, G. J., "Snapping of Low Pinned Arches on an Elastic Foundation," *Journal of Applied Mechanics*, Vol. 40, No. 3, Sept. 1973, pp. 741–774.

[10]Simitses, G. J.. *Elastic Stability of Structures*, Prentice-Hall. Englewood Cliffs, NJ, 1976; second printing, R. E. Kreiger Publishing Co., Melbourne. FL, 1986.

[11]Roorda, J., "Stability of Structures with Small Imperfections," *Journal of Engineering Mechanics Division*, ASCE, Vol. 91, EM1, 1965, pp. 87–108.

[12]Onat, E. T. and Shu. L. S., "Finite Deformation of a Rigid Perfectly Plastic Arch," *Journal of Applied Mechanics*, Vol. 29, No. 3, 1962, pp. 549–553.

[13]Franciosi, V., Augusti, G., and Sparacio, R., "Collapse of Arches Under Repeated Loading," *Journal of the Structural Division*, ASCE, Vol. 90, ST1, Jan. 1964, pp. 165–179.

[14]Lee, L. H. N. and Murphy, L. M., "Inelastic Buckling of Shallow Arches," *Journal of Engineering Mechanics Division*, ASCE, Vol. 94, EM1, Jan. 1968, pp. 225–239.

[15]Augusti, G., "Buckling of Inelastic Arches: Simple Model," *Meccanica*, Vol. 3, 1968. pp. 102–105.

[16]Batterman, S. C. "Plastic Stability of Arches: Re-Consideration of a Model," *Israel Journal of Technology*, Vol. 9, 1971, pp. 467–476.

[17]Kamatsu. S., "Braced Steel Arches," *Steel Framed Structures: Stability and Strength*, edited by R. Narayanan, Elsevier Applied Science Publishers Ltd. London. 1985, Chap. 9.

71

[18]Huang, N. C. and Nachbar, W., "Dynamic Snap-Through of Imperfect Viscoelastic Shallow Arches," Univ. of California at La-Jolla, LaJolla, CA, TR-AF-AFOSR 1226-67, March 1967.

[19]Krajcinovic, D., "Creep Buckling of a Tied Arch," *Stability of Structures Under Static and Dynamics Loads*, American Society of Chemical Engineers, New York, 1977.

[20]Botros, F. R. and Bienek, M. P., "Creep Buckling of Structures," *Proceedings of the AIAA/ASME/ASCE/AHS 24th SDM Conference:* AIAA Paper 83-0864, May 1983.

[21]Hsu, C. S., "On the Dynamic Stability of Elastic Bodies with Prescribed Initial Conditions," *Int'l J. Eng. Sci.*, Vol. 4, 1966, pp. 1-21.

[22]Hsu, C. S., "The Effects of Various Parameters on the Dynamic Stability of a Shallow Arch," *Journal of Applied Mechanics*, Vol. 34, No. 2, 1967, pp. 349-358.

[23]Lock, M. H., "The Snapping of a Shallow Sinusoidal Arch Under a Step Pressure Load," *AIAA Journal*, Vol. 4, July 1966, pp. 1249-1256.

[24]Simitses, G. J., "Suddenly-Loaded Structural Configurations," *J. of Eng. Mech.*, Div. ASCE, Vol. 110, No. 9, 1984, pp. 1320-1334.

[25]Walker, K. P., "Research and Development Programs for Non-linear Structural Modeling with Advanced Time Temperature Dependent Constitutive Relations," NASA-CR 165533, 1981.

[26]Chan, K. S., Bodner, S. R., Walker, K. P., and Lindholm, U. S., "A Survey of Unified Constitutive Theories," NASA CR-23925, 1984.

[27]Riff, R., Carlson, R. L., and Simitses, G. J., "The Thermodynamically Consistent Constitutive Equations For Nonisothermal Large Strain, Elasto-Plastic, Creep Behavior," *AIAA Journal*, Vol. 25, Jan. 1987, pp. 114-122.

[28]Simitses, G. J., Carlson, R. L., and Riff, R., "Formulation of the Nonlinear Analysis of Shell-Like Structures, Subjected to Time-Dependent Mechanical and Thermal Loading," NASA Rept. 1986.

[29]Zienkiewicz, O. C. and Cheung, Y. K., *The Finite Element Method in Structural and Continuum Mechanics*, McGraw-Hill, New York, 1967.

[30]Oden, J. T., *Finite Elements of Nonlinear Continua*, McGraw-Hill, New York, 1972.

[31]Ramm, E. "Strategies for Tracing the Nonlinear Response Near Limit Points," *Proceedings Europe-U.S. Workshop on "Nonlinear Finite Element Analysis in Structural Mechanics,"* Springer-Verlag, New York, 1981.

NON–ISOTHERMAL BUCKLING BEHAVIOR OF VISCOPLASTIC SHELL STRUCTURES

Richard Riff
School of Aerospace Engineering
Georgia Institute of Technology
Atlanta, Georgia 30332

Abstract

The buckling behavior of thin metallic shell structures under transient thermomechanical loads is investigated. The analysis is based on nonlinear geometric and constitutive relations, and all the field equations are expressed in a rate form. The employed constitutive equations are thermodynamically consistent and they are capable of capturing all non–isothermal, elasto–viscoplastic characteristics of the response. The solution scheme is capable of predicting response which includes pre– and post–buckling with creep and plastic effects. The solution procedure is demonstrated through several examples which include both creep and snap–through behavior.

Introduction

The prediction of inelastic behavior of metallic materials at elevated temperatures has increased in importance in recent years. The operating conditions within the hot section of a rocket motor or a modern gas turbine engine present an extremely harsh thermomechanical environment. Large thermal transients are induced each time the engine is started or shut down. Additional thermal transient from an elevated ambient, occur whenever the engine power level is adjusted to meet flight requirements. The structural elements employed to construct such hot sections, as well as any engine components located therein, must be capable of withstanding such extreme conditions. Failure of a component would, due to the critical nature of the hot section, lead to and immediate and catastrophic loss in power and thus cannot be tolerated. Consequently, assuring satisfactory long term perfor- mance for such components is a major concern for the designer.

The problem of inelastic analysis of shell structures has been investigated recently by Kojic' and Bathe [1]. They used the "effective-stress-function" algorithm to compute plastic and creep effects on the behavior of shell like structures. The effects of inelastic material behavior on stability of shells found their way into the literature since the late 1970's. The paper by Miyazaki and Ando [2] deals with creep buckling of perfect spherical shells subjected to pressure loading and considers only the effects of steady-state creep. Xirochakis and Jones [3] have studied axisymmetric and bifurcation creep buckling of externally pressurized spherical shells under the condition of secondary creep only. Botros and Bienek [4] presented a numerical treatment of the creep buckling of these configurations. Their work includes the effects of elastic strain, primary and secondary creep strains and creep recovery. The influence of temperature and viscous effects on dynamic buckling of shells has been considered by Wojewodzki and Bukowski [5,6]. The book by Owen and Hinton [7] gives a list of references for the applications of finite element methods to the problem of creep buckling of structures.

Assistant Professor, Member AIAA

As far as the author know no work has been reported on the non-isothermal buckling behavior of elasto-viscoplastic shell structures.The purpose of this paper is to demonstrate the effect of highly nonlinear material behavior on the snap through and creep buckling of shells.

Elasto–Thermo–Viscoplastic Constitutive Relations

In a previous works [8-11], following the ideas of Lechmann [12,13] the authors have presented a complete set of constitutive relations for nonisothermal, large strain, elasto–viscoplastic behavior of metals. It was shown there [8] that the metric tensor in the convected (material) coordinate system can be linearly decomposed into elastic and (visco) plastic parts. So a yield function was assumed, which is dependent on the rate of change of stress on the metric, on the temperature and on a set of internal variables. Moreover, a hypoelastic law was chosen to describe the thermo-elastic part of the deformation.

A time and temperature dependent viscoplasticity model was formulated in this convected material system to account for finite strains and rotations. The history and temperature dependence were incorporated through the introduction of internal variables. The choice of these variables, as well as their evolution, was motivated by thermodynamic considerations.

The constitutive relation will be rephrased here in some different form. For brevity we compile only some notations and fundamental relations which are used in the formulation of the intended constitutive law. For details, see Refs. 8 and 11.

Concerning the formulation of constitutive laws it is advantageous to use a material (convected) coordinate system. The transformation from the underformed state (metric $\overset{\circ}{g}_{ik}$) to the deformed state (g_{ik}) can be represented by the tensor:

$$f^i_k = \overset{\circ}{g}{}^{ir} g_{rk} \quad or \quad (f^{-1})^i_k = g^{ir} \overset{\circ}{g}_{rk} \tag{1}$$

The total deformation rate is defined by

$$\dot{d}^i_k = \frac{1}{2} g^{ir} \dot{g}_{rk} = -\frac{1}{2} g_{ir} \dot{g}^{rk} = \frac{1}{2}(f^{-1})^i_r (\dot{f})^r_{.k} = -\frac{1}{2}(\dot{f}^{-1})^i_{.r} f^r_k \tag{2}$$

here (˙) denotes time material derivative. The rate of change of the metric tensor is given by

$$\dot{g}_{ik} = v_{i,k} + v_{k,i} \tag{3}$$

and $v_{i,k}$ are the material velocities gradients. Hence,

$$d_{ik} = \frac{1}{2}(v_{i,k} + v_{k,i}) \tag{4}$$

The expression

$$\overset{\triangledown}{f}{}^i_k = (\dot{f})^i_{.k} + d^i_k f^r_k - d^r_k f^i_r = sym\{(\dot{f})^i_{.k}\} \tag{5}$$

represents the symmetric part of $(\dot{f})^i_k$ or the covariant derivative with respect to time, also called the convected derivation, which is due to Zaremba and Jaumann.

74

The total deformation can be decomposed according to

$$f^i_k = \overset{\circ}{g}{}^{im}\overset{*}{g}_{mr}\, g_{sk} = \overset{(i)}{f^i_r}\overset{(r)}{f^r_k} \tag{6}$$

where the superscript $(\overset{*}{\ })$ relates to a fictitious configuration defined by a fictitious reversible process with frozen internal variables. The decomposition of Eq. (6) leads to an additive decomposition of the deformation rate

$$\dot{d}^i_k = \overset{(r)}{\dot{d}^i_k} + \overset{(i)}{\dot{d}^i_k} \tag{7}$$

$\overset{(r)}{\dot{d}^i_k}$ is related to the reversible deformations, whereas $\overset{(i)}{\dot{d}^i_k}$ denotes the remaining part of the deformation rate.

For the description of the stress state, we introduce the Kirchoff stress tensor s^i_k, which is connected with the real Cauchy stress tensor σ^i_k, by the relation:

$$s^i_k = \frac{\overset{\circ}{\rho}}{\rho}\sigma^i_k \tag{8}$$

Assuming that the elastic behavior is not affected essentially by inelastic deformations, the following hypoelastic incremental law was chosen [8]

$$\overset{(r)}{\dot{d}^i_k} = \frac{1}{2G}\overset{\triangledown}{t^i_k} + \{\frac{1}{9K}\dot{s}^r_r + \alpha\dot{T}\}\delta^i_k \tag{9}$$

with
$$
\begin{array}{ll}
t^i_k & : \text{ weighted stress deviator} \\
G & : \text{ shear modulus} \\
K & : \text{ bulk modulus} \\
\alpha & : \text{ coefficient of thermal expansion}
\end{array}
$$

The following constitutive relations were established [8] for the inelastic behavior.
yield condition:
$$F = (t^i_k - c\overset{\circ}{\rho}\, g\beta^i_k)(t^k_i - c\overset{\circ}{\rho}\, g\beta^k_i) - k^2(A,T) = f^2 - k^2 > 0 \tag{10}$$

accompanying equilibrium state:
$$\overline{F} = (\overline{t}^i_k - c\overset{\circ}{\rho}\, g\beta^i_k)(\overline{t}^k_i - c\overset{\circ}{\rho}\, g\beta^k_i) - k^2(A,T) = \overline{f}^2 - k^2 = 0 \tag{11}$$

evolution law for inelastic deformations:
$$\overset{(i)}{\dot{d}^i_k} = 2\dot{\lambda}(\overline{t}^i_k - c\overset{\circ}{\rho}\, g\beta^i_k) \tag{12}$$

with
$$\dot{\lambda} = \frac{1}{4\eta}\left(\sqrt{\frac{(t^i_k - c\overset{\circ}{\rho}\, g\beta^i_k)(t^k_i - c\overset{\circ}{\rho}\, g\beta^k_i)}{k^2}} - 1\right) \tag{13}$$

and
$$\overline{t}^i_k = \frac{1}{1 + 4\eta\dot{\lambda}}(t^i_k - c\overset{\circ}{\rho}\, g\beta^i_k) + c\overset{\circ}{\rho}\, g\beta^i_k \tag{14}$$

75

evolution laws for the internal variables:

$$\dot{A} = \frac{1}{\overset{\circ}{\rho}} \overset{(i)}{\dot{t}_k^i \, d_i^k} \tag{15}$$

$$\overset{\nabla}{\beta_k^i} = \xi \overset{(i)}{d_k^i} \tag{16}$$

if

$$F = 0 \quad and \quad \frac{\partial F}{\partial s_k^i} \overset{\nabla}{s_k^i} + \frac{\partial F}{\partial T} \dot{T} > 0 \tag{17}$$

then

$$\dot{d}_k^i = \overset{(r)}{d_k^i} \tag{18}$$

$$\overset{(i)}{\dot{d}_k^i} = 0 \quad and \quad \overset{\nabla}{d_k^i} = 2\ddot{\lambda}(t_k^i - c \, \overset{\circ}{\rho} \, g\beta_k^i) \tag{19}$$

with

$$\ddot{\lambda} = \frac{1}{8\eta k^2} \{2(t_k^i - c \, \overset{\circ}{\rho} \, g\beta_k^i) \overset{\nabla}{t_i^k} - \frac{\partial k^2}{\partial T} \dot{T}\} \tag{20}$$

if

$$F = 0 \quad and \quad \frac{\partial F}{\partial s_k^i} \overset{\nabla}{s_k^i} + \frac{\partial F}{\partial T} \dot{T} \leq 0 \tag{21}$$

or

$$F < 0 \tag{22}$$

then

$$\begin{aligned}
\dot{d}_k^i &= \overset{(r)}{d_k^i} \\
\dot{A} &= 0 \\
\overset{\nabla}{\beta_k^i} &= 0
\end{aligned} \tag{23}$$

Within the developed frame the elasto–viscoplastic behavior is governed by the scalar material functions $c(s_k^i, T, A, \beta_k^i)$, $k^2(A, T)$, $g(s_k^i, A, T, \beta_k^i)$, $\xi(A, T, \beta_k^i)$, and $\eta(A, T, \beta_k^i)$. These material functions can be determined from a series of monotonic and cyclic processes with proportional and nonproportional paths at different temperature levels [11].

Formulation and Solution Schemes

The rate form of the constitutive equations suggests that a rate approach be taken toward the entire problem so that flow is viewed as history dependent process rather than an event. For this purpose, a complete true ab-initio rate theory of kinematics and kinetics for continuum and curved thin structures, without any restriction on the magnitude of the transformation was presented in Ref. 11. It is implemented with respect to a body- fixed system of convected coordinates, and it is valid for finite strains and finite rotations. The time dependence and large strain behavior are incorporated through the introduction of the time rates of change of the metric and of the curvature.

76

A nonlinear, thermodynamic theory of shells was derived in ref. 11 from three dimensional continuum mechanics in a natural and comprehensive way. All the approximations had been thrown into a postulated two dimensional form of the first law of thermodynamics.

The derived shell theory, in the least restricted form, before any simplifying assumptions are imposed, has the following desirable features:

(a) The two-dimensional, impulse-integral form of the equations of motions and the Second Law of Thermodynamics (Clausius- Duhem inequality) for a shell follow naturally and exactly from their three-dimensional counterparts.

(b) Unique and concrete definitions of shell variables such as stress resultants and couples, rate of deformation, spin and entropy resultants can be obtained in terms of weighted integrals of the three-dimensional quantities through the thickness.

(c) There are no series expansions in the thickness direction.

(d) There is no need for making use of the Kirchhoff Hypotheses in the kinematics.

(e) All approximations can be postponed until the descretization process of the integral forms of the First Law of Thermo- dynamics.

(f) A by-product of the descent from three-dimensional theory is that the two-dimensional temperature field (that emerges) is not a through-the-thickness average, but a true point by point distribution. This is contrary to what one finds in the literature concerning thermal stresses in the shell.

The obtained complete rate field equations consist of the principles of the rate of the virtual power and the rate of conservation of energy, of the constitutive relations, and of boundary and initial conditions. These equations provide a sound basis for the formulation of the adopted finite element solution procedures.

The quasi-linear nature of the principle of the rate of virtual power suggests the adoption of an incremental approach to numerical integration with respect to time. The availability of the field formulation provides assurance of the completeness of the incremental equations and allows the use of any convenient procedure for spatial integration over the domain V. In the present instance, the choice has been made in favor of a simple expansion in time for the construction of incremental solutions from the results of finite element spatial integration of the governing equations.

The procedure employed permits the rates of the field formulation to be interpreted as increments in the numerical solution. This is particularly convenient for the construction of incremental boundary condition histories.

To develop geometrically nonlinear, doubly curved finite shell elements the basic equations of nonlinear shell theories have to be transferred into the finite element model. As these equations in general are written in tensor notation, their implementation into the finite element matrix formulation re- quires considerable effort. The nonlinear element matrices are directly derived from the incrementally formulated nonlinear shell equations, by using a tensor-oriented procedure. For this formulation, we use the "natural" degrees of freedom per mid-surface shell node: three incremental velocities and the rates of rotations about the material coordinates in a mixed form.

77

Finite element solution of any boundary-value problem involves the solution of the equilibrium equations (global) together with the constitutive equations (local). Both sets of equations are solved simultaneously in a step by step manner. The incremental form of the global and local equations can be achieved by taking the integration over the incremental time step $\Delta t = t_{j+1} - t_j$. The rectangular rule has been applied to execute the resulting time integration.

Clearly, the numerical solution involves iteration. A simplified version of the Riks-Wempner [14] constant-arc-length method has been utilized. This iteration procedure which is a genera- lization of the displacement control method also allows to trace the non-linear response beyond bifurcation points. In contrast to the conventional Newton-Raphson techniques, the iteration of the method takes place in the velocity and load rate space. The load step of the first solution in each increment is limited by controlling the length ds of the tangent. Either the length is kept constant in each step or it is adapted to the characteris- tics of the solution. In each step the triangular-size stiffness matrix has to be checked for negative diagonal terms, indicating that a critical point is reached.

Applications

Two different material representing different sensitivity to creep and high temperature were chosen for the numerical experimitations.

The first is the carbon steel C-45 (DIN 1720) with $E = 10^7$ psi, $\nu = 0.3$ and $\sigma_y = 2.7 \times 10^4$ psi at room temperature. The viscoplastic properties (the scalar material functions) were obtained in Ref. 11. The C-45 has low resistance to temperature and high strain rate sensitivity. The second is Hastelloy-X a nickel-base alloy used for burner-liner parts, turbine-exhaust weldments, afterburner parts, and other parts requiring high resistance to temperature effects. Material properties used for Hastelloy-X were based on data from Refs. 15 and 16.

The first example is of hinged spherical cap made of C-45 carbon steel and loaded by a con-centrated force at the appex (Fig. 1). The hypothetical elastic response is shown in Fig. 2 by the dash line. The true behavior for our material is elasto-viscoplastic, the full curve in Fig. 2. Note that this curve represents quasi-static (steady state) elasto-viscoplastic response, as described by the constitutive law. According to this, snapping occurs at a load of 32.3 lbs, primarily because of the low yield strenght. Then, the post-limit point behavior seems to be driven by viscoplastic behavior.

It is expected here that for loads between 4 lbs and 32.3 lbs (especially for the higher range) the behavior will be a combination of creep and snap-through buckling. This is demonstrated by Fig. 3 for different temperatures. The applied load of 25 lbs is reached quasi-statically and then it is kept constant. Note the different creep buckling behavior and the differnt critical time to creep for the different temperatures.

The second example considers a clamped spherical cap subjected to uniform pressure and made from Hastelloy-X (Fig. 4). Fig. 5 describes the different load deflection curves of the center point for different temperatures for this example. The critical creep collapse time is reduced by 45

In the next example (Fig. 7) the central deflection time history and the influence of temperature change of a thin, imperfect, cylind- rical shell panel made of carbon steel C-45 is shown. The panel (Fig. 6) is simply supported on all sides, and subjected to inplane loads along the generator. The
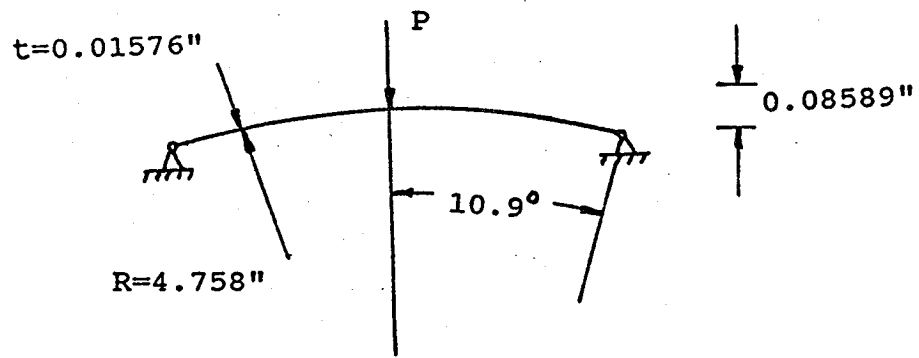
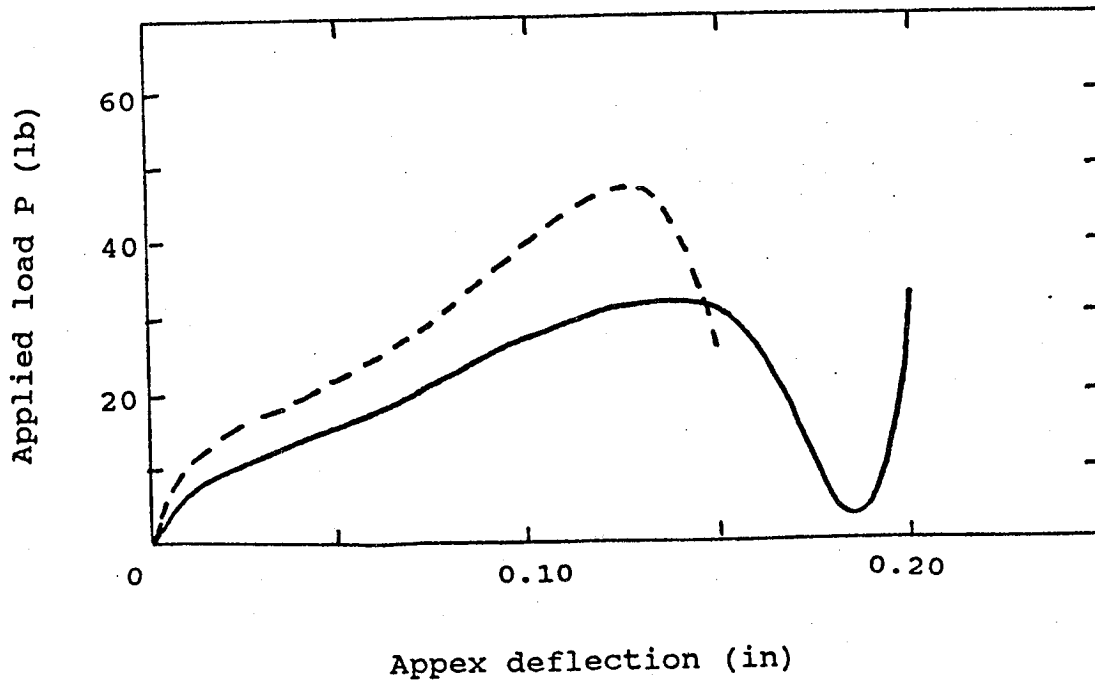Fig. 1. Spherical cap under appex load
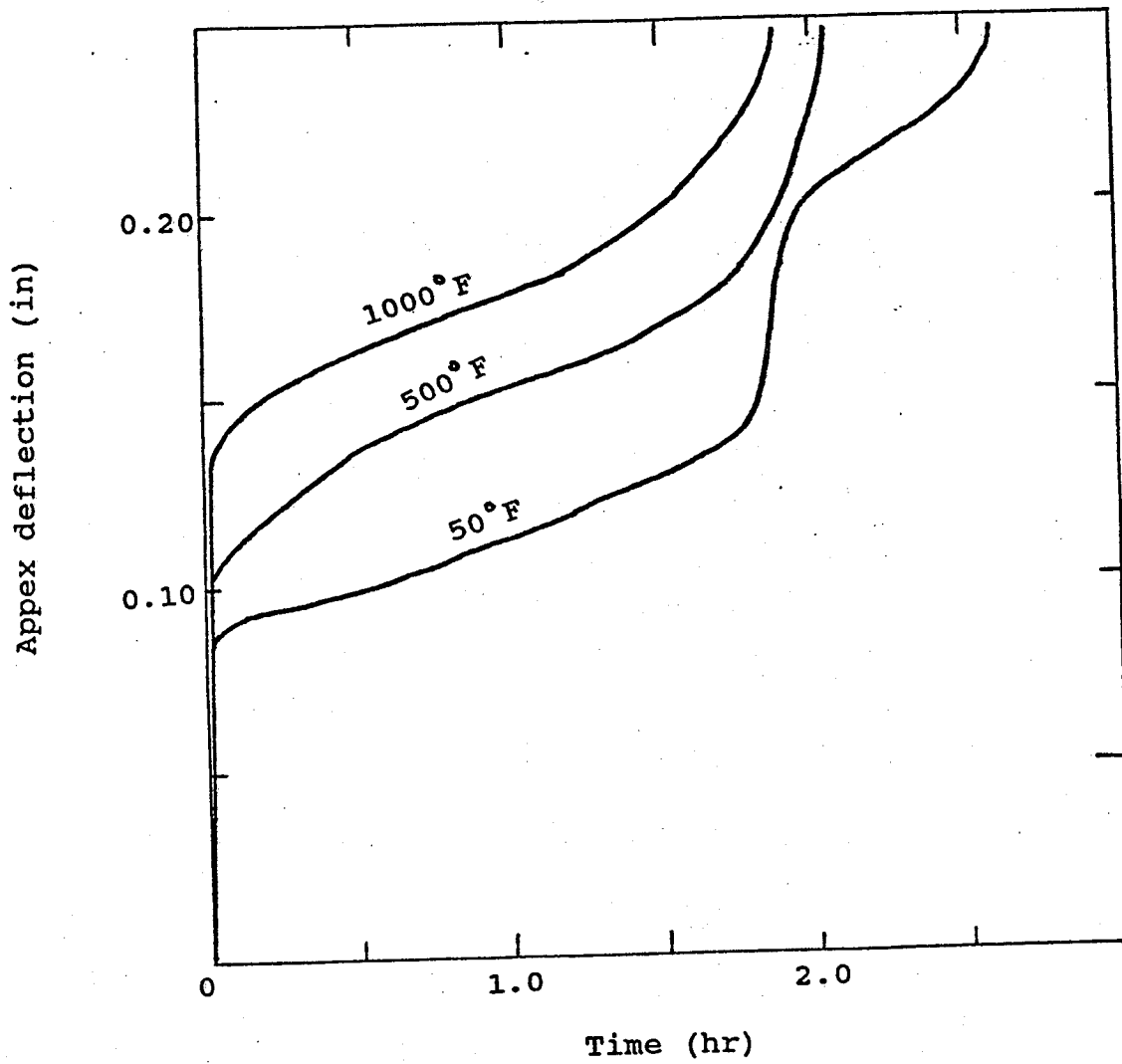

Fig. 2. Load deflection curves

79

Fig. 3. Appex deflection time history
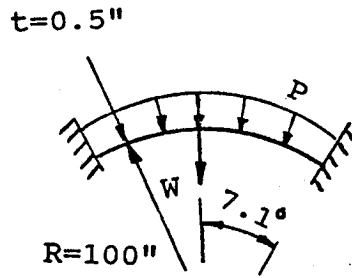
t=0.5"

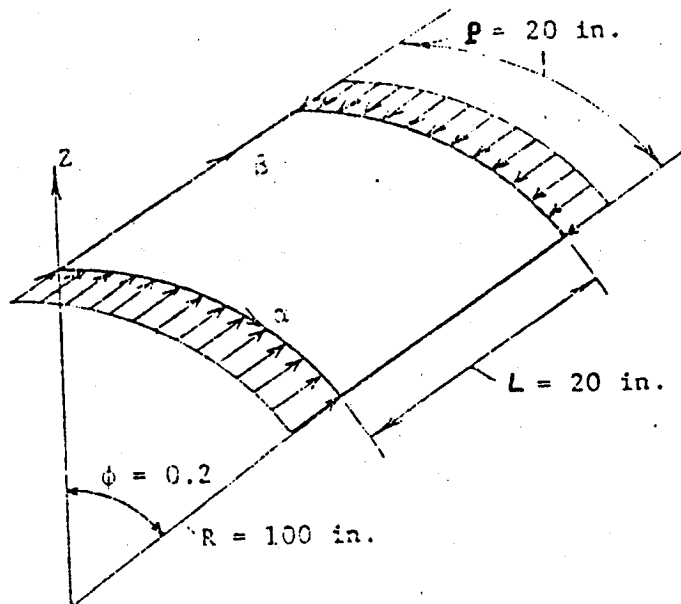Fig. 4. Spherical cap subjected
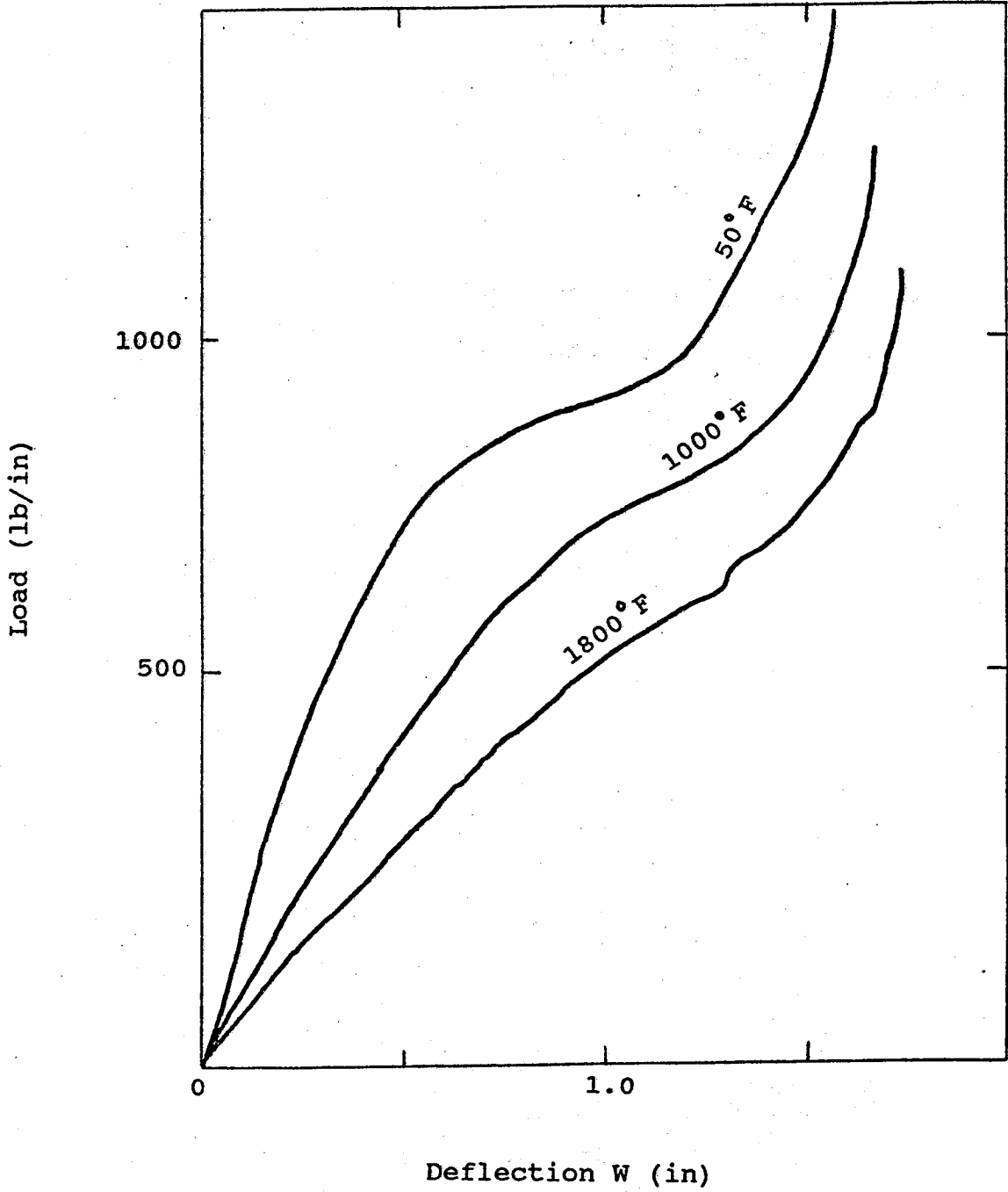to uniform pressure

Fig. 6. Cylindrical panel

Fig. 5. Load deflection curves for different
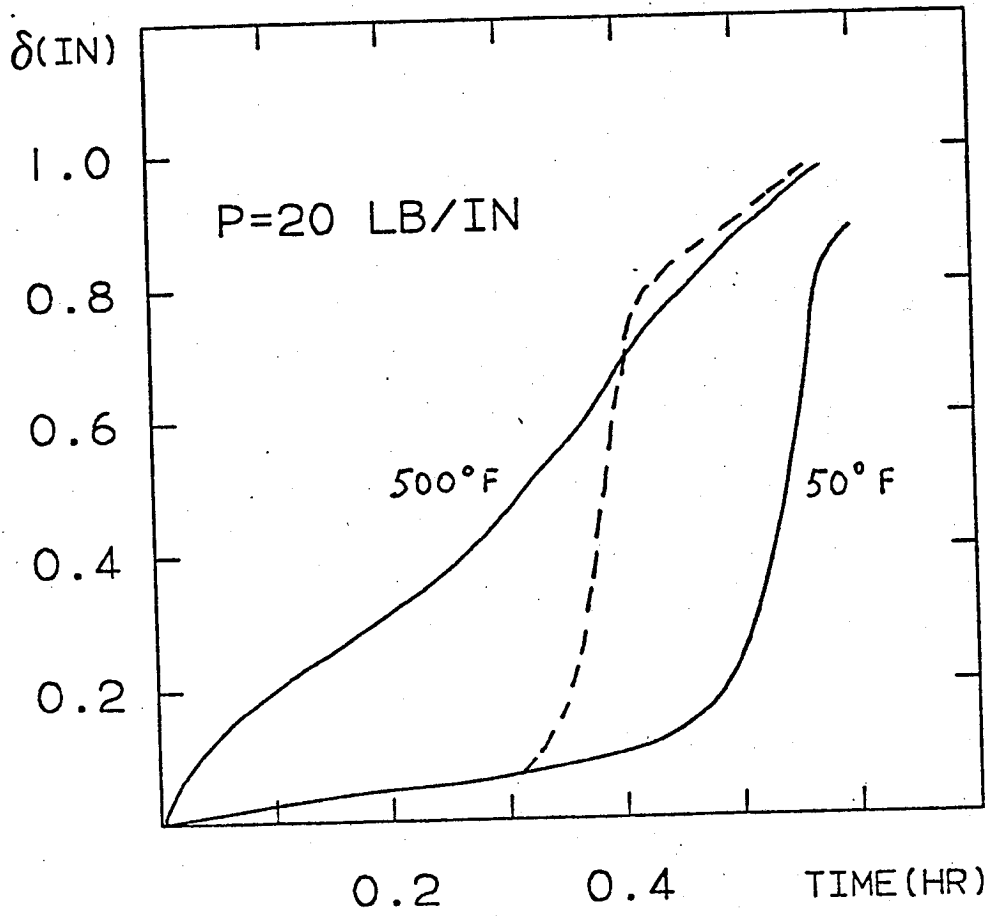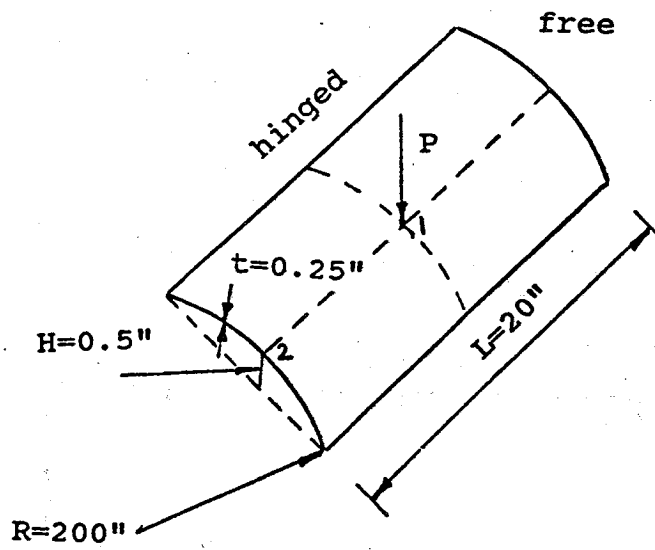temperatures

82

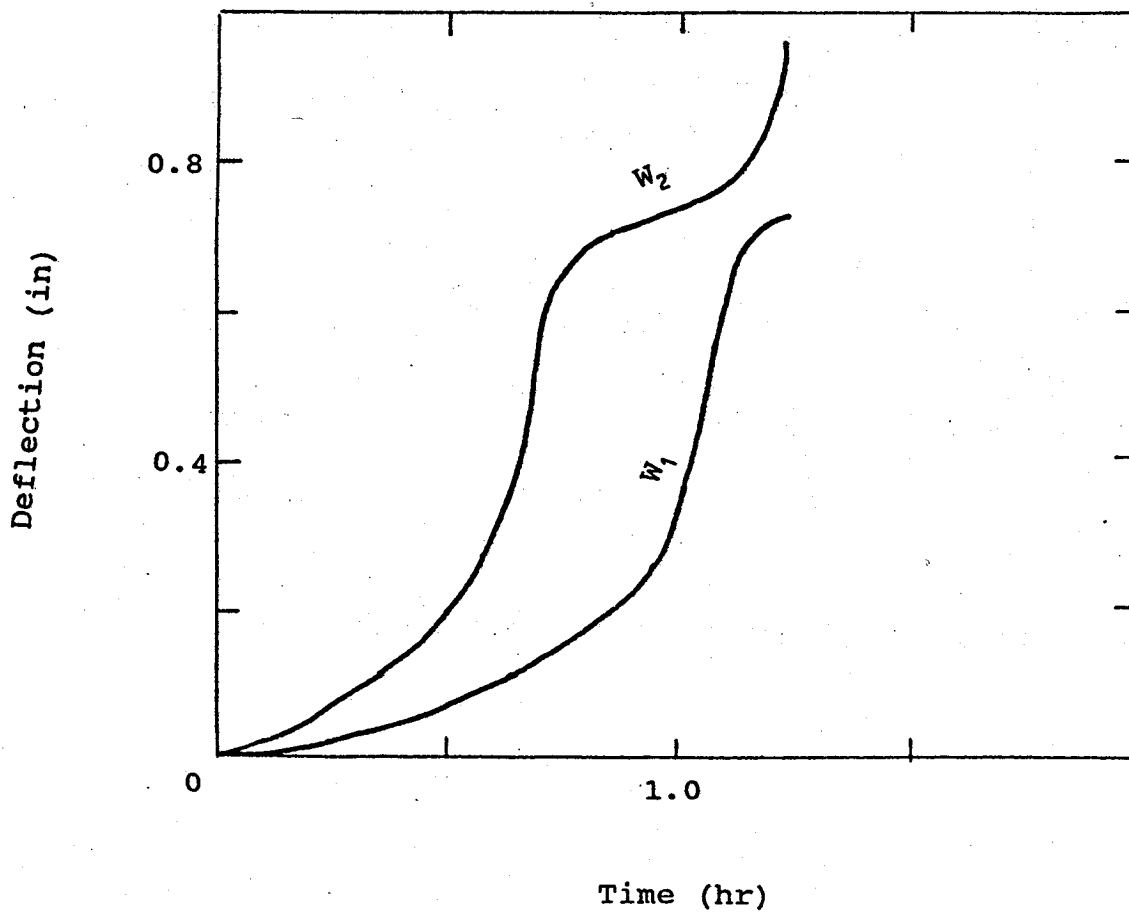Fig. 7. cylindrical panel creep behavior

Fig. 8. Shallow cylindrical panel

Fig. 9. Deflection time history

84

applied load of 20 lbs/in is well below the linear critical (buckling) load for this geometry, which is 42.15 lbs/in. At a temperature of 50x F the shell is in a primary creep state for the first 28 minutes, reaching a deflection of 0.2 in. and the critical time for creep buckling (this implies that the deflection becomes unbounded) is 35 minutes. At temperature of 500x F the shell 'maps' into its post-buckled configuration almost immediately but the critical time for creep buckling remains almost unchanged. The dashed line in the figure represents a non-isothermal process where the temperature was suddenly increased from 50x F to 500x F after 0.3 hrs. As a result the shell snaps-through to its post buckled position at 500x F with small over-shoot and reaches its critical time of creep buckling two minutes sooner (33 min.).

The last example is of shallow cylindrical panel made from Hastelloy-X and subjected to a concentrated force at the center of the panel (Fig. 8). Fig. 9 shows the deflection time history of points 1 and 2 to $P = 0.6P_{cl}$ which was kept constant.

Discussion

The study shows that in the presence of high temperature and viscoplasticity, the process of shell buckling assume an entirely new character. While the stability phenomena still exist under sufficiently large loads, buckling develops, as a time and temperature dependent deformation process under constant or variable thermomechanical loads of magnitude smaller than the purely elastic critical values. If the elastic behavior of a structure displays limit points and snap-through phenomena, the deformation process of creep buckling become even more compli- cated and it usually exhibits a combination of snapping and creep responses.

Acknowledgement

References

1. M. Kojic and K. J. Bathe, "Thermo-Elastic-Plastic and Creep Analysis of Shell Structures", Computer and Structures, Vol. 26, No. 1/2, 1987, pp. 135-143.

2. G. Miyazaki and Y. Ando, "Parametric Analysis of Creep Buckling of a Shallow Spherical Shell using the Finite Element Method", Nuclear Engineering and Design, 1977.

3. P. C. Xirochakis and N. Jones, "Axisymmetric and Bifuraca- tion Creep Buckling of Exter- nally Pressurized Spherical Shells", Solids and Structures, Vol. 16, 1980, pp. 131-148.

4. F. R. Botros and M. P. Bienek, "Creep Buckling of Struc- tures", Proceedings of the AIAA/ ASME/ ASCE/ AHS 24th SDM Conference, AIAA Paper No. 83-0864, May 1983.

5. W. Wojewodzki and R. Bukowski, "The Influence of the Yield Function Nonlinearity and Temperature in Dynamic Buckling of Viscoplastic Cylindrical Shells", Applied Mechanics, Vol. 51, 1984, pp. 114-120.

6. R. Bukowski and W. Wojewodzki, "Dynamic Buckling of Visco- plastic Spherical Shell", Solids and Structures , Vol. 20, No. 8,1984, pp. 761-776.

7. D. R. J. Owen, and E. Hinton, Finite Elements in Plasticity, Pineridge Press, Swansea, U.K., 1980.

8. R. Riff, R. L. Carlson, and G. J. Simitses., "Thermody- namically Consistent Constitutive Equations for Noniso- thermal Large -Strain, Elastoplastic, Creep Behavior," AIAA, Vol, 25, 1987, pp. 114-122.

9. R. Riff and G. J. Simitses, "Thermo-Elasto-Viscoplastic Analysis of Problems in Extension And Shear", Computer and Structures, Vol. 29, No. 2, 1988, pp. 293-300.

10. G. J. Simitses and R. Riff., "Non-Isothermal Elasto Visco- plastic Snap-Through and Creep Buckling of Shallow Arches" Proceedings of the 28th Structures, Structural Dynamics and Material Conference, Montrey, California, April 1987, pp. 466-472.

11. Simitses, G.J., Carlson, R.L., and Riff, R., "Formulation of the Nonlinear Analysis of Shell-Like Structures, Subjected to Time-Dependent Mechanical and Thermal Loading" NASA Report, 1986.

12. Th. Lehmann, "On large elastic-plastic deformation", In Proceedings of the Symposium on Foundation of Plasticity (Edited by A. Sawszuk), pp. 57-85, Noordhoff Netherlands, 1973.

13. Th. Lehmann, "On a generalized constitutive law in thermoplasticity", In Proceedings of the Symposium Plasticity Today (edited by A. sawczuk and C. Biancki), pp. 115-134, Udine, 1983.

14. Ramm, E., "Strategies for Tracing the Nonlinear Response Near Limit points", Proceedings Europe-U.S. Workshop on "Nonlinear Finite Element Analysis in Structural Mechanics", Bochum, 1980, Springer-Verlay 1981.

15. "Turbine Engine Hot Section Technology", NASA CP-2493, 1987

16. "Nonlinear Constitutive Relations For High Temperature Applications", NASA CP-2369, 1984

REPORT DOCUMENTATION PAGE

1. AGENCY USE ONLY (Leave blank)	2. REPORT DATE November 1991	3. REPORT TYPE AND DATES COVERED Final Contractor Report – March 90

4. TITLE AND SUBTITLE

Analysis of Shell-Type Structures Subjected to Time-Dependent Mechanical and Thermal Loading

6. AUTHOR(S)

G.J. Simitses

5. FUNDING NUMBERS

WU–505–63–5B
G–NAG3–534

7. PERFORMING ORGANIZATION NAME(S) AND ADDRESS(ES)

Georgia Institute of Technology
School of Aerospace Engineering
Atlanta, Georgia 30332

8. PERFORMING ORGANIZATION REPORT NUMBER

None

9. SPONSORING/MONITORING AGENCY NAMES(S) AND ADDRESS(ES)

National Aeronautics and Space Administration
Lewis Research Center
Cleveland, Ohio 44135–3191

10. SPONSORING/MONITORING AGENCY REPORT NUMBER

NASA CR–189051

11. SUPPLEMENTARY NOTES

12a. DISTRIBUTION/AVAILABILITY STATEMENT

Unclassified - Unlimited
Subject Category 39

12b. DISTRIBUTION CODE

13. ABSTRACT (Maximum 200 words)

This report deals with the development of a general mathematical model and solution methodologies for analyzing structural response of thin, metallic shell-like structures under dynamic and/or static thermomechanical loads. In the mathematical model, geometric as well as material-type of nonlinearities are considered. Traditional as well as novel approaches are reported and detailed applications are presented in the appendices. The emphasis for the mathematical model, the related solution schemes, and the applications, is on thermal viscoelastic and viscoplastic phenomena, which can predict creep and ratchetting.

14. SUBJECT TERMS

Finite elements; Creep; Viscoelastic; Viscoplastic; Ratching; Thermal transient; Solution schemes; Sample problems

15. NUMBER OF PAGES
88

16. PRICE CODE
A05

17. SECURITY CLASSIFICATION OF REPORT Unclassified	18. SECURITY CLASSIFICATION OF THIS PAGE Unclassified	19. SECURITY CLASSIFICATION OF ABSTRACT Unclassified	20. LIMITATION OF ABSTRACT

FOURTH CLASS MAIL

ADDRESS CORRECTION REQUESTED

U.S.MAIL

NASA